Interactions of transmembrane peptides and proteins with lipid membranes studied by mass spectrometry

Interactions of transmembrane peptides and proteins with lipid membranes studied by mass spectrometry

Interacties van transmembraan peptiden en eiwitten met lipide membranen bestudeerd met behulp van massaspectrometrie

(met een samenvatting in het Nederlands)

Proefschrift

ter verkrijging van de graad van doctor aan de Universiteit Utrecht op gezag van de Rector Magnificus, prof. dr. W. H. Gispen, ingevolge het besluit van het College voor Promoties in het openbaar te verdedigen op woensdag 27 november 2002 des middags te 12.45 uur

door

Jeroen Adrianus Antonius Demmers

geboren op 7 september 1975, te Bergen op Zoom

Promotoren:

Prof. dr. J. A. Killian
Prof. dr. A. J. R. Heck
Prof. dr. J. Haverkamp

verbonden aan de Faculteit Scheikunde der Universiteit Utrecht

"Human life occurs only once, and the reason we cannot determine which of our decisions are good and which are bad is that in a given situation we can make only one decision; we are not granted a second, third, or fourth life in which to compare various decisions."

— Milan Kundera in *The Unbearable Lightness of Being* (1984)

Aan mijn ouders

Table of contents

CHAPTER 1

General introduction

Biological membranes and life

Life can be scientifically thought of as a set of phenomena in which groups of molecules form temporary associations that are far from thermodynamic equilibrium. These complexes contain more information, order and structure than their surroundings. The energetic situation is maintained by the system itself at the expense of order, information and structure outside the system. The implication is that the living entity, such as a cell, should be separated from the rest of the universe by a discrete boundary, such as a cell membrane, by which it is then still able to communicate with the surroundings [1]. Cell membranes play a crucial role in homeostasis, the ability to maintain a steady chemical balance in a changing environment, and in biological communication between the inside and outside of a cell, between different cells and between different organelles in one cell; that is to say, they are not passive sacs, but active surfaces with an enormous diversity of functions. As soon as they stop working, the cell is not capable of living anymore. Therefore, membranes are indispensable for life. Membranes form boundaries not only of the cell as a whole, but also between compartments in eukaryotic cells, as they surround sub-cellular compartments such as organelles.

Building blocks of membranes

Biological membranes are dynamic, supramolecular assemblies that are composed of lipids and specific proteins (Figure 1), such as highly selective pumps, channels, receptors, and energy transducers, which mediate distinctive functions of membranes. According to the fluid-mosaic model [2], membrane proteins are 'dissolved in two-dimensional solutions of oriented lipids' and are held together by non-covalent interactions [3]. The lipids and proteins in biomembranes are present in a mass ratio ranging from about 1:4 to 4:1. Additionally, membranes contain carbohydrates that are linked to lipids and proteins.
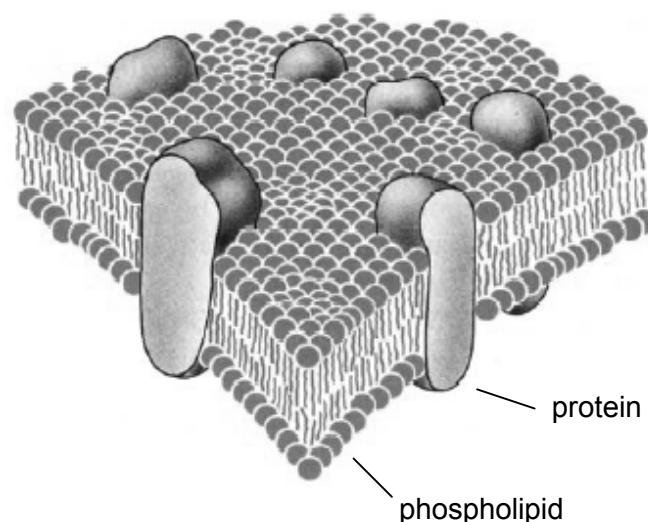

Figure 1 – Schematic representation of a phospholipid bilayer membrane containing several integral membrane proteins, according to the Singer-Nicolson fluid-mosaic model [2].

Membrane lipids have both water-soluble and water-insoluble moieties. It is this common amphipathic feature that enables the formation of the lipid bilayer. The first insights into the ambivalent lipid molecules forming continuous double layers (bilayers) of 4 to 5 nm thick with a hydrophilic outside and a hydrophobic inside, came from Gorter and Grendel and was proposed in 1925 [4,5]. The interactions between lipids are very tight and result in the membrane being virtually impermeable for most water-soluble molecules. Moreover, these interactions make that the membranes can form very extensive structures, that they close on themselves so that there are no edges with exposed hydrocarbon chains, and that they are self-sealing.

Cell membranes are composed of a large variety of lipids. The most abundant type of membrane lipids are the phospholipids (Figure 2). Phospholipids are derived from either glycerol, the phosphoglycerides, or from sphingosine, the sphingolipids. Many different types of lipid headgroups exist, which differ in charge, size, shape and their capacity to form hydrogen bonds. Phospholipids are rooted in the membrane bilayer by virtue of their hydrophobic tails, which are derived from fatty acids (long hydrocarbon chains with terminal carboxylates). These fatty acid chains usually contain an even number of carbon atoms, typically between 14 and 24, and they may be saturated or unsaturated. The 16- and 18-carbon atoms are the most common ones in biological membranes. Other important classes of membrane lipids are the glycolipids (carbohydrate-containing lipids) and the sterols, which contain a series of fused rings. One such sterol, cholesterol, is a major component of the membranes of many animal cells and is a key regulator of membrane fluidity.
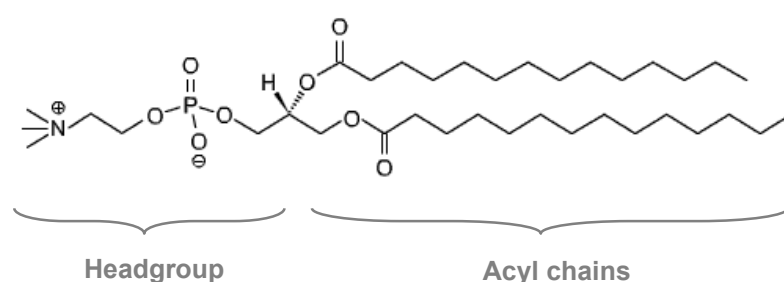
Figure 2 – Structural formula of the phospholipid 1,2-dimyristoyl-*sn*-glycero-3-phosphocholine (DMPC). In many schematic representations of lipid bilayer the headgroup of the phospholipid is indicated as a circle or ellipse and the acyl chains as solid lines.

Biological membranes are usually organized as lamellar lipid bilayers. However, they do contain lipids that on their own preferably adopt non-lamellar structures, such as the inverted hexagonal H_{II} phase [6,7]. The presence of such lipids is believed to be essential for the correct functioning of the membrane [7,8], most probably by providing specific packing properties, thereby affecting protein functioning. Alternatively, they could facilitate the temporal and local

formation of non-bilayer structures that may play a role in processes like membrane fusion and fission.

The proteins are either entirely spanning the membrane (integral membrane proteins) or bound to the membrane surface (peripheral membrane proteins). Integral membrane proteins interact extensively with the hydrocarbon chains of lipids by means of non-polar, hydrophobic interactions between the hydrophobic part of the protein and the hydrophobic interior of the membrane, whereas the non-polar regions are located outside the membrane in the aqueous environment. In contrast, the interactions between peripheral membrane proteins with the membrane are primarily electrostatic and hydrogen-bond based, although they can also be bound to integral membrane proteins or be anchored to the lipid bilayer by a covalently attached hydrophobic chain.

Permeability of lipid membranes

The major function of lipid bilayers is to act as permeability barriers. Still, some small solute molecules are capable of crossing the bilayer. For a molecule to cross the bilayer it must (1) enter the membrane, overcoming any interfacial resistance or free energy barrier to do this, (2) diffuse across the bilayer, and (3) exit the membrane on the opposite side, again overcoming any possible interfacial resistance. The permeability coefficients of several small solute molecules have been measured in two well-defined synthetic lipid bilayer systems: lipid vesicles (microscopic sacs that enclose a volume with a molecularly thin lipid bilayer membrane) and planar lipid bilayer membranes (for reviews: see [9-12]). Water, although highly polar, can surprisingly easily penetrate the membrane bilayer, in contrast to ions and small polar molecules [13]. Although the partition coefficient of water inside the membrane is low, the permeability coefficient of 3.4×10^{-3} cm/s [13] suggests that water can penetrate the bilayer at a rate of about 4000 water molecules per second per phospholipid molecule in the membrane, when a concentration gradient of 1.0 M is present [9]. Hence, a very low steady-state concentration of solute in the membrane core is not inconsistent with a relatively large net flux across the bilayer [14]. This remarkably high permeability for protons across the membrane may be explained by transient hydrogen-bonded chains of water extending across the membrane [10,15]. It should be noted, however, that the above mentioned experiments were carried out on lipid bilayers without any protein components present.

Integral membrane proteins

While lipids form a permeability barrier and establish compartments, specific membrane proteins mediate most other functions, especially in passive or active transport processes, and are responsible for many dynamic processes carried out by membranes. In general, membranes can perform a variety of functions, mostly carried out by different repertoires of proteins. Open reading frames encoding proteins with predicted transmembrane domains are exceptionally

abundant in sequence databases (20-50%), with the higher percentages corresponding to higher organisms [16]. The importance of membrane proteins is illustrated by the fact that the majority of all pharmaceuticals are targeted to this class of proteins, especially the family of G protein coupled receptors. This is one of the reasons why there is a large interest in obtaining structural information about membrane proteins.

In order to study integral membrane proteins, they have to be extracted from the membrane and to be purified. These hydrophobic proteins can be solubilized only by detergents or organic solvents. The ideal detergent to dissociate the protein from other membrane constituents to study structural properties, should not disturb the conformation of the protein and should be removable following purification. Sodium dodecyl sulfate is highly efficient in solubilization, but denatures the protein. Milder detergent molecules are, for instance, sodium cholate and octyl glucoside. An excess detergent is added so that at most one protein is present in a detergent micelle. However, since many membrane processes are vectorial, the functional properties of these membrane proteins can only be studied in their natural environment: the membrane. For instance, transport of nutrients or transduction of signals from one compartment to the other can only be studied with the membrane itself present. Therefore, in addition to studies of proteins dissolved in detergent micelles, proteins are also reconstituted in bilayers of synthetic phospholipids, resulting in functionally active membrane model systems that form a powerful experimental approach to the elucidation of membrane processes.

Methods for the investigation of membrane protein structure

In order to understand membrane protein functioning, insight into protein structure is necessary. However, the water-insoluble characteristics of these proteins makes primary, secondary and tertiary structure determination in general much more difficult than for water-soluble or globular proteins. A widely used method to obtain secondary structure information is circular dichroism (CD) spectroscopy, where regular secondary structures result in defined spectroscopic shapes, because of the distinct electronic environments sensed by the polypeptide amide groups within these structures. In addition, attenuated total reflection Fourier transform infrared (ATR-FTIR) and Raman spectroscopy can be used to obtain secondary structure information, since in these techniques vibrational bands from the polypeptide backbone are sensitive to secondary structure and can thus be used to quantify the amount of α- and β-structures [17]. Like CD spectroscopy, it can be applied to dried films, as well as to aqueous membrane suspensions, to proteins in detergent, to reconstituted vesicles or to oriented membrane systems. Moreover, detailed structural information, as well as information about the orientation of proteins in a lipid environment, can be obtained by solid-state nuclear magnetic spin resonance (NMR) spectroscopy [18-22]. Global conformational changes in ion channels can also be studied by cryo-electron microscopy [23].

The only experimental techniques to date that are capable of providing high-resolution (atomic scale) three-dimensional structures of membrane proteins are NMR spectroscopy [24]

and X-ray crystallography [25]. However, for both of these methods, severe limitations exist with respect to membrane proteins; on the one hand due to the relatively slow motions undertaken by integral membrane proteins *in situ* and usually also in detergent complexes (NMR), on the other hand because of major difficulties in obtaining well-diffracting crystals from such hydrophobic proteins (X-ray crystallography; see next section for details).

Three-dimensional structures of integral membrane proteins in detail

In the Protein Data Bank (PDB) of the Research Collaboratory for Structural Bioinformatics (RCSB) [26] over 16,000 protein, peptide and virus structures have been deposited to date. Only a very small fraction of these structures belong to integral membrane proteins (an up-to-date overview of all membrane proteins of which crystallographic structures have been determined to at least 4 Å is available on http://blanco.biomol.uci.edu/ from the Stephen White Laboratory at UC Irvine (CA)). At this moment, some 45 three-dimensional structures of membrane proteins have been resolved, comprising about 0.25% of the total number of structures deposited in the PDB. This percentage is in sharp contrast with the estimated 20-50% of the total genome of an organism encoding for membrane proteins [16], which illustrates that the experimental procedures to resolve three-dimensional structures of globular proteins are less well applicable to integral membrane proteins. For protein crystallography, the general procedure of solubilizing the proteins in detergent solutions and adding small amphipathic molecules to facilitate packing properties in the crystals has been proven to be successful for only a small number of proteins. Other promising novel techniques for crystallization of membrane proteins are being developed, such as using antibodies to solubilize the proteins [27] and using continuous lipidic phases as crystallization media [28]. Also in solid-state NMR spectroscopy, novel methods are being developed that look promising, for instance by making use of reverse micelles dissolved in a low-viscosity fluid [29,30] or by magic angle spinning (MAS-) NMR spectroscopy on oriented membrane systems [31,32]. These developments in both X-ray crystallography and NMR spectroscopy may contribute to gain insight into structural properties of more membrane proteins in the near future.

The first glimpse of the three-dimensional structure of a membrane protein came from high-resolution electron microscopy pioneering studies of two-dimensional crystals of bacteriorhodopsin of *Halobacterium halobium* [33,34]. The fundamental observation that this protein has a number of membrane spanning α-helices had a great impact on subsequent theories and experiments on membrane proteins. The first X-ray picture of a membrane protein, the photosynthetic reaction center from the purple bacterium *Rhodopseudomonas viridis,* was published in 1982 [35] (higher-resolution structures some years later [36,37]). Subsequently, a number of other structures of large membrane proteins have been resolved (e.g. [38-43]).

In addition to the α-helix as a membrane-spanning secondary structure element, there is the β-barrel motif, which was first found in the X-ray structure of an outer membrane protein:

porin [44]. In a β-barrel, the hydrophobic residues occur with a periodicity along the sequence such that they form a continuous surface, whereas the polar side chains are all on one side of the pleated sheet, forming the lining of the water-filled pore.

In this thesis, the focus will be on α-helical transmembrane peptides and α-helical integral membrane proteins.

Potassium channel KcsA: a typical α-helical integral membrane protein

A recent major breakthrough in understanding structure-function relationships in membrane proteins was the elucidation of the first structure of an ion channel: the potassium channel from *Streptomyces lividans,* KcsA [45]. The polypeptide of KcsA comprises 160 residues folded into two transmembrane α-helices, a pore helix and a cytoplasmic tail of 33 residues. Four subunits arranged around a central fourfold symmetry axis form the channel (Figure 3). The subunits pack together in such a way that there is a hole in the center which forms the ion pore through the membrane [45]. The structural elements that build up the ion channel show sequence similarity among all K^+ channels [46].

The structure of the KcsA potassium channel gives a good impression about the general lay-out of integral membrane proteins. The hydrophobic transmembrane segments, which can be tilted, span the lipids bilayer in an α-helical conformation. Moreover, belts of aromatic residues are observed in the interfacial region (Trp residues are colored black in Figure 3), where these residues are assumed to interact specifically. The next two sections will discuss the structural characteristics of transmembrane α-helices in more detail.

Structural characteristics of membrane-spanning α-helices

Membrane-spanning α-helices are composed of a stretch of predominantly non-polar amino acid residues, so that Van der Waals interactions can be established between the hydrophobic face of these α-helices and the acyl chains of membrane lipids. The principle of hydrophobic matching, in which the hydrophobic length of a transmembrane protein segment matches the hydrophobic thickness of the lipid bilayer, was introduced by Mouritsen and Bloom [47] and is believed to be an important determinant in protein-lipid interactions. The α-helix is favorable because this structure satisfies the hydrogen bonding potential of the polypeptide backbone. An alternate structure which lacks a single hydrogen bond would be less stable by about 5 kcal/mol [48], and therefore, a continuous helix without turns is most favorable. Typical transmembrane α-helices are estimated to vary in length from 15 to 28 residues [49] and may be tilted with respect to the bilayer normal, as can be deduced from available three-dimensional structures of membrane proteins. The α-helices are connected by hydrophilic loop structures that are enriched in amino acid residues with polar and ionizable side chains and are not located within the membrane.
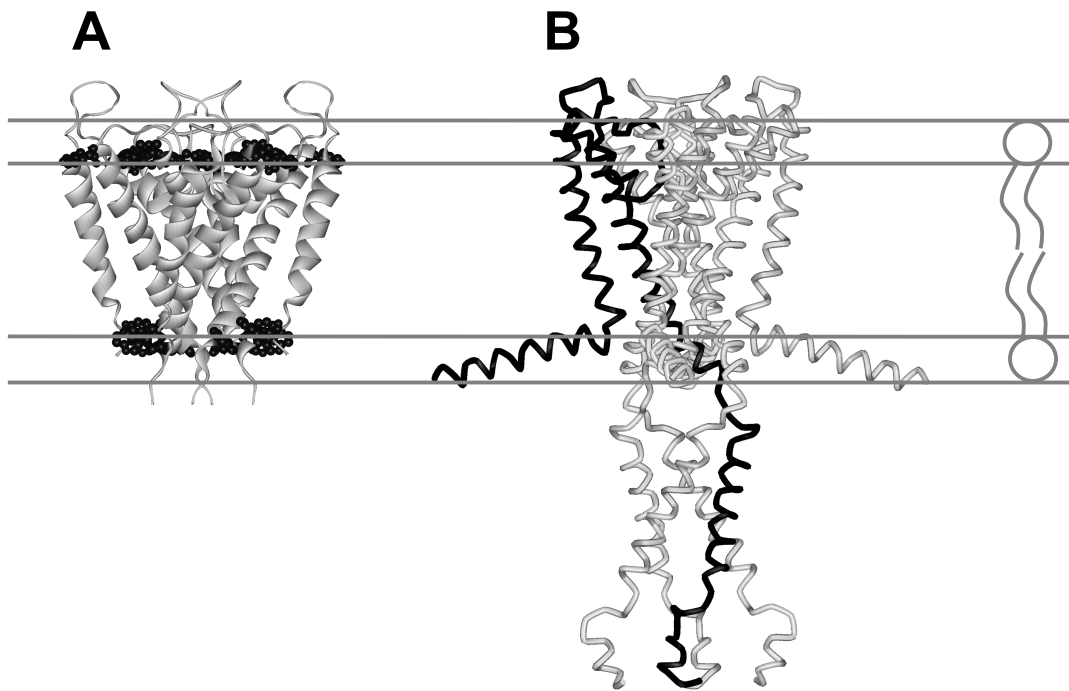
Figure 3 – Left panel: Crystal structure of the potassium channel KcsA [45] without its cytoplasmic N- and C-terminal tails (PDB entry: 1BL8). Trp residues, which form aromatic belts at the borders of the hydrophobic transmembrane domain, are indicated by black balls and sticks. Using site-directed spin-labeling methods and EPR spectroscopy, Cortes *et al.* [50] proposed a model for the architecture of the full-length ion channel based on this crystal structure (**right panel**). In this model, one of the monomers is colored black. Note that the boundaries of the lipid bilayer are not known with certainty and the drawing is only meant to indicate the approximate location of the membrane.

Although the general lay-out of transmembrane α-helices consists of non-polar amino acid residues, many of the known three-dimensional structures of membrane proteins have ionizable or polar residues in their membrane spanning domains [51-54]. These residues are likely to play important functional and/or structural roles in membrane proteins. Because it costs a lot of energy to transfer a charged residue from water to the hydrophobic inside of the membrane [48,55], these groups must be stabilized, for instance by ion pairing [56]. Additional polar interactions, like hydrogen bonds or interactions with carbonyl groups, may be required [57,58].

A rather special residue that is often found in transmembrane segments is proline. The structure of bacteriorhodopsin shows proline residues in three of the seven transmembrane helices, whereas rhodopsin has prolines in five out of seven helices. Remarkably, the helices are not particularly bent, although proline residues in water-soluble proteins have been shown to break the regular α-helix structure and to be present in regions of the helix where there is a distortion or irregularity [59]. Several studies have indicated a bias toward proline residues in

transmembrane segments of integral membrane proteins, especially those involved in transport [60,61]. The significance is not known, although a reasonable explanation would be that the lack of hydrogen bonding capacity within the helix itself can stabilize polar interactions between neighboring helices.

Structural characteristics of membrane spanning domains in the membrane-water interfacial region

Compared to the hydrophobic core of the membrane, the membrane–water interfacial (phospholipid headgroup) region presents a chemically complex environment, which offers many possibilities for non-covalent interactions with protein side chains [62]. Therefore, the interface is thought to play an important role in membrane association of proteins and peptides. The carbonyl moieties of the lipids, the phospholipid headgroups and water molecules around the lipid head groups present opportunities for dipole–dipole interactions and allow hydrogen bonding with appropriate amino acid side chains. In addition, electrostatic interactions might occur between, for example, positively charged amino acid side chains and negatively charged lipid phosphate groups. Residues that flank the hydrophobic membrane-spanning segments of membrane proteins will interact with the interface on each side of the membrane and thereby may determine the precise interfacial positioning of these segments or influence their orientation in the membrane [63-67].

A remarkable feature that pops up in many transmembrane α-helices is the distribution of aromatic amino acid residues. Not only do membrane proteins have a significantly higher Trp content than soluble proteins [68], they are found with a high frequency near the ends of transmembrane α-helices, which are expected to be located in the membrane interfacial region [69]. Localization of aromatic amino acids in the membrane interface is for instance observed in the photosynthetic reaction center [70], the potassium channel KcsA [45], bacterial porins [71], and in gramicidin A [72]. Also, several studies on smaller membrane-associated peptides have shown that there are indeed specific interactions of aromatic amino acid residues with the membrane interface [73-75]. A variety of roles have been proposed for interfacial aromatic residues, including positioning or anchoring the transmembrane segments in the membrane and stabilization of the helix with respect to the membrane environment [75]. In a recently resolved crystal structure of a specific phosphatidylcholine transfer protein (PC-TP), the positively charged choline headgroup of the co-crystallized PC engages in cation π interactions within a cage formed by the faces of two Tyr and one Trp residues [76], also indicating a specific interaction with aromatic side chains.

Another feature that is common in transmembrane proteins is the occurrence of charged residues such as arginine and lysine next to the transmembrane segments, and therefore acting as 'flanking residues'. Although the role of these charged residues in membrane proteins as topological determinants is well established [77], they may also play a role in membrane

anchoring in the interfacial region [75]. An interesting example is provided by bacteriorhodopsin, where a bound lipid headgroup contacts both aromatic and positively charged residues, with the aromatic residues located deeper in the membrane than the basic ones [78].

Model membranes and designed transmembrane peptides

Biological membranes are complex in terms of diversity of their protein and lipid components. In order to study membrane proteins, they often need to be concentrated, purified and reconstituted. Moreover, membrane proteins are often too large to investigate them in detail. Therefore, model membrane systems have been developed consisting of natural or designed peptides and phospholipids to study interactions of protein transmembrane segments with surrounding lipids at the molecular level (Figure 4). An important advantage of such systems is the well-defined composition, which can be systematically varied in order to study these interactions.
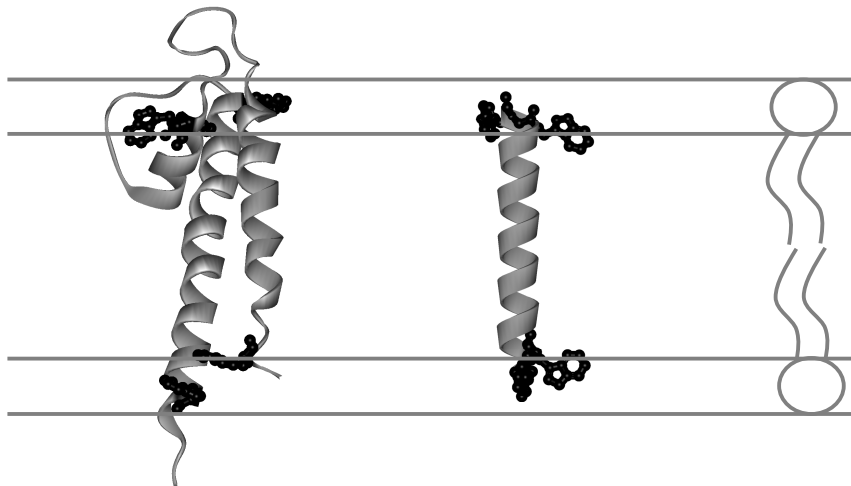

Figure 4 – Three-dimensional structure of a KcsA K$^+$ channel monomer, incorporated in a lipid phospholipid bilayer (**left**). Trp residues are indicated by black balls and sticks. The structure on the **right** is a representation of a synthetic α-helical peptide with Trp as flanking residues incorporated in a lipid bilayer in a transmembrane orientation, and, as such, it serves as a model for a transmembrane segment of a typical integral membrane protein. Note that the boundaries of the lipid bilayer are not known with certainty and the drawing is only meant to indicate the approximate location of the membrane.

A large number of the studies on peptide-lipid interactions has been focused on the naturally occurring peptides gramicidin A (e.g. [79-81]), alamethicin (e.g. [82,83]), and melittin (e.g. [84,85]). Nowadays, designed synthetic peptides are often being used as model transmembrane segments of integral membrane proteins in protein-lipid interaction studies. These peptides have the general architecture of transmembrane segments of membrane proteins and can be considered as 'consensus' transmembrane segment sequences. Examples of such sequences are the acetyl-GXXL(AL)$_n$XXA-ethanolamine/amide peptides, the so-called XALP

peptides, where X stands for any amino acid residue that flanks the hydrophobic core region. Such peptides and derivatives of these, especially those with Trp and Lys as the flanking X residues, have been extensively used to investigate protein-membrane interactions with a broad variety of techniques, like DSC, ^{31}P-NMR spectroscopy [86-88], ^{2}H-NMR, ESR, IR, tryptophan fluorescence, CD, and sucrose gradient centrifugation [89,90], and atomic force microscopy [91,92]. De Planque and co-workers have used XALP peptides to investigate the effect on lipid organization of variations in hydrophobic length of the peptide with respect to the bilayer hydrophobic thickness. They concluded from their work that in particular protein-lipid interactions in the membrane-water interface are important for determining the structure and dynamics of proteins and lipids in membranes [75,89,90,93]. Besides the XALP peptides, many other related sequences have been used in studies on interactions between model transmembrane peptides and lipids (see e.g. [94-100]).

Mass spectrometry

Mass spectrometry on biomolecules

As discussed above, membrane proteins and their interactions with lipid bilayers are not easy to characterize. There are a number of biophysical techniques available and they have given major insights into properties of membrane proteins and their interactions with the membrane environment. However, they all have their specific restrictions and, therefore, it would be advantageous when this repertoire of tools could be extended by other techniques such as mass spectrometry, which offers in principle complementary possibilities for investigating such interactions.

Mass spectrometry (MS) has developed in the last decade to a mature tool to study biomolecules in general and proteins in particular. It has been proven to be an indispensable tool in determining the primary structure of proteins including possible modifications using tandem MS (see below). More recently, it has also been shown to be a valuable tool in studies on secondary and tertiary protein structures, for instance in combination with hydrogen/deuterium exchange or charge-state distribution investigations (e.g. [101]). Nowadays, MS is also used to study quaternary structures of proteins and protein complexes and their interactions with enzymes, ligands or substrates. However, little is known about the potential of MS to study membrane proteins and only very few applications have used MS successfully in studying this class of proteins.

The basis of MS is (1) the production of ions from neutral analytes and to bring them into the gas-phase, and (2) the separation according to their mass-over-charge (m/z) values and the detection of those ions. Its current prominent role in the analysis of biological macromolecules is due to two major technical breakthroughs in 1988 and 1989: the development of matrix-assisted laser desorption/ionization (MALDI)-MS and electrospray ionization (ESI)-MS (see below for extended description). Before these landmarks, electron ionization, chemical ionization, field ionization, and field desorption were used to ionize molecules to bring them in the gas-phase. These techniques were limited to low and medium molecular weight compounds, since higher-mass compounds were easily decomposed because of the high energy levels involved. In the early 1980s, fast atom bombardment (FAB) MS [102,103] and plasma desorption (PD) MS [104] had been developed and using these methods it was possible to analyze compounds of higher mass (e.g. biomolecules) up to several tens of kDa. FAB involves the bombardment of a solid analyte and matrix (a small organic species, e.g. glycerol or *m*-nitrobenzyl alcohol) mixture by a fast particle beam, which is a neutral inert gas, typically Ar or Xe. The particle beam is incident at the analyte surface, where it transfers much of its energy to the surroundings, setting up momentary collisions and disruptions. Disadvantages are the low upper mass limit, the low ionization efficiency that is influenced by the chemical properties of matrix and sample [105], and the high background matrix peaks. The ionization energy involved

is sufficient to induce fragmentation of the analyte ions, which may be wanted or unwanted. Therefore, this ionization technique could be referred to as 'semi-soft' ionization.

The revolutionary invention of the 'soft' ionization techniques MALDI and ESI, however, allowed analysis of biomolecules in the mass range of over 100 kDa. These techniques deposit relatively little energy in the ions. Nowadays, they are routine techniques for molecular mass determinations of all types of biomolecules. Especially for peptide and protein analysis the sensitivity of these techniques are considered extremely good even at the femtomole level. In the following sections the principles of MALDI and ESI are discussed in more detail and the focus will be on peptides and proteins (for review see [106]).

Electrospray ionization mass spectrometry

Electrospray ionization (ESI), developed in 1989 by Fenn *et al.* [107], produces gaseous ionized molecules from a liquid solution. This is accomplished by creating a fine spray of highly charged droplets from the tip of a metal nozzle (or metal-coated glass capillary in case of nano-flow ESI) in the presence of a strong electric field (Figure 5). The highly charged droplets are then electrostatically attracted to the mass spectrometer inlet. By evaporation of the solvent by heat or application of a drying gas, the droplets decrease in size and the electric field density on its surfaces increases. The mutual repulsion between like charges on this surface becomes so great that it exceeds the forces of surface tension, and ions begin to leave the droplet through what is known as a Taylor cone. The ions are then directed into an orifice through electrostatic lenses leading to the mass analyzer. ESI is conducive to the formation of multiply charged molecules (such as $[M + nH]^{n+}$), which is an important feature since the mass spectrometer measures m/z values, where m is the mass of an ion and z is its charge. Therefore, it is possible to observe very large molecules with an instrument that has a relatively low m/z range, which makes it ideal for the analysis of intact proteins. Furthermore, the technique is very sensitive and there is no matrix interference. There is experimental evidence [108-110] that ESI is a softer ionization technique compared to other ionization methods, since it allows the production of charged non-covalently bound protein complexes in the gas-phase when relatively low voltages are applied. When only information on the mass of the analyte is needed, sample preparation can be achieved by dissolving the sample in a protic volatile organic solvent system that is homogeneous and contains low amounts of salt. In addition, excellent results have been obtained by aqueous buffer solutions at neutral pH values, in which the protein retains its secondary and tertiary structure. For extended reviews on ESI: see Refs. [106,111].
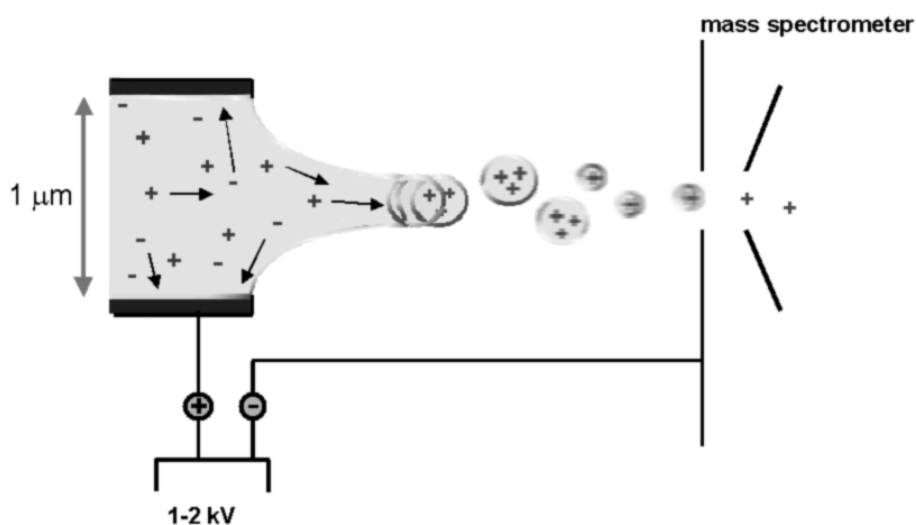
Figure 5 – Schematic representation of the nano-flow ESI process in the positive ion mode. Multiply charged positively droplets are formed that are accelerated in the electric field; at the same time they decrease in size by evaporation of the solvent. Subsequently, they divide into smaller droplets, finally resulting in the formation of positively charged analyte ions entering the mass analyzer inlet.

Matrix-assisted laser desorption/ionization mass spectrometry

Matrix-assisted laser desorption/ionization (MALDI), developed in the late 1980s [112], is a method that allows for the ionization and transfer of a sample from a condensed phase to the gas phase (for a review on MALDI-MS see Ref. [113]). It requires a solid matrix with which the sample is co-crystallized, and laser light as the ionizing beam to sputter the sample from the probe surface. The matrix is a non-volatile solid organic compound (usually 2,5-dihydroxybenzoic acid, α-cyano-4-hydroxycinnamic acid or sinapinic acid) that plays a key role by absorbing the light energy which causes the material to vaporize. The matrix absorbs most of the incident energy and is believed to facilitate the ionization process when sample and matrix are in the gas-phase. In MALDI-MS, in general singly charged peptides or proteins are generated. The charged molecules are directed by electrostatic lenses from the ionization source into the mass analyzer. Subsequently, time-of-flight analysis is often used to separate the ions according to their mass-to-charge ratio. MALDI involves efficient energy transfer and allows relatively small quantities of sample to be analyzed which make it very attractive for the analysis of biological compounds. MALDI-MS is quite tolerant for heterogeneous samples and for salts. Although there are some examples of membrane proteins that have been analyzed successfully by MALDI-MS (e.g. [114,115]), a potential problem is the hydrophobicity of these proteins that may disturb the co-crystallization process.

Separation and detection: quadrupole time-of-flight analysis

A quadrupole (Q) mass analyzer separates ions on basis of the stability of the ion trajectory through four parallel rods, in which opposing rods carry charges of the same sign. By applying an alternating radio frequency (RF) voltage on top of a direct current (DC) voltage, ions traveling at a relatively low velocity with different m/z values follow different trajectories through the rods. At a particular voltage, ions with one m/z value traverse the quadrupole, while others collide with the rods and are lost. By scanning the voltages while keeping the ratio between the DC and RF voltages constant, ions with different m/z values pass successively through the mass analyzer. A quadrupole analyzer is suitable for coupling with ESI, since it can operate at relatively high pressures and does not require high accelerating fields.

In hybrid mass spectrometers, a quadrupole analyzer can be coupled to a time-of-flight (ToF) analyzer, resulting in a Q-ToF mass spectrometer as shown in Figure 6, which is used in most experiments described in this thesis. The ToF analyzer is one of the simplest mass analyzing devices and is commonly used in combination with MALDI and ESI. ToF is based on accelerating a set of ions to a detector with the same amount of kinetic energy (U_k). Since $U_k = \frac{1}{2} m \cdot v^2$, where m stands for the mass of the ion and v for the velocity of the ion, ions will travel a certain distance d (which is given by the length of the ToF tube) within a time t, where t is dependent on the m/z of the ion. Thus, the m/z values of the ions are determined from the ions' time of arrival at the detector. ToF reflectron analysis has been developed to increase the resolution of the conventional ToF analyzer. While the ToF analyzer has limited resolving power, the addition of the reflectron serves to reduce the kinetic energy distribution of the ions that reach the detector and, as a result, achieve higher resolution. However, this improved resolution comes at the expense of sensitivity and mass range. For an extensive review on the fundamentals of ToF analysis, see Ref. [116].

In the Q-ToF hybrid mass spectrometer in Figure 6, the ions are extracted orthogonally into the ToF tube to correct for spatial or velocity spread of the ions in the direction of the ion source and so to improve resolution [116]. The quadrupole operates in the RF-only mode, when it acts as a wide band-pas filter transmitting ions across the entire m/z range. In the tandem MS (MS/MS) mode, the quadrupole acts as a m/z filter for selection of the precursor ion for collision induced dissociation in the collision cell (see next section).

Ions are detected by converting their kinetic energy into an electrical current. Among the four most common types of detectors, the electron multiplier and scintillation counter are the most frequently used. An electron multiplier is made up of a series of approximately ten dynodes, each made of a secondary emitting material maintained at ever-increasing potentials. Ions strike the dynode surface, which results in the emission of electrons. These secondary electrons are then attracted to the next dynode and then the next, resulting in a cascade. The typical current gain is about 10^6. The scintillation counter (photomultiplier conversion dynode) detector is similar to an electron multiplier. The ions initially strike a dynode, thus releasing electrons. However, in this case the electrons then strike a phosphorous screen. When the

phosphorous screen is struck by an electron, it releases photons that are then detected by a photomultiplier.

Tandem mass spectrometry for protein sequence determination

Mass spectrometry is important in obtaining protein sequence information. Primary structural information on peptides and proteins can be obtained by collision-induced dissociation (CID) MS. Peptides are linear biopolymers built up from amino acids, which allows the relatively straightforward interpretation of the fragmentation data. The process is initiated by converting some of the kinetic energy from the peptide ion into vibrational energy. This is achieved by introducing the mass selected precursor ion, usually an $[M+n\text{H}]^{n+}$ or $[M+n\text{Na}]^{n+}$ ion, into the collision cell where it collides with neutral gas molecules, resulting in fragment ions that can be monitored. The fragment ions produced in this process can be separated into two classes. One class retains the charge on the N-terminal region while cleavage is observed from the C-terminal region. This fragmentation can occur at three different positions, each of which is sequence designated as types a_n, b_n, and c_n (nomenclature according to [117]). The second class of fragment ions generated from the N-terminal region retains the charge on the C-terminal region, while cleavage is observed from the N-terminal. Like the first class, this fragmentation can occur at three different positions, types x_n, y_n, and z_n.
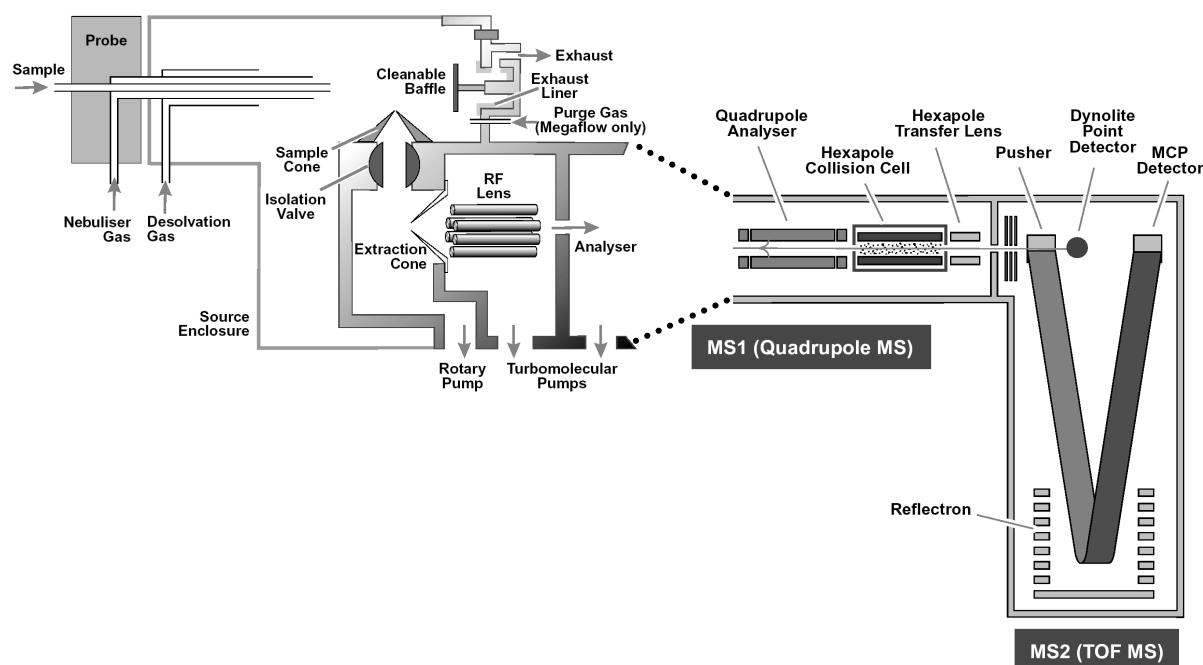

Figure 6 – Schematic representation of an orthogonal Q-ToF hybrid mass analyzer, equipped with a Z-spray nano-flow ESI setup (source: Micromass Ltd., UK).

There are several limitations for complete sequencing. Neither leucine and isoleucine, nor lysine and glutamine can be differentiated because they have (almost) the same residual mass. Furthermore, sequence information generally can be obtained only for relatively small peptides up to approximately 5 kDa. However, for larger peptides at least partial sequence information can be revealed and even partial information can be very informative. Indeed, peptide sequencing in combination with peptide fingerprints of a proteolytically digested protein is now the method of first choice in identifying proteins.

Hydrogen/deuterium exchange in protein structure determination

The analysis of hydrogen/deuterium (H/D) exchange kinetics of protein backbone amide protons has long been used as a source of structural and dynamic information [118-121]. The idea is that some of the solvent exposed hydrogen atoms in proteins are capable of switching places with hydrogen atoms from the solvent molecules surrounding the protein. If an isotope of hydrogen is used as the solvent, such as in deuterium oxide, its higher mass gets incorporated into the protein and the change in mass can be monitored. The exchange of hydrogens occurs at a specific rate, which is a function of several variables, including solvent accessibility (and, thus, protein structure), temperature, and pH. There are three kinds of hydrogens in proteins (Figure 7). Hydrogens covalently bound to carbon (gray) essentially do not exchange, whereas the ones on the side chains (bold and underlined) can exchange very fast. The ones at the backbone amide positions (bold) exchange at rates that are very sensitive to the structure of the protein. Each amino acid, except proline, has one amide hydrogen. Therefore, hydrogen exchange rates can be measured along the entire length of the protein backbone. The backbone amide hydrogens can be involved in formation of hydrogen bonds in secondary structural elements like, α-helices and β-strands. Therefore, their exchange rates are a reflection of structure and structural stability. Hydrogen exchange measurements can be used to sense changes in protein structure on a specific time scale. Some amide hydrogens, such as those at the surface of folded proteins, exchange very rapidly. The rate of exchange of these hydrogens can be used to sense binding to other proteins and to analyze complexes. Other hydrogens are buried in the hydrophobic core of the protein and may not exchange for hours, days, or even months. Therefore, the movements of proteins and the rate of such movements can be studied by H/D exchange.

Protein H/D and hydrogen/tritium (H/T) exchange studies were initiated in the mid-1950s [118,122]. Since then, the usual methods to measure incorporated labels have been tritium counting and various spectroscopic techniques (infrared, Raman, UV absorbance), which give information at an unresolved level. Also NMR methods and neutron crystallography have been used, by which high resolution data can be obtained. In addition, MS can be used to measure H/D exchange kinetics, which will be further explained in the next section.

H/D kinetics monitored by mass spectrometry

The combination of ESI-MS and solution-phase H/D exchange, which began in the early 1990s is an informative way of studying global secondary, tertiary and even quaternary structures of proteins. One of the first examples was published by Katta and Chait [123] on the conformational changes in bovine ubiquitin induced by addition of organic solvents to protein solutions. Since then the method has been successfully used in studies on protein folding/unfolding and structure elucidation [124-133], protein interfaces [134], DNA-protein interactions [135], non-covalent protein-protein interactions [136], protein-ligand interactions [137], enzyme-inhibitor complexes [138] and amyloid formation [139-141]. For reviews on H/D exchange and mass spectrometry see Refs. [136,142-145].
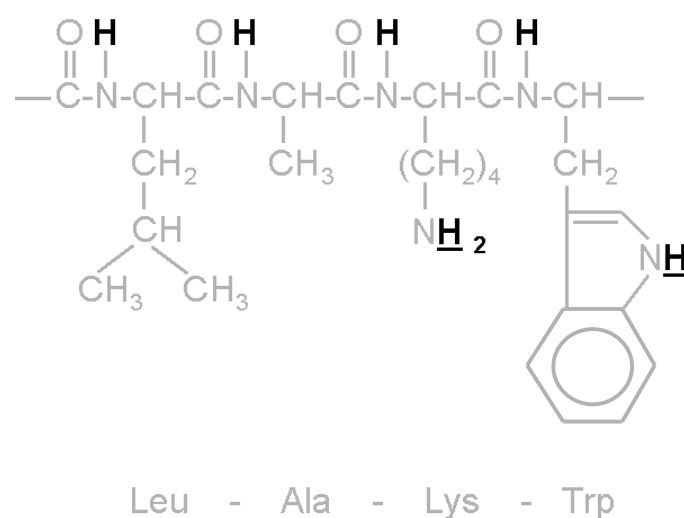
Figure 7 — Structural formula of a peptide sequence: hydrogens covalently bound to carbon (gray) are virtually unexchangeable, hydrogens linked to nitrogen (and oxygen) atoms in side chains (underlined) exchange very fast and backbone amide hydrogens (black) in an unstructured polypeptide have intermediate exchange rates. The exchange rates of amide hydrogens are therefore a reflection of the polypeptide secondary structure.

An example of how NMR spectroscopy and ESI-MS in combination with H/D exchange are complementary techniques, was shown by Miranker *et al.* [129], using two populations of protein conformers. The first population has molecules that are completely exchanged and others that are not exchanged at all. The second population has 50% of the protons exchanged. Because NMR spectroscopy monitors the average proton occupancy, the two populations are indistinguishable. However, ESI-MS can distinguish the two populations on the basis of their mass difference. Another successful application of H/D exchange combined with ESI-MS was published by Robinson *et al.* [128]. The conformation of a protein bound to the molecular chaperone GroEL was investigated by monitoring directly its hydrogen exchange

kinetics using electrospray ionization mass spectrometry. The bound protein was weakly protected from exchange to an extent closely similar to that of an uncomplexed molten globule state of the protein.

Standard procedures nowadays in MS are continuous labeling of a protein in deuterated buffer solution at neutral pH values. The exchange reaction is quenched by lowering the pH to 2.5 and the temperature to 0°C. The whole protein can be analyzed, but an alternative way to obtain detailed information is to digest the deuterated protein first with porcine pepsin and to subsequently monitor the deuterium content of the proteolytic fragment peptides. This works best at low pH values and can tolerate being at 0°C.

In addition to ESI-MS, MALDI-MS has been successfully used in combination with solution-phase H/D exchange since several years [134,146-151]. The advantages of this technique may be the suitability for fast, high-throughput screening and its tolerance of relatively impure samples. Disadvantages, however, may be the artifacts in amount of incorporated deuteriums because of back-exchange with matrix molecules.

Hydrogen/deuterium exchange and collision induced dissociation mass spectrometry

As mentioned above, NMR spectroscopy can be used to monitor the hydrogen exchange at individual amide bonds in order to obtain information on local solvent accessibility or dynamics. When using MS as the preferred method, the individual sites of deuterium incorporation in a peptide could in principle be probed by fragmentation in CID MS. Several studies have shown that this method can give high resolution data on H/D exchange of individual amide bond hydrogen atoms [127,131,139,152-156]. Other studies, however, have indicated that hydrogen mobility within peptide ions is sufficiently rapid to scramble their position prior to CID [157-159], which results in loss of isotopic information.

Analysis of membrane peptides and proteins by mass spectrometry

Like for virtually any other biophysical tool, the study of membrane proteins presents a special challenge for MS approaches as well. Problems include the purification and sample handling of these proteins because of their high hydrophobicity, and the extremely low solubility in aqueous solvents and hence the use of detergents. Whereas ESI-MS is incompatible with membrane proteins dissolved in detergent solutions, a number of recent papers have shown the potential of MALDI-MS in this respect. In order to analyze proteins in aqueous detergent solutions, it has been tried to examine the effect of detergents on the MALDI-MS analysis and to modify sample preparation and admission procedures [160-162]. A study on the analysis of integral membrane proteins in detergent-solubilized state by MALDI-MS with modified (hydrophobic) matrix mixtures was published by Hillenkamp and co-workers [114], who could detect the intact non-covalently bound trimer of porin. Alternatively, integral membrane proteins can be analyzed with

MALDI-MS by using α-cyano-4-hydroxycinnamic acid in a formic acid/water/isopropyl mixture as the matrix [115]. Generally, even low concentrations of detergents like sodium dodecyl maltoside, which are necessary for solubilization of membrane proteins, suppress MALDI-MS signals dramatically, although it has been reported that above the critical micelle concentrations for sodium dodecyl sulfate (SDS) and 3-[(3-cholamidopropyl)dimethylammonio]-1-propanesulfonate (CHAPS) peaks with a sufficient signal to noise ratio were obtained [163,164].

A number of papers have been published about the use of ESI-MS to investigate transmembrane peptides and intact integral membrane proteins dissolved in organic solvents such as formic acid, methanol, chloroform, hexafluoroisopropanol and mixtures hereof [165-169]. Although organic solvents in general denature proteins in such a way that the tertiary and mostly also the secondary structural elements are lost during the measurement, for many types of experiments maintenance of these structural elements is not a prerequisite, as long as the primary structure remains intact.

A general approach for identification of proteins involves the combination of MS with high-pressure liquid chromatography (HPLC) and limited proteolytic digestion or chemical cleavage. Peptide mass fingerprints are easily generated for water-soluble proteins and this is widely used for identification of proteins that are separated by two-dimensional gel electrophoresis [170]. Membrane proteins possess loop domains that are in the aqueous phase surrounding the membrane and limited proteolytic digestion is applicable to this class of proteins as well. Often, proteolytic fragments from these parts of the protein are sufficient for successful identification of the protein, except that the presence of detergents may affect the signal-to-noise ratio. This method has been applied successfully to identify integral membrane proteins [171-177]. However, to obtain a peptide mass fingerprint of the membrane-embedded part of an integral membrane protein is much more difficult, since many of the widely used proteases (like trypsin and endoproteinase Glu-C) target charged residues, which are not very often found in transmembrane segments. Furthermore, potential cleavage sites in the membrane-embedded domain are not easily accessible for proteases. However, in-gel chemical cleavage by cyanogen bromide (CNBr) at methionine residues has shown to be a potential tool to circumvent these problems [178-181]. This specific chemical cleavage procedure in combination with MS can also be used for conformational studies on membrane proteins [182] and topology determination studies on integral membrane proteins [183].

To our knowledge, until now no studies have been published on mass spectrometric analysis of membrane peptides or proteins in their natural environment, the phospholipid membrane. Yet this would be of great interest, because it would allow their secondary and tertiary structural elements to stay intact during analysis and hence provide useful information on the characteristics of this class of biomolecules.

Outline of this thesis

Although information is available in literature on the structure of membrane proteins, the exact way in which membrane proteins are embedded in the lipid bilayer is not yet well understood. Limited insight is existing in their interactions with the surrounding lipids and with the membrane-water interface in particular, where many interactions of membrane proteins with substrates, enzymes and ligands take place. Insight into the exact positioning of the transmembrane segment(s) of such proteins with respect to the membrane-water interface, as well as into their structural properties, are essential to understand the functioning of these proteins. An accepted way to systematically study integral membrane proteins and their interactions with the surrounding lipid membrane, is to use designed model transmembrane peptides in well-defined vesicular systems. These hydrophobic peptides are about as long as a typical transmembrane segment of such a protein and form α-helices in lipid bilayers. In Chapters 2, 3 and 4 experiments are described using such peptides in order to study specific characteristics of these peptides in a lipid environment. Extending on this, in Chapter 5 a full-length naturally occurring integral membrane protein embedded in a lipid environment is studied. The scope of this thesis is to investigate the opportunities of MS for studying these membrane peptides and proteins in membrane systems.

In Chapter 2, it will be shown that it is possible to study the precise positioning of transmembrane peptides in lipid bilayers. Therefore, a novel method was developed to implement MS in membrane peptide and protein research, referred to as 'proteoliposome spraying' method. By combining H/D exchange and nano-flow ESI-MS, the numbers of incorporated deuterium atoms in two different designed transmembrane peptides that are incorporated in lipid bilayer membranes can be analyzed. This 'proteoliposome spraying' method involves direct introduction of the vesicle suspension into the MS-inlet. Several distinct H/D exchange rates can be observed for the exchangeable hydrogens depending on their position in the transmembrane peptides. Assignments are confirmed by CID MS measurements, which allow analysis of exchange of individual peptide amide linkages.

In Chapter 3, this method is used to get more detailed insights into the architecture of various transmembrane peptides and into the positioning of such peptides in lipid bilayer membranes. Several variables such as (1) the influence of the length of the peptide hydrophobic core sequence, (2) the role of the flanking tryptophan residues, and (3) the influence of putative helix breakers, are investigated. The results are discussed in a biochemical and biophysical context.

In Chapter 4, I shall move from biophysical chemistry towards a physical chemistry related subject, which is about possible complications in H/D exchange studies that might result from gas-phase migration of deuterium atoms incorporated in the peptides (referred to as 'scrambling'). Our systematic studies of this phenomenon suggest that the extent of deuterium scrambling is strongly influenced by experimental factors, such as the exact amino acid sequence

of the peptide, the nature of the charge carrier and, therefore, most likely by the gas-phase structure of the peptide ion.

In Chapter 5, I shall move back to biophysical chemistry, where a 'real' integral membrane protein is explored: the potassium channel KcsA. The intention was to extend the studies presented in Chapters 2 and 3 to a larger membrane protein and to investigate the interactions of this protein with lipids. In these experiments, non-covalent complexes of phospholipid molecules and KcsA are observed. Moreover, it is possible to probe preferential binding of certain classes of lipids to the protein. The results are discussed in the context of results of biochemical assays with identical protein-membrane systems.

In Chapter 6, the results presented in this thesis are summarized and discussed in the context of the present literature.

References

1. Gee, H. (1999) What is life? *Nature Science Update*, http://www.nature.com/nsu/990422/990422-9.html.
2. Singer, S.J. & Nicolson, G.L. (1972) The fluid mosaic model of the structure of cell membranes. *Science* **175**, 720-31.
3. Jacobson, K. (1983) Lateral diffusion in membranes. *Cell Motil.* **3**, 367-73.
4. Gorter, E. & Grendel, F. (1925) On bimolecular layers of lipoids on the chromocytes of the blood. *J. Exp. Med.* **41**, 439-43.
5. Gorter, E. & Grendel, F. (1997) On biomolecular layers of lipoids on the chromocytes of the blood (Reprinted from Proceedings of the Koninklijke Nederlandse Akademie van Wetenschappen, vol. 29, p. 314-317, 1926). *Proc. K. Ned. Akad. Wet.* **100**, 118-21.
6. Epand, R.M. (1998) Lipid polymorphism and protein-lipid interactions. *Biochim. Biophys. Acta-Rev. Biomembr.* **1376**, 353-68.
7. de Kruijff, B. (1997) Lipid polymorphism and biomembrane function. *Curr. Opin. Chem. Biol.* **1**, 564-9.
8. de Kruijff, B. (1997) Biomembranes. Lipids beyond the bilayer. *Nature* **386**, 129-30.
9. Deamer, D.W. & Bramhall, J. (1986) Permeability of lipid bilayers to water and ionic solutes. *Chem. Phys. Lipids* **40**, 167-88.
10. Deamer, D.W. (1987) Proton permeation of lipid bilayers. *J. Bioenerg. Biomembr.* **19**, 457-79.
11. Bloom, M., Evans, E. & Mouritsen, O.G. (1991) Physical-Properties of the Fluid Lipid-Bilayer Component of Cell-Membranes - a Perspective. *Q. Rev. Biophys.* **24**, 293-397.
12. Lieb, W.R. & Stein, W.D. (1986) Non-Stokesian nature of transverse diffusion within human red cell membranes. *J. Membr. Biol.* **92**, 111-9.
13. Walter, A. & Gutknecht, J. (1986) Permeability of small nonelectrolytes through lipid bilayer membranes. *J. Membr. Biol.* **90**, 207-17.
14. Gennis, R.B. in *Biomembranes: Molecular Structure and Function.* Edited by C.R. Cantor, New York: Springer-Verlag; 1989.
15. Nagle, J.F. (1987) Theory of passive proton conductance in lipid bilayers. *J. Bioenerg. Biomembr.* **19**, 413-26.
16. Arkin, I.T. & Brunger, A.T. (1998) Statistical analysis of predicted transmembrane alpha-helices. *Biochim. Biophys. Acta* **1429**, 113-28.
17. Vigano, C., Manciu, L., Buyse, F., Goormaghtigh, E. & Ruysschaert, J.M. (2000) Attenuated total reflection IR spectroscopy as a tool to investigate the structure, orientation and tertiary structure changes in peptides and membrane proteins. *Biopolymers* **55**, 373-80.

18. Cross, T.A., Tian, F., Cotten, M., Wang, J., Kovacs, F. & Fu, R. (1999) Correlations of structure, dynamics and function in the gramicidin channel by solid-state NMR spectroscopy. *Novartis Found Symp.* **225**, 4-16.

19. Fu, R. & Cross, T.A. (1999) Solid-state nuclear magnetic resonance investigation of protein and polypeptide structure. *Annu. Rev. Biophys. Biomol. Struct.* **28**, 235-68.

20. Opella, S.J., Ma, C. & Marassi, F.M. (2001) Nuclear magnetic resonance of membrane-associated peptides and proteins. *Methods Enzymol.* **339**, 285-313.

21. Bechinger, B. (2000) Understanding peptide interactions with the lipid bilayer: a guide to membrane protein engineering. *Curr. Opin. Chem. Biol.* **4**, 639-44.

22. van der Wel, P.C.A., Strandberg, E., Killian, J.A. & Koeppe, I., R.E. (2002) Geometry and Intrinsic Tilt of a Tryptophan-Anchored Transmembrane alpha-Helix Determined by (2)H NMR. *Biophys. J.* **83**, 1479-88.

23. Saibil, H.R. (2000) Conformational changes studied by cryo-electron microscopy. *Nat. Struct. Biol.* **7**, 711-4.

24. Arora, A. & Tamm, L.K. (2001) Biophysical approaches to membrane protein structure determination. *Curr. Opin. Struct. Biol.* **11**, 540-7.

25. Nollert, P., Navarro, J. & Landau, E.M. (2002) Crystallization of membrane proteins *in cubo. Methods Enzymol.* **343**, 183-99.

26. Berman, H.M., Westbrook, J., Feng, Z., Gilliland, G., Bhat, T.N., Weissig, H., Shindyalov, I.N. & Bourne, P.E. (2000) The Protein Data Bank. *Nucleic Acids Res.* **28**, 235-42.

27. Kovari, L.C., Momany, C. & Rossmann, M.G. (1995) The use of antibody fragments for crystallization and structure determinations. *Structure* **3**, 1291-3.

28. Landau, E.M. & Rosenbusch, J.P. (1996) Lipidic cubic phases: a novel concept for the crystallization of membrane proteins. *Proc. Natl. Acad. Sci. U. S. A.* **93**, 14532-5.

29. Wand, A.J., Ehrhardt, M.R. & Flynn, P.F. (1998) High-resolution NMR of encapsulated proteins dissolved in low-viscosity fluids. *Proc. Natl. Acad. Sci. U. S. A.* **95**, 15299-302.

30. Babu, C.R., Flynn, P.F. & Wand, A.J. (2001) Validation of protein structure from preparations of encapsulated proteins dissolved in low viscosity fluids. *J. Am. Chem. Soc.* **123**, 2691-2.

31. Watts, A. (1998) Solid-state NMR approaches for studying the interaction of peptides and proteins with membranes. *Biochim. Biophys. Acta* **1376**, 297-318.

32. Warschawski, D.E., Traikia, M., Devaux, P.F. & Bodenhausen, G. (1998) Solid-state NMR for the study of membrane systems: the use of anisotropic interactions. *Biochimie* **80**, 437-50.

33. Henderson, R. & Unwin, P.N. (1975) Three-dimensional model of purple membrane obtained by electron microscopy. *Nature* **257**, 28-32.

34. Henderson, R., Baldwin, J.M., Ceska, T.A., Zemlin, F., Beckmann, E. & Downing, K.H. (1990) Model for the structure of bacteriorhodopsin based on high-resolution electron cryo-microscopy. *J. Mol. Biol.* **213**, 899-929.

35. Michel, H. (1982) Three-dimensional crystals of a membrane protein complex. The photosynthetic reaction centre from *Rhodopseudomonas viridis. J. Mol. Biol.* **158**, 567-72.

36. Deisenhofer, J., Epp, O., Miki, K., Huber, R. & Michel, H. (1984) X-ray structure analysis of a membrane protein complex. Electron density map at 3 A resolution and a model of the chromophores of the photosynthetic reaction center from *Rhodopseudomonas viridis. J. Mol. Biol.* **180**, 385-98.

37. Deisenhofer, J., Epp, O., Miki, K., Huber, R. & Michel, H. (1985) *Nature* **318**, 618-24.

38. Koepke, J., Hu, X.C., Muenke, C., Schulten, K. & Michel, H. (1996) The crystal structure of the light-harvesting complex II (B800- 850) from *Rhodospirillum molischianum. Structure* **4**, 581-97.

39. McDermott, G., Prince, S.M., Freer, A.A., Hawthornthwaitelawless, A.M., Papiz, M.Z., Cogdell, R.J. & Isaacs, N.W. (1995) Crystal-Structure of an Integral Membrane Light-Harvesting Complex from Photosynthetic Bacteria. *Nature* **374**, 517-21.

40. Kuhlbrandt, W. & Wang, D.N. (1991) 3-Dimensional Structure of Plant Light-Harvesting Complex Determined by Electron Crystallography. *Nature* **350**, 130-4.

41. Kuhlbrandt, W., Wang, D.N. & Fujiyoshi, Y. (1994) Atomic Model of Plant Light-Harvesting Complex by Electron Crystallography. *Nature* **367**, 614-21.

42. Dutzler, R., Campbell, E.B., Cadene, M., Chait, B.T. & MacKinnon, R. (2002) X-ray structure of a ClC chloride channel at 3.0 A reveals the molecular basis of anion selectivity. *Nature* **415**, 287-94.

43. Toyoshima, C., Nakasako, M., Nomura, H. & Ogawa, H. (2000) Crystal structure of the calcium pump of sarcoplasmic reticulum at 2.6 A resolution. *Nature* **405**, 647-55.

44. Weiss, M.S., Abele, U., Weckesser, J., Welte, W., Schiltz, E. & Schulz, G.E. (1991) Molecular Architecture and Electrostatic Properties of a Bacterial Porin. *Science* **254**, 1627-30.

45. Doyle, D.A., Cabral, J.M., Pfuetzner, R.A., Kuo, A.L., Gulbis, J.M., Cohen, S.L., Chait, B.T. & Mackinnon, R. (1998) The Structure of the Potassium Channel   Molecular Basis of K+ Conduction and Selectivity. *Science* **280**, 69-77.

46. MacKinnon, R., Cohen, S.L., Kuo, A., Lee, A. & Chait, B.T. (1998) Structural conservation in prokaryotic and eukaryotic potassium channels. *Science* **280**, 106-9.

47. Mouritsen, O.G. & Bloom, M. (1984) Mattress model of lipid-protein interactions in membranes. *Biophys. J.* **46**, 141-53.

48. Engelman, D.M., Steitz, T.A. & Goldman, A. (1986) Identifying nonpolar transbilayer helices in amino acid sequences of membrane proteins. *Annu. Rev. Biophys. Biophys. Chem.* **15**, 321-53.

49. Killian, J.A. (1998) Hydrophobic mismatch between proteins and lipids in membranes. *Biochim. Biophys. Acta* **1376**, 401-15.

50. Cortes, D.M., Cuello, L.G. & Perozo, E. (2001) Molecular architecture of full-length KcsA: role of cytoplasmic domains in ion permeation and activation gating. *J. Gen. Physiol.* **117**, 165-80.

51. Kaback, H.R. (1986) Active transport in *Escherichia coli*: passage to permease. *Annu. Rev. Biophys. Biophys. Chem.* **15**, 279-319.

52. Lemmon, M.A. & Engelman, D.M. (1994) Specificity and Promiscuity in Membrane Helix Interactions. *Q. Rev. Biophys.* **27**, 157-218.

53. Ubarretxena-Belandia, I. & Engelman, D.M. (2001) Helical membrane proteins: diversity of functions in the context of simple architecture. *Curr. Opin. Struct. Biol.* **11**, 370-6.

54. Popot, J.L. & Engelman, D.M. (2000) Helical membrane protein folding, stability, and evolution. *Annu. Rev. Biochem.* **69**, 881-922.

55. Honig, B.H. & Hubbell, W.L. (1984) Stability of "salt bridges" in membrane proteins. *Proc. Natl. Acad. Sci. U. S. A.* **81**, 5412-6.

56. Engelman, D.M. & Zaccai, G. (1980) Bacteriorhodopsin is an inside-out protein. *Proc. Natl. Acad. Sci. U. S. A.* **77**, 5894-8.

57. Warshel, A., Russell, S.T. & Churg, A.K. (1984) Macroscopic models for studies of electrostatic interactions in proteins: limitations and applicability. *Proc. Natl. Acad. Sci. U. S. A.* **81**, 4785-9.

58. Kyte, J. & Doolittle, R.F. (1982) A simple method for displaying the hydropathic character of a protein. *J. Mol. Biol.* **157**, 105-32.

59. Piela, L., Nemethy, G. & Scheraga, H.A. (1987) Proline-induced constraints in alpha-helices. *Biopolymers* **26**, 1587-600.

60. Deber, C.M., Brandl, C.J., Deber, R.B., Hsu, L.C. & Young, X.K. (1986) Amino acid composition of the membrane and aqueous domains of integral membrane proteins. *Arch. Biochem. Biophys.* **251**, 68-76.

61. Brandl, C.J. & Deber, C.M. (1986) Hypothesis about the function of membrane-buried proline residues in transport proteins. *Proc. Natl. Acad. Sci. U. S. A.* **83**, 917-21.

62. Killian, J.A. & von Heijne, G. (2000) How proteins adapt to a membrane-water interface. *Trends Biochem. Sci.* **25**, 429-34.

63. Monne, M., Nilsson, I., Johansson, M., Elmhed, N. & von Heijne, G. (1998) Positively and negatively charged residues have different effects on the position in the membrane of a model transmembrane helix. *J. Mol. Biol.* **284**, 1177-83.

64. Braun, P. & von Heijne, G. (1999) The aromatic residues Trp and Phe have different effects on the positioning of a transmembrane helix in the microsomal membrane. *Biochemistry* **38**, 9778-82.

65. Ridder, A.N.J.A., Morein, S., Stam, J.G., Kuhn, A., de Kruijff, B. & Killian, J.A. (2000) Analysis of the role of interfacial tryptophan residues in controlling the topology of membrane proteins. *Biochemistry* **39**, 6521-8.

66. White, S.H. & Wimley, W.C. (1998) Hydrophobic interactions of peptides with membrane interfaces. *Biochim. Biophys. Acta* **1376**, 339-52.

67. Hristova, K., Wimley, W.C., Mishra, V.K., Anantharamiah, G.M., Segrest, J.P. & White, S.H. (1999) An amphipathic alpha-helix at a membrane interface: a structural study using a novel X-ray diffraction method. *J. Mol. Biol.* **290**, 99-117.

68. Schiffer, M., Chang, C.H. & Stevens, F.J. (1992) The functions of tryptophan residues in membrane proteins. *Protein Eng.* **5**, 213-4.

69. Reithmeier, R.A. (1995) Characterization and modeling of membrane proteins using sequence analysis. *Curr. Opin. Struct. Biol.* **5**, 491-500.

70. Deisenhofer, J. & Michel, H. (1989) Nobel lecture. The photosynthetic reaction centre from the purple bacterium *Rhodopseudomonas viridis*. *EMBO J.* **8**, 2149-70.

71. Cowan, S.W., Schirmer, T., Rummel, G., Steiert, M., Ghosh, R., Pauptit, R.A., Jansonius, J.N. & Rosenbusch, J.P. (1992) Crystal-Structures Explain Functional-Properties of 2 *Escherichia Coli* Porins. *Nature* **358**, 727-33.

72. Kovacs, F., Quine, J. & Cross, T.A. (1999) Validation of the single-stranded channel conformation of gramicidin A by solid-state NMR. *Proc. Natl. Acad. Sci. U. S. A.* **96**, 7910-5.

73. Ladokhin, A.S., Selsted, M.E. & White, S.H. (1997) Bilayer interactions of indolicidin, a small antimicrobial peptide rich in tryptophan, proline, and basic amino acids. *Biophys. J.* **72**, 794-805.

74. Wimley, W.C. & White, S.H. (1996) Experimentally determined hydrophobicity scale for proteins at membrane interfaces. *Nat. Struct. Biol.* **3**, 842-8.

75. de Planque, M.R.R., Kruijtzer, J.A.W., Liskamp, R.M.J., Marsh, D., Greathouse, D.V., Koeppe, R.E., II, de Kruijff, B. & Killian, J.A. (1999) Different membrane anchoring positions of tryptophan and lysine in synthetic transmembrane alpha-helical peptides. *J. Biol. Chem.* **274**, 20839-46.

76. Roderick, S.L., Chan, W.W., Agate, D.S., Olsen, L.R., Vetting, M.W., Rajashankar, K.R. & Cohen, D.E. (2002) Structure of human phosphatidylcholine transfer protein in complex with its ligand. *Nat. Struct. Biol.* **9**, 507-11.

77. von Heijne, G. (1989) Control of topology and mode of assembly of a polytopic membrane protein by positively charged residues. *Nature* **341**, 456-8.

78. Essen, L.O., Siegert, R., Lehmann, W.D. & Oesterhelt, D. (1998) Lipid patches in membrane protein oligomers: Crystal structure of the bacteriorhodopsin-lipid complex. *Proc. Natl. Acad. Sci. U. S. A.* **95**, 11673-8.

79. Urry, D.W. (1971) The gramicidin A transmembrane channel: a proposed pi(L,D) helix. *Proc. Natl. Acad. Sci. U. S. A.* **68**, 672-6.

80. Weinstein, S., Durkin, J.T., Veatch, W.R. & Blout, E.R. (1985) Conformation of the gramicidin A channel in phospholipid vesicles: a fluorine-19 nuclear magnetic resonance study. *Biochemistry* **24**, 4374-82.

81. Wallace, B.A. (1998) Recent Advances in the High Resolution Structures of Bacterial Channels: Gramicidin A. *J. Struct. Biol.* **121**, 123-41.

82. Bechinger, B. (1997) Structure and functions of channel-forming peptides: magainins, cecropins, melittin and alamethicin. *J. Membr. Biol.* **156**, 197-211.

83. Sansom, M.S. (1998) Models and simulations of ion channels and related membrane proteins. *Curr. Opin. Struct. Biol.* **8**, 237-44.

84. Ladokhin, A.S. & White, S.H. (1999) Folding of amphipathic alpha-helices on membranes: energetics of helix formation by melittin. *J. Mol. Biol.* **285**, 1363-9.

85. Dempsey, C.E. (1990) The actions of melittin on membranes. *Biochim. Biophys. Acta* **1031**, 143-61.

86. Morein, S., Killian, J.A. & Sperotto, M.M. (2002) Characterization of the thermotropic behavior and lateral organization of lipid-peptide mixtures by a combined experimental and theoretical approach: effects of hydrophobic mismatch and role of flanking residues. *Biophys. J.* **82**, 1405-17.

87. Morein, S., Koeppe, I.R., Lindblom, G., de Kruijff, B. & Killian, J.A. (2000) The effect of peptide/lipid hydrophobic mismatch on the phase behavior of model membranes mimicking the lipid composition in *Escherichia coli* membranes. *Biophys. J.* **78**, 2475-85.

88. Strandberg, E., Morein, S., Rijkers, D.T.S., Liskamp, R.M.J., van der Wel, P.C.A. & Killian, J.A. (2002) Lipid dependence of membrane anchoring properties and snorkeling behavior of aromatic and charged residues in transmembrane peptides. *Biochemistry* **41**, 7190-8.

89. de Planque, M.R.R., Greathouse, D.V., Koeppe, R.E., II, Schafer, H., Marsh, D. & Killian, J.A. (1998) Influence of lipid/peptide hydrophobic mismatch on the thickness of diacylphosphatidylcholine bilayers. A 2H NMR and ESR study using designed transmembrane alpha-helical peptides and gramicidin A. *Biochemistry* **37**, 9333-45.

90. de Planque, M.R., Goormaghtigh, E., Greathouse, D.V., Koeppe, R.E., 2nd, Kruijtzer, J.A., Liskamp, R.M., de Kruijff, B. & Killian, J.A. (2001) Sensitivity of single membrane-spanning alpha-helical peptides to hydrophobic mismatch with a lipid bilayer: effects on backbone structure, orientation, and extent of membrane incorporation. *Biochemistry* **40**, 5000-10.

91. Rinia, H.A., Boots, J.W., Rijkers, D.T., Kik, R.A., Snel, M.M., Demel, R.A., Killian, J.A., van der Eerden, J.P. & de Kruijff, B. (2002) Domain formation in phosphatidylcholine bilayers containing transmembrane peptides: specific effects of flanking residues. *Biochemistry* **41**, 2814-24.

92. Rinia, H.A., Kik, R.A., Demel, R.A., Snel, M.M.E., Killian, J.A., van der Eerden, J.P.J.M. & de Kruijff, B. (2000) Visualization of highly ordered striated domains induced by transmembrane peptides in supported phosphatidylcholine bilayers. *Biochemistry* **39**, 5852-8.

93. de Planque, M.R.R., Boots, J.W.P., Rijkers, D.T.S., Liskamp, R.M.J., Greathouse, D.V. & Killian, J.A. (2002) The Effects of Hydrophobic Mismatch between Phosphatidylcholine Bilayers and Transmembrane alpha-Helical Peptides Depend on the Nature of Interfacially Exposed Aromatic and Charged Residues. *Biochemistry* **41**, 8396-404.

94. Pare, C., Lafleur, M., Liu, F., Lewis, R.N. & McElhaney, R.N. (2001) Differential scanning calorimetry and (2)H nuclear magnetic resonance and Fourier transform infrared spectroscopy studies of the effects of transmembrane alpha-helical peptides on the organization of phosphatidylcholine bilayers. *Biochim. Biophys. Acta* **1511**, 60-73.

95. Zhang, Y.P., Lewis, R.N., Hodges, R.S. & McElhaney, R.N. (2001) Peptide models of the helical hydrophobic transmembrane segments of membrane proteins: interactions of acetyl-K2-(LA)12-K2-amide with phosphatidylethanolamine bilayer membranes. *Biochemistry* **40**, 474-82.

96. Zhang, Y.P., Lewis, R.N., Hodges, R.S. & McElhaney, R.N. (1995) Interaction of a peptide model of a hydrophobic transmembrane alpha-helical segment of a membrane protein with phosphatidylethanolamine bilayers: differential scanning calorimetric and Fourier transform infrared spectroscopic studies. *Biophys. J.* **68**, 847-57.

97. Zhang, Y.P., Lewis, R.N., Henry, G.D., Sykes, B.D., Hodges, R.S. & McElhaney, R.N. (1995) Peptide models of helical hydrophobic transmembrane segments of membrane proteins. 1. Studies of the conformation, intrabilayer orientation, and amide hydrogen exchangeability of Ac-K2-(LA)12-K2-amide. *Biochemistry* **34**, 2348-61.

98.   Harzer, U. & Bechinger, B. (2000) Alignment of lysine-anchored membrane peptides under conditions of hydrophobic mismatch: a CD, 15N and 31P solid-state NMR spectroscopy investigation. *Biochemistry* **39**, 13106-14.

99.   Bechinger, B. (2001) Membrane insertion and orientation of polyalanine peptides: a (15)N solid-state NMR spectroscopy investigation. *Biophys. J.* **81**, 2251-6.

100.   Liu, L.P. & Deber, C.M. (1998) Guidelines for membrane protein engineering derived from de novo designed model peptides. *Biopolymers* **47**, 41-62.

101.   Simmons, D.A. & Konermann, L. (2002) Characterization of transient protein folding intermediates during myoglobin reconstitution by time-resolved electrospray mass spectrometry with on-line isotopic pulse labeling. *Biochemistry* **41**, 1906-14.

102.   Barber, M., Bordoli, R.S., Sedgewick, R.D. & Tyler, A.N. (1981) Fast atom bombardment of solids: a new ion source for mass spectrometry. *J. Chem. Soc. - Chem. Comm.* **325**, 325-7.

103.   Barber, M., Bordoli, R.S., Sedgewick, R.D. & Tyler, A.N. (1981) Fast atom bombardment of solids as an ion source in mass spectroscopy. *Nature* **293**, 270-5.

104.   Sundqvist, B., Roepstorff, P., Fohlman, J., Hedin, A., Hakansson, P., Kamensky, I., Lindberg, M., Salehpour, M. & Sawe, G. (1984) Molecular weight determinations of proteins by californium plasma desorption mass spectrometry. *Science* **226**, 696-8.

105.   Williams, D.H., Bradley, C.V., Santikarn, S. & Bojesen, G. (1982) Fast-atom-bombardment mass spectrometry. A new technique for the determination of molecular weights and amino acid sequences of peptides. *Biochem. J.* **201**, 105-17.

106.   Mann, M., Hendrickson, R.C. & Pandey, A. (2001) Analysis of proteins and proteomes by mass spectrometry. *Annu. Rev. Biochem.* **70**, 437-73.

107.   Fenn, J.B., Mann, M., Meng, C.K., Wong, S.F. & Whitehouse, C.M. (1989) Electrospray ionization for mass spectrometry of large biomolecules. *Science* **246**, 64-71.

108.   Collette, C., Drahos, L., De Pauw, E. & Vekey, K. (1998) Comparison of the internal energy distributions of ions produced by different electrospray sources. *Rapid Commun. Mass Spectrom.* **12**, 1673-8.

109.   Collette, C. & De Pauw, E. (1998) Calibration of the internal energy distribution of ions produced by electrospray. *Rapid Commun. Mass Spectrom.* **12**, 165-70.

110.   Jones, J.L., Dongre, A.R., Somogyi, A. & Wysocki, V.H. (1994) Sequence Dependence of Peptide Fragmentation Efficiency Curves Determined by Electrospray-Ionization Surface-Induced Dissociation Mass-Spectrometry. *J. Am. Chem. Soc.* **116**, 8368-9.

111.   Loo, J.A. (2000) Electrospray ionization mass spectrometry: a technology for studying noncovalent macromolecular complexes. *Int. J. Mass Spectrom.* **200**, 175-86.

112.   Karas, M. & Hillenkamp, F. (1988) Laser desorption ionization of proteins with molecular masses exceeding 10,000 daltons. *Anal. Chem.* **60**, 2299-301.

113.   Karas, M. (1996) Matrix-assisted laser desorption ionization MS: a progress report. *Biochem. Soc. Trans.* **24**, 897-900.

114.   Rosinke, B., Strupat, K., Hillenkamp, F., Rosenbusch, J., Dencher, N., Kruger, U. & Galla, H.J. (1995) Matrix-Assisted Laser Desorption/Ionization Mass-Spectrometry (Maldi-Ms) of Membrane-Proteins and Noncovalent Complexes. *J. Mass Spectrom.* **30**, 1462-8.

115.   Cadene, M. & Chait, B.T. (2000) A robust, detergent-friendly method for mass spectrometric analysis of integral membrane proteins. *Anal. Chem.* **72**, 5655-8.

116.   Chernushevich, I.V., Loboda, A.V. & Thomson, B.A. (2001) An introduction to quadrupole-time-of-flight mass spectrometry. *J. Mass Spectrom.* **36**, 849-65.

117.   Roepstorff, P. & Fohlman, J. (1984) Proposal for a common nomenclature for sequence ions in mass spectra of peptides. *Biomed. Mass Spectrom.* **11**, 601.

118.   Hvidt, A. & Nielsen, S.O. (1966) Hydrogen exchange in proteins. *Adv. Protein Sci.* **21**, 287-386.

119. Englander, S.W., Sosnick, T.R., Englander, J.J. & Mayne, L. (1996) Mechanisms and Uses of Hydrogen Exchange. *Curr. Opin. Struct. Biol.* **6**, 18-23.

120. Englander, S.W. & Kallenbach, N.R. (1984) *Q. Rev. Biophys.* **19**, 521-655.

121. Clarke, J. & Itzhaki, L.S. (1998) Hydrogen exchange and protein folding. *Curr. Opin. Struct. Biol.* **8**, 112-8.

122. Linderstrøm-Lang, K.U. in *Deuterium exchange and protein structure.* Edited by A. Neuberger, London: Methuen; 1958.

123. Katta, V. & Chait, B.T. (1991) Conformational changes in proteins probed by hydrogen-exchange electrospray-ionization mass spectrometry. *Rapid Commun. Mass. Spectrom.* **5**, 214-7.

124. Chen, J., Walter, S., Horwich, A.L. & Smith, D.L. (2001) Folding of malate dehydrogenase inside the GroEL-GroES cavity. *Nat. Struct. Biol.* **8**, 721-8.

125. Deng, Y.Z. & Smith, D.L. (1999) Rate and equilibrium constants for protein unfolding and refolding determined by hydrogen exchange-mass spectrometry. *Anal. Biochem.* **276**, 150-60.

126. Maier, C.S., Schimerlik, M.I. & Deinzer, M.L. (1999) Thermal denaturation of *Escherichia coli* thioredoxin studied by hydrogen/deuterium exchange and electrospray ionization mass spectrometry: monitoring a two-state protein unfolding transition. *Biochemistry* **38**, 1136-43.

127. Anderegg, R.J., Wagner, D.S., Stevenson, C.L. & Borchardt, R.T. (1994) The Mass Spectrometry of Helical Unfolding in Peptides. *J. Am. Soc. Mass Spectrom.* **5**, 425-33.

128. Robinson, C.V., Gross, M., Eyles, S.J., Ewbank, J.J., Mayhew, M., Hartl, F.U., Dobson, C.M. & Radford, S.E. (1994) Conformation of GroEL-bound alpha-lactalbumin probed by mass spectrometry. *Nature* **372**, 646-51.

129. Miranker, A., Robinson, C.V., Radford, S.E., Aplin, R.T. & Dobson, C.M. (1993) Detection of transient protein folding populations by mass spectrometry. *Science* **262**, 896-900.

130. Tuma, R., Coward, L.U., Kirk, M.C., Barnes, S. & Prevelige, P.E., Jr. (2001) Hydrogen-deuterium exchange as a probe of folding and assembly in viral capsids. *J. Mol. Biol.* **306**, 389-96.

131. Eyles, S.J., Speir, J.P., Kruppa, G.H., Gierasch, L.M. & Kaltashov, I.A. (2000) Protein conformational stability probed by Fourier transform ion cyclotron resonance mass spectrometry. *J. Am. Chem. Soc.* **122**, 495-500.

132. Deng, Y. & Smith, D.L. (1999) Hydrogen exchange demonstrates three domains in aldolase unfold sequentially. *J. Mol. Biol.* **294**, 247-58.

133. Wang, L., Lane, L.C. & Smith, D.L. (2001) Detecting structural changes in viral capsids by hydrogen exchange and mass spectrometry. *Protein Sci.* **10**, 1234-43.

134. Mandell, J.G., Baerga-Ortiz, A., Akashi, S., Takio, K. & Komives, E.A. (2001) Solvent accessibility of the thrombin-thrombomodulin interface. *J. Mol. Biol.* **306**, 575-89.

135. Gonzalez de Peredo, A., Saint-Pierre, C., Latour, J.M., Michaud-Soret, I. & Forest, E. (2001) Conformational changes of the ferric uptake regulation protein upon metal activation and DNA binding; first evidence of structural homologies with the diphtheria toxin repressor. *J. Mol. Biol.* **310**, 83-91.

136. Smith, D.L., Deng, Y. & Zhang, Z. (1997) Probing the non-covalent structure of proteins by amide hydrogen exchange and mass spectrometry. *J. Mass Spectrom.* **32**, 135-46.

137. Anderegg, R.J. & Wagner, D.S. (1995) Mass spectrometric characterization of a protein ligand interaction. *J. Am. Chem. Soc.* **117**, 1374-7.

138. Wang, F., Blanchard, J.S. & Tang, X.J. (1997) Hydrogen exchange/electrospray ionization mass spectrometry studies of substrate and inhibitor binding and conformational changes of *Escherichia coli* dihydrodipicolinate reductase. *Biochemistry* **36**, 3755-9.

139. Kraus, M., Janek, K., Bienert, M. & Krause, E. (2000) Characterization of intermolecular beta-sheet peptides by mass spectrometry and hydrogen isotope exchange. *Rapid Commun. Mass Spectrom.* **14**, 1094-104.

140. Kheterpal, I., Zhou, S., Cook, K.D. & Wetzel, R. (2000) Abeta amyloid fibrils possess a core structure highly resistant to hydrogen exchange. *Proc. Natl. Acad. Sci. U. S. A.* **97**, 13597-601.

141.   Tito, P., Nettleton, E.J. & Robinson, C.V. (2000) Dissecting the hydrogen exchange properties of insulin under amyloid fibril forming conditions: a site-specific investigation by mass spectrometry. *J. Mol. Biol.* **303**, 267-78.

142.   Engen, J.R. & Smith, D.L. (2001) Investigating protein structure and dynamics by hydrogen exchange MS. *Anal. Chem.* **73**, 256A-65A.

143.   Miranker, A., Robinson, C.V., Radford, S.E. & Dobson, C.M. (1996) Investigation of protein folding by mass spectrometry. *FASEB J.* **10**, 93-101.

144.   Ehring, H. (1999) Hydrogen exchange/electrospray ionization mass spectrometry studies of structural features of proteins and protein/protein interactions. *Anal. Biochem.* **267**, 252-9.

145.   Engen, J.R. & Smith, D.L. (2000) Investigating the higher order structure of proteins. Hydrogen exchange, proteolytic fragmentation, and mass spectrometry. *Methods Mol. Biol.* **146**, 95-112.

146.   Villanueva, J., Canals, F., Villegas, V., Querol, E. & Aviles, F.X. (2000) Hydrogen exchange monitored by MALDI-TOF mass spectrometry for rapid characterization of the stability and conformation of proteins. *FEBS Lett.* **472**, 27-33.

147.   Andersen, M.D., Shaffer, J., Jennings, P.A. & Adams, J.A. (2001) Structural characterization of protein kinase A as a function of nucleotide binding. Hydrogen-deuterium exchange studies using matrix-assisted laser desorption ionization-time of flight mass spectrometry detection. *J. Biol. Chem.* **276**, 14204-11.

148.   Powell, K.D. & Fitzgerald, M.C. (2001) Measurements of protein stability by H/D exchange and matrix-assisted laser desorption/ionization mass spectrometry using picomoles of material. *Anal. Chem.* **73**, 3300-4.

149.   Mandell, J.G., Falick, A.M. & Komives, E.A. (1998) Measurement of amide hydrogen exchange by MALDI-TOF mass spectrometry. *Anal. Chem.* **70**, 3987-95.

150.   Mandell, J.G., Falick, A.M. & Komives, E.A. (1998) Identification of protein-protein interfaces by decreased amide proton solvent accessibility. *Proc. Natl. Acad. Sci. U. S. A.* **95**, 14705-10.

151.   Powell, K.D., Wales, T.E. & Fitzgerald, M.C. (2002) Thermodynamic stability measurements on multimeric proteins using a new H/D exchange- and matrix-assisted laser desorption/ionization (MALDI) mass spectrometry-based method. *Protein Sci.* **11**, 841-51.

152.   Akashi, S. & Takio, K. (2000) Characterization of the interface structure of enzyme-inhibitor complex by using hydrogen-deuterium exchange and electrospray ionization Fourier transform ion cyclotron resonance mass spectrometry. *Protein Sci.* **9**, 2497-505.

153.   Deng, Y.Z., Pan, H. & Smith, D.L. (1999) Selective Isotope Labeling Demonstrates That Hydrogen Exchange at Individual Peptide Amide Linkages Can Be Determined by Collision Induced Dissociation Mass Spectrometry. *J. Am. Chem. Soc.* **121**, 1966-7.

154.   Akashi, S., Naito, Y. & Takio, K. (1999) Observation of hydrogen-deuterium exchange of ubiquitin by direct analysis of electrospray capillary-skimmer dissociation with courier transform ion cyclotron resonance mass spectrometry. *Anal. Chem.* **71**, 4974-80.

155.   Kim, M.Y., Maier, C.S., Reed, D.J. & Deinzer, M.L. (2001) Site-Specific Amide Hydrogen/Deuterium Exchange in *E. coli* Thioredoxins Measured by Electrospray Ionization Mass Spectrometry. *J. Am. Chem. Soc.* **123**, 9860-6.

156.   Kaltashov, I.A. & Eyles, S.J. (2002) Crossing the phase boundary to study protein dynamics and function: combination of amide hydrogen exchange in solution and ion fragmentation in the gas phase. *J. Mass Spectrom.* **37**, 557-65.

157.   McLafferty, F.W., Guan, Z.Q., Haupts, U., Wood, T.D. & Kelleher, N.L. (1998) Gaseous Conformational Structures of Cytochrome *C*. *J. Am. Chem. Soc.* **120**, 4732-40.

158.   Harrison, A.G. & Yalcin, T. (1997) Proton mobility in protonated amino acids and peptides. *Int. J. Mass Spectrom.* **165**, 339-47.

159. Johnson, R.S., Krylov, D. & Walsh, K.A. (1995) Proton Mobility Within Electrosprayed Peptide Ions. *J. Mass Spectrom.* **30**, 386-7.

160. Marx, M.K., Mayer-Posner, F., Soulimane, T. & Buse, G. (1998) Matrix-assisted laser desorption/ionization mass spectrometry analysis and thiol-group determination of isoforms of bovine cytochrome *c* oxidase, a hydrophobic multisubunit membrane protein. *Anal. Biochem.* **256**, 192-9.

161. Gharahdaghi, F., Kirchner, M., Fernandez, J. & Mische, S.M. (1996) Peptide-mass profiles of polyvinylidene difluoride-bound proteins by matrix-assisted laser desorption/ionization time-of-flight mass spectrometry in the presence of nonionic detergents. *Anal. Biochem.* **233**, 94-9.

162. Bornsen, K.O., Gass, M.A., Bruin, G.J., von Adrichem, J.H., Biro, M.C., Kresbach, G.M. & Ehrat, M. (1997) Influence of solvents and detergents on matrix-assisted laser desorption/ionization mass spectrometry measurements of proteins and oligonucleotides. *Rapid Commun. Mass Spectrom.* **11**, 603-9.

163. Amado, F.M.L., Santana-Marques, M.G., Ferrer-Correia, A.J. & Tomer, K.B. (1997) Analysis of Peptide and Protein Samples Containing Surfactants by MALDI-MS. *Anal. Chem.* **69**, 1102-6.

164. Breaux, G.A., Green-Church, K.B., France, A. & Limbach, P.A. (2000) Surfactant-aided, matrix-assisted laser desorption/ionization mass spectrometry of hydrophobic and hydrophilic peptides. *Anal. Chem.* **72**, 1169-74.

165. Bouchard, M., Benjamin, D.R., Tito, P., Robinson, C.V. & Dobson, C.M. (2000) Solvent effects on the conformation of the transmembrane peptide gramicidin A: Insights from electrospray ionization mass spectrometry. *Biophys. J.* **78**, 1010-7.

166. Barnidge, D.R., Dratz, E.A., Jesaitis, A.J. & Sunner, J. (1999) Extraction method for analysis of detergent-solubilized bacteriorhodopsin and hydrophobic peptides by electrospray ionization mass spectrometry. *Anal. Biochem.* **269**, 1-9.

167. Le Coutre, J., Whitelegge, J.P., Gross, A., Turk, E., Wright, E.M., Kaback, H.R. & Faull, K.F. (2000) Proteomics on full-length membrane proteins using mass spectrometry. *Biochemistry* **39**, 4237-42.

168. Whitelegge, J.P., Gundersen, C.B. & Faull, K.F. (1998) Electrospray-ionization mass spectrometry of intact intrinsic membrane proteins. *Protein Sci.* **7**, 1423-30.

169. Whitelegge, J.P., le Coutre, J., Lee, J.C., Engel, C.K., Prive, G.G., Faull, K.F. & Kaback, H.R. (1999) Toward the bilayer proteome, electrospray ionization-mass spectrometry of large, intact transmembrane proteins. *Proc. Natl. Acad. Sci. U. S. A.* **96**, 10695-8.

170. Santoni, V., Molloy, M. & Rabilloud, T. (2000) Membrane proteins and proteomics: un amour impossible? *Electrophoresis* **21**, 1054-70.

171. Vu-Hai, M.T., Huet, J.C., Echasserieau, K., Bidart, J.M., Floiras, C., Pernollet, J.C. & Milgrom, E. (2000) Posttranslational modifications of the lutropin receptor: mass spectrometric analysis. *Biochemistry* **39**, 5509-17.

172. Tsatsos, P.H., Reynolds, K., Nickels, E.F., He, D.Y., Yu, C.A. & Gennis, R.B. (1998) Using matrix-assisted laser desorption ionization mass spectrometry to map the quinol binding site of cytochrome bo3 from *Escherichia coli. Biochemistry* **37**, 9884-8.

173. Michel, H., Griffin, P.R., Shabanowitz, J., Hunt, D.F. & Bennett, J. (1991) Tandem mass spectrometry identifies sites of three post-translational modifications of spinach light-harvesting chlorophyll protein II. Proteolytic cleavage, acetylation, and phosphorylation. *J. Biol. Chem.* **266**, 17584-91.

174. Simpson, R.J., Connolly, L.M., Eddes, J.S., Pereira, J.J., Moritz, R.L. & Reid, G.E. (2000) Proteomic analysis of the human colon carcinoma cell line (LIM 1215): Development of a membrane protein database. *Electrophoresis* **21**, 1707-32.

175. Friso, G. & Wikstrom, L. (1999) Analysis of proteins from membrane-enriched cerebellar preparations by two-dimensional gel electrophoresis and mass spectrometry. *Electrophoresis* **20**, 917-27.

176. Shevchenko, A., Loboda, A., Ens, W. & Standing, K.G. (2000) MALDI quadrupole time-of-flight mass spectrometry: A powerful tool for proteomic research. *Anal. Chem.* **72**, 2132-41.

177. Mundt, A.A., Cuillel, M., Forest, E. & Dupont, Y. (2001) Peptide mapping and disulfide bond analysis of the cytoplasmic region of an intrinsic membrane protein by mass spectrometry. *Anal. Biochem.* **299**, 147-57.

178. Hellman, U., Wernstedt, C., Gonez, J. & Heldin, C.H. (1995) Improvement of an "In-Gel" digestion procedure for the micropreparation of internal protein fragments for amino acid sequencing. *Anal. Biochem.* **224**, 451-5.

179. van Montfort, B.A., Canas, B., Duurkens, R., Godovac-Zimmermann, J. & Robillard, G.T. (2002) Improved in-gel approaches to generate peptide maps of integral membrane proteins with matrix-assisted laser desorption/ionization time-of-flight mass spectrometry. *J. Mass Spectrom.* **37**, 322-30.

180. Soskic, V., Nyakatura, E., Roos, M., Muller-Esterl, W. & Godovac-Zimmermann, J. (1999) Correlations in palmitoylation and multiple phosphorylation of rat bradykinin B2 receptor in Chinese hamster ovary cells. *J. Biol. Chem.* **274**, 8539-45.

181. Roos, M., Soskic, V., Poznanovic, S. & Godovac-Zimmermann, J. (1998) Post-translational modifications of endothelin receptor B from bovine lungs analyzed by mass spectrometry. *J. Biol. Chem.* **273**, 924-31.

182. Gelasco, A., Crouch, R.K. & Knapp, D.R. (2000) Intrahelical arrangement in the integral membrane protein rhodopsin investigated by site-specific chemical cleavage and mass spectrometry. *Biochemistry* **39**, 4907-14.

183. Leite, J.F., Amoscato, A.A. & Cascio, M. (2000) Coupled proteolytic and mass spectrometry studies indicate a novel topology for the glycine receptor. *J. Biol. Chem.* **275**, 13683-9.

CHAPTER 2

Electrospray Ionization Mass Spectrometry as a Novel Tool to Analyze Hydrogen/Deuterium Exchange Kinetics of Transmembrane Peptides in Lipid Bilayers

Jeroen A.A. Demmers [1,2], Johan Haverkamp [2], Albert J.R. Heck [2], Roger E. Koeppe II [3] & J. Antoinette Killian [1]

[1] Department of Biochemistry of Membranes, Center for Biomembranes and Lipid Enzymology, Institute of Biomembranes, Utrecht University, Padualaan 8, 3584 CH Utrecht, The Netherlands
[2] Department of Biomolecular Mass Spectrometry, Bijvoet Center for Biomolecular Research and Utrecht Institute for Pharmaceutical Sciences, Utrecht University, Sorbonnelaan 16, 3584 CA Utrecht, The Netherlands
[3] Department of Chemistry and Biochemistry, University of Arkansas, Fayetteville, Arkansas 72701, USA

Abstract

A novel method is described to study the precise positioning of transmembrane peptides in a phospholipid bilayer combining hydrogen/deuterium (H/D) exchange and nano-electrospray ionization mass spectrometry (nano-ESI-MS). The method was tested by using model systems consisting of designed α-helical transmembrane peptides (WALP16 and WALP16(+10)) incorporated in large unilamellar vesicles of DMPC. Both peptides consist of an alternating leucine/alanine hydrophobic core sequence flanked by tryptophan residues as interfacial anchor residues. In the case of WALP16(+10), this sequence is extended at both ends by five-amino acid glycine/alanine tails extending into the aqueous phase surrounding the bilayer. H/D exchange of labile hydrogens in these peptides was monitored in time after dilution of the vesicles in buffered deuterium oxide. It was found that the peptides can be measured by direct introduction of the proteoliposome suspension into the mass spectrometer. Several distinct H/D exchange rates were observed (corresponding to half-life values varying from ≤ 2 to $\approx 2 \times 10^4$ min). Fast exchange rates were assigned to the water-exposed tails of WALP16(+10). For both WALP16 and WALP16(+10), intermediate exchange rates were assigned to the residues close to the membrane/water interface, and the slow exchange rates to the membrane-embedded hydrophobic core. These assignments were confirmed by results from collision induced dissociation tandem mass spectrometry experiments, which allowed analysis of exchange of individual peptide amide linkages. This proteoliposome nano-ESI-MS technique is shown to be an extremely sensitive and powerful tool for revealing site-specific information on peptide-membrane interactions.

Introduction

Membrane proteins are biologically important because they are responsible for crucial functions in the cell, such as signal transduction, hormone reception, and transport of proteins, nutrients, and ions across cell membranes. The way in which membrane proteins are embedded in the lipid bilayer and interact with surrounding lipids is of fundamental significance for membrane protein structure and function. Insight into the exact positioning of the transmembrane segment(s) of such proteins with respect to the membrane-water interface and their structural and dynamic properties is hereby essential.

The analysis of hydrogen/deuterium (H/D) exchange kinetics of protein backbone amide protons has long been used as a source of structural and dynamic information [1-3]. The H/D exchange process of amide hydrogens with solvent deuteriums can take place only when these hydrogens are exposed to the solvent. For a membrane-incorporated peptide, the rate of H/D exchange is influenced by the extent of solvent permeation to the site of exchange in different regions of the bilayer, as well as by the participation of amide hydrogens in the hydrogen-bonding network that defines secondary and tertiary structure [2].

Until now, H/D exchange in membrane peptides and proteins has mostly been studied using FTIR and NMR spectroscopic techniques. Although both techniques have given useful insight into the structure and dynamics of peptides in membranes, both exhibit some

disadvantages. FTIR spectroscopy can determine the total amount of deuterium uptake but does not give information about specific sites of deuterium exchange [4-6]. Usually, such studies on membrane peptides require bilayers that are not hydrated in excess water, and the use of buffers is not trivial. In contrast, high-resolution NMR techniques can determine exchange rates of specific amide hydrogens. However, such NMR studies typically use micellar systems, which are not ideal alternatives for membrane systems. Moreover, relatively large amounts of material, long measuring times, and a low pH are required. The latter may not be physiologically relevant. Nevertheless, H/D exchange rates have been measured for individual assigned amide protons of various membrane associated peptides and proteins in detergent solutions [6-9]. Another NMR approach makes use of trapping techniques and subsequent transfer of the peptide from an aqueous membrane environment to isotropic media [10]. Also, solid-state NMR techniques have been used to study H/D exchange kinetics of individual amide backbone hydrogens of a helical transmembrane peptide [11]. However, the limited sensitivity is a disadvantage of all NMR methods.

In recent years, several studies have been reported in which mass spectrometry (MS) was used to investigate H/D exchange behavior of water-soluble peptides and proteins [12-16]. From the observed H/D exchange patterns, information can be extracted on protein folding [13,15] and non-covalent complex formation [14]. Information on the exchange of hydrogens at individual peptide amide linkages may be obtained by MS using limited proteolysis [16] or collision induced dissociation MS (CID MS), as has been shown for the α-helical peptide melittin [17] as well as for several peptic fragments of cytochrome *c* [18]. The results of these latter studies indicate that H/D exchange measured by CID MS may in some cases be an appropriate tool to investigate the amount of secondary structure in a peptide.

In this study, we apply nano-electrospray ionization MS (nano-ESI-MS) as a tool to measure H/D exchange in water-insoluble transmembrane peptides. In this approach, the peptides are reconstituted in fully hydrated dispersed phospholipid bilayers, which are then directly introduced into the mass spectrometer. We tested this technique by using well-defined model transmembrane peptides, WALP16 and WALP16(+10) (Table 1). The WALP16 peptide consists of an alternating Leu/Ala hydrophobic core sequence flanked by tryptophan residues, which are found in many membrane proteins near the membrane/water interfacial region and are assumed to interact in a specific way with the membrane interface [19-21]. Moreover, it forms a transmembrane α-helix in phosphatidylcholine bilayers [20] and therefore it may resemble a consensus transmembrane α-helical segment of intrinsic membrane proteins. The length of WALP16 (22.5 Å, [22]) is similar to the hydrophobic thickness of a 1,2-dimyristoyl-*sn*-glycero-3-phosphocholine (DMPC) bilayer in the fluid state (≈23 Å, [23]), which implies that in this lipid system, WALP16 is completely embedded in the hydrophobic region of the bilayer. The WALP16(+10) peptide has alternating Gly/Ala extensions at both termini of WALP16. These tails were designed to have sufficient hydrophilicity to penetrate into the water phase surrounding the bilayer and to adopt no secondary structure because of the α-helix breaking Gly

residues. Since the tail hydrogens therefore should be accessible to the aqueous phase and not involved in hydrogen bonding they are expected to exchange much more rapidly than those in the hydrophobic core of the peptide. The membrane incorporation of both peptides is schematically depicted in Figure 1.

The results of the experiments described here show that our proteoliposome nano-ESI-MS technique may be an extremely powerful and sensitive tool to analyze the exact positioning of membrane peptides in a lipid bilayer and to reveal site-specific information on peptide-membrane interactions. We believe that this method could be equally well applied to study the positioning of larger transmembrane proteins in model or biological membranes.
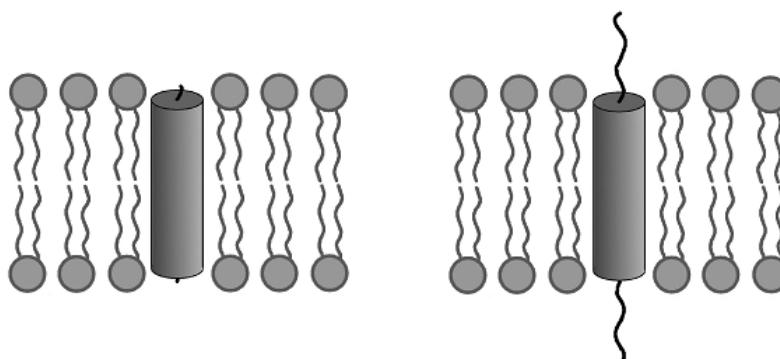

Figure 1 − Schematic representation of the incorporation of (A) WALP16 and (B) WALP16(+10) in a DMPC bilayer. The cylinder implies the α-helical transmembrane region; the Gly/Ala extensions of WALP16(+10) are denoted by randomly ordered strings.

Table I − Amino acid sequences of the peptides used, their molecular masses, and their numbers of exchangeable hydrogen atoms.

Peptide	Amino acid sequence	Monoisotopic molecular mass (amu)	No. of exch. hydrogens
WALP16	[a]`ac-GWWLALALALALAWWA-etn`[b]	1,896.05	22
WALP16(+10)	`ac-GAGAGAWWLALALALALAWWAGAGAG-etn`	2,536.35	32

[a]ac, acetyl
[b]etn, ethanolamine

Materials and methods

Chemicals - Trifluoroacetic acid (TFA) and 1,4-dioxane (p.A.) were obtained from Merck (Darmstadt, Germany) 2,2,2-trifluoroethanol (TFE) from Sigma (St. Louis, MO). Deuterium oxide (>99.9 % D) was obtained from Aldrich Chemical Company, Inc. (Milwaukee, WI, USA). D_2O was stored under nitrogen at 4 °C. Acetonitrile (HPLC gradient grade) was obtained from Biosolve Ltd. (Valkenswaard, The Netherlands). Sodium iodide was from OPG Farma Company (Utrecht, The Netherlands). Ammonium acetate was from Fluka (Switzerland). The phospholipid 1,2-dimyristoyl-*sn*-glycero-3-phosphocholine (DMPC) was obtained from Avanti

Polar Lipids Inc. (Birmingham, AL). The peptide WALP16 was synthesized as described by Killian *et al.* [20]. WALP16(+10) was synthesized from Fmoc-Gly Sasrin resin and cleaved with 10% ethanolamine in dichloromethane at 24°C for 48 hours. Details will be published elsewhere (D.V. Greathouse and R. Goforth, manuscript in preparation). The peptides were tested for purity by electrospray mass spectrometry and found to be essentially pure.

Procedure for peptide incorporation into phospholipid vesicles - Peptides were first dissolved in a small volume of TFA (10 µl per mg of peptide) and dried under a nitrogen stream. To remove residual TFA, the peptides were subsequently dissolved in TFE (1 mg/ml) followed by evaporation of the solvent in a rotavapor. Peptides were then again dissolved in TFE to a final concentration of 1 mg/ml. Dry mixed films of WALP16 or WALP16(+10) and DMPC (peptide to lipid ratio1:25) were prepared as follows. Peptide solutions in TFE (1 ml; 0.46 mM) were added to DMPC solutions in methanol (1 ml; 12 mM) and vigorously vortexed. The solvent was removed by evaporation in a rotavapor. The mixed films were then dried for 24 hr under vacuum. The films were hydrated at about 40ºC, well above the gel-to-liquid crystalline phase transition temperature of the phospholipid (24°C [24]) in 0.5 ml 10 mM ammonium acetate buffer (pH 7.5). This results in the formation of extended bilayers, as was confirmed by ^{31}P NMR measurements, performed as described previously [20]. Large unilamellar vesicles (LUVETs) were prepared by extrusion through a 400-nm filter at room temperature and kept at 4°C until use.

Before the start of H/D exchange, LUVETs were preincubated at 30°C for at least 30 min. LUVETs suspensions were then 50 times diluted in deuterated ammonium acetate buffer at 30°C (10 mM, pH 7.5), containing approximately 0.1 mM NaI. At selected time points, 2 µl of this diluted DMPC/peptide suspension was transferred into a gold-coated glass capillary and the measurement was started as quickly as possible. The deadtime between dilution and measurement was at a minimum 1.5 min.

Mass spectrometry measurements - MS measurements were performed on a quadrupole time-of-flight (Q-Tof) instrument (Micromass Ltd., Manchester, UK) operating in positive ion mode, equipped with a Z-spray nano-electrospray source. Nano-electrospray needles were made from borosilicate glass capillaries (Kwik-Fil, World Precision Instruments Inc., Sarasota, FL) on a P-97 puller (Sutter Instrument Co., Novato, CA). A special procedure was developed to pull needles with a relatively large tip opening (several tens of µm), which resulted in higher flow rates than typical for nano-ESI-MS. The needles were coated with a thin gold layer (approx. 500 Å) using an Edwards Scancoat six Pirani 501 (at 40 mV, 1 kV, for 200 sec). The nano-ES needle was positioned approx. 5 mm before the orifice of the mass spectrometer. For MS experiments the quadrupole was set in the RF-only mode to act simply as an ion guide to efficiently link the electrospray ion source with the high sensitivity reflectron time-of-flight analyzer. In MS/MS mode, the quadrupole was used to select precursor ions, which were fragmented in the hexapole collision cell, generating product ions that were subsequently mass analyzed by the orthogonal time-of-flight mass analyzer. The potential between the nanospray needle and the orifice of the

mass spectrometer was typically set to 1800 V, the cone voltage was 140 V. The nanospray needle was constantly kept at approximately 30°C. For CID MS measurements the collision energy was set to 135 V. Argon was used as collision gas. The quadrupole mass resolution parameters were set to a relatively large mass window in order to select the entire isotope envelope of the precursor ions. The reflectron time-of-flight parameters were set such that the fragment ions were detected at more than unit mass resolution, as required to obtain isotopically resolved H/D profiles. Increases in deuterium content (in Da) were calculated by using the average mass-to-charge (m/z) values of the isotope clusters of the undeuterated peptide and the (partly) deuterated peptides.

Results and discussion

ESI-MS – By using the proteoliposome nano-ESI-MS technique as described in this paper, high-quality spectra can be obtained of peptides in model membranes. Figures 2 A and B show typical positive ion spectra of LUVETs of WALP16 and WALP16(+10), respectively, reconstituted in DMPC bilayers dispersed in 10 mM ammonium acetate buffer. In both cases the monomers, dimers, trimers and tetramers of DMPC are observed as $[M+H]^+$ as well as $[M+Na]^+$ ions (22 mass units higher). Also the peptide ion peaks are clearly visible, in spite of the relatively low peptide/lipid ratio. The $[M+Na]^+$ ions of WALP16 as well as of WALP16(+10) are more abundant than the corresponding $[M+H]^+$ ions. The spectrum of the WALP/DMPC LUVETs indicates that the vesicles are destabilized during the ionization process in such a way that only smaller aggregates of phospholipid molecules are observed. The largest singly charged multimer was found to be the $[16M+H]^+$ ion of DMPC (not shown), with an intensity of about four orders of magnitude lower than the intensity of the $[M+H]^+$ ion of DMPC.

Figure 3 shows the overall deuterium content in time of WALP16 and WALP16(+10) reconstituted in DMPC bilayers upon dilution in buffered deuterium oxide. As shown in Figure 3 A, within the deadtime of the experiment, approx. six hydrogens have exchanged for WALP16 and 15 for WALP16(+10). From the first time point at 2 min to approx. 100 min, the exchange is slower, as can also be observed in Figure 3 B, in which the exchange is monitored during much longer incubation times. At longer incubation times, exchange becomes very slow. From the total number of exchangeable hydrogens (22 for WALP16 and 32 for WALP16(+10); see Table 1), it can be concluded that even after several days, not all exchangeable hydrogens have exchanged completely. For both peptides approx. ten hydrogens remain protected from exchange. This appears to be in good agreement with the model shown in Figure 1, in which WALP16 is incorporated in the DMPC bilayer with its hydrophobic core embedded inside the phospholipid bilayer, whereas the 5-amino acid tails of WALP16(+10) at both sides extend into the aqueous phase surrounding the bilayer.
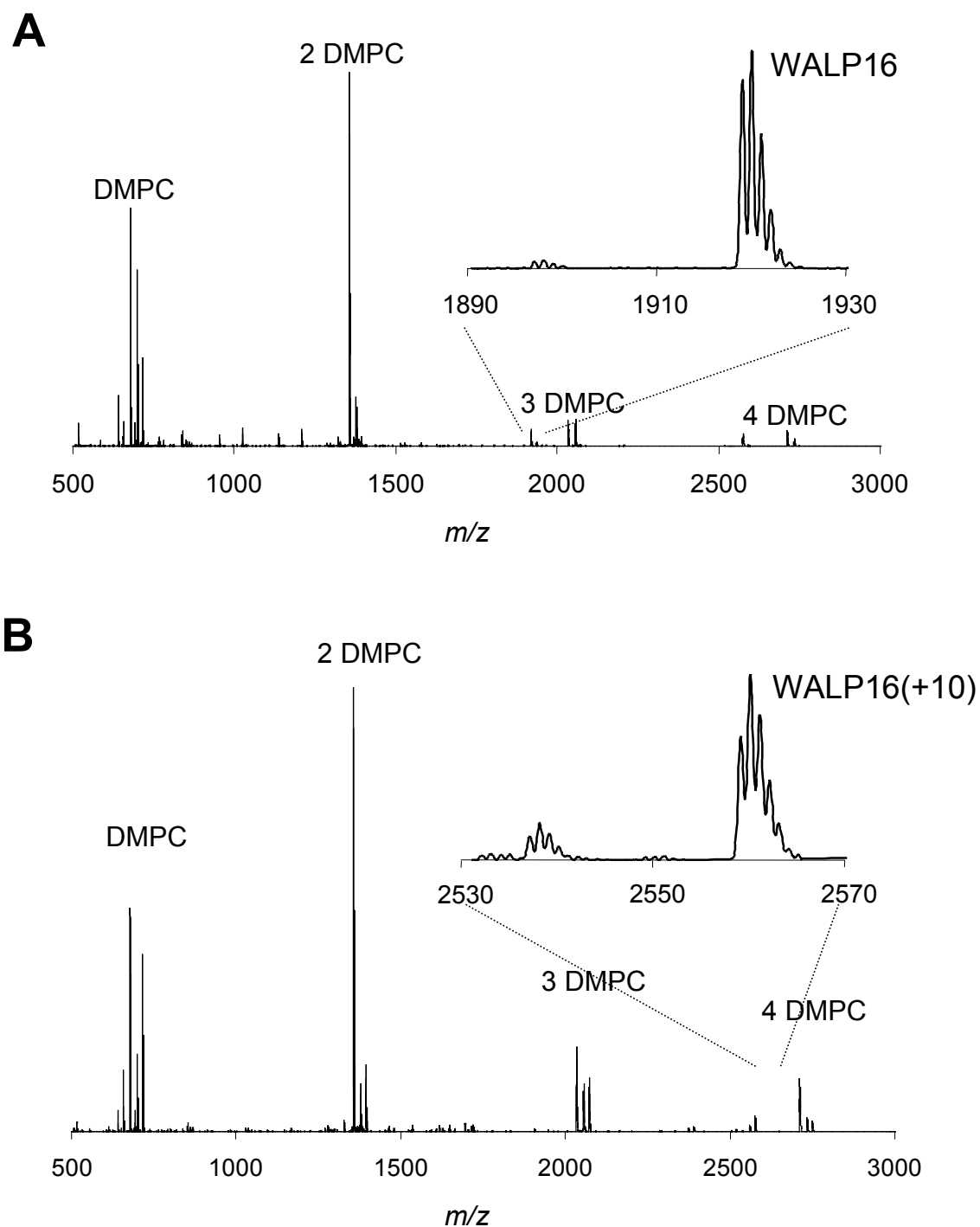
Figure 2 – Nano-ESI-MS spectrum of LUVETs of **(A)** WALP16/DMPC (1:25) and **(B)** WALP16(+10)/DMPC (1:25). The [M+Na]$^+$ ions of the DMPC monomer, dimer and trimer are most abundant; the isotope envelopes of the [M+Na]$^+$ ions of the WALP16 and WALP16(+10) peptides are observed around m/z 1919 (**A**) and m/z 2559 (**B**); the [M+H]$^+$ ions are around m/z 1897 (**A**) and m/z 2537 (**B**), respectively. For the recording of each spectrum ~200 nl of a vesicle suspension containing ~20 µM peptide was used.
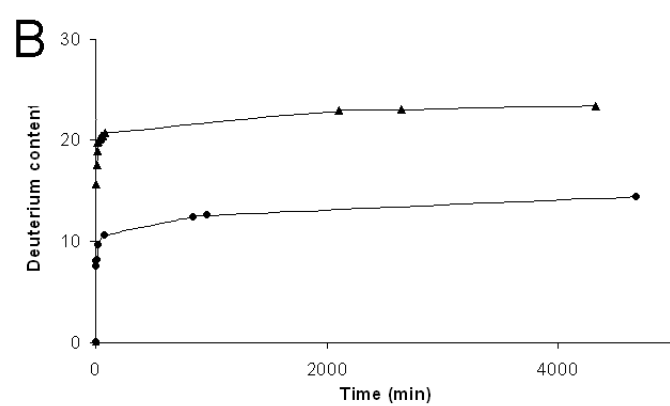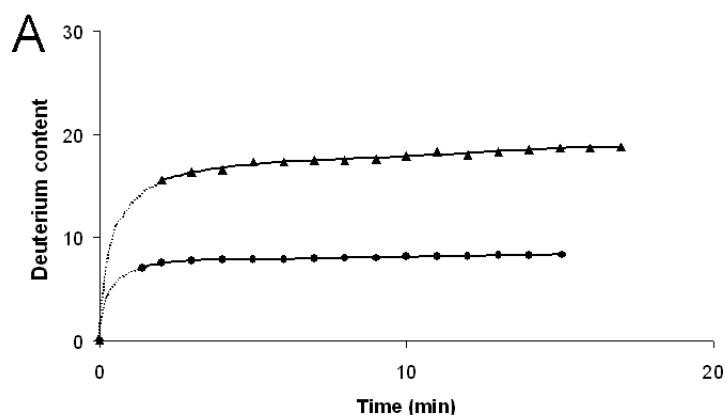
Figure 3 − Deuterium content of WALP16 (●) and WALP16(+10) (▲) incorporated in DMPC bilayers as a function of incubation time. Panel **(A)** shows the time envelope from 0 to 15 min. The dotted line between 0 and 2 min represents an estimated extrapolation of the curve, as no data points were available in this region. Panel **(B)** shows the time envelope from 0 to 5×10^3 min.

The various exchange rates can be quantified by using the expression [25]:

$$(1/H_t) \cdot H = e^{(-k_{ex}t)} \qquad \textbf{(1)}$$

where H is the amount of protected hydrogens, H_t is the total amount of exchangeable hydrogens, k_{ex} is the H/D exchange rate constant and t is the time the peptide is incubated in D_2O. From equation **(1)**, it follows that in plots of $\ln(H)$ versus t, the slope is inversely proportional to k_{ex}, and populations of hydrogens having different rate constants can thus be distinguished. In this way, from plots over the entire time interval, roughly three populations of exchangeable hydrogens could be discerned. These are summarized in Table II and will be discussed below.

Both peptides contain a number of fast-exchanging hydrogens (half-lives ≤ 3min). These hydrogens have already exchanged completely at the time of the first measurements. They are most likely unprotected by hydrogen bonding and readily accessible to the solvent. As shown in Table II, WALP16 has about six and WALP16(+10) about 15 fast-exchanging hydrogens. Therefore, these hydrogens comprise most likely the two terminal backbone hydrogens of WALP16 and the terminal extensions of WALP16(+10), corresponding to approx. ten additional fast-exchanging hydrogens. Also the four indole hydrogens of the tryptophans in both peptides may exchange very fast. For both the WALP16 and WALP16(+10) hydrogens, it is not possible

to obtain the exact half-life values for these populations, because no data points are available at these very early times.

Table II – H/D exchange half-life values (in min) of populations of hydrogens of WALP16 and WALP16(+10), calculated from logarithmic plots of the data in Figure 3 (see text for details).

	WALP16		WALP16(+10)	
	No. of hydrogens	Half-life (min)	No. of hydrogens	Half-life (min)
Fast	6	≤ 3	15	≤ 2
Intermediate	1.5	1.4×10^1	2	1.9×10^1
-	2	2.4×10^2	2	7.0×10^1
-	2	3.4×10^3	2	3.5×10^2
Slow	10	1.8×10^4	10	2.3×10^4

Fast exchange was defined as between 0 and 2 min, intermediate exchange from 2-1,000 min and slow exchange starting from about 1,000 min. The number of hydrogens in each population is indicated (estimated errors in these numbers are in all cases 0.5).

The population of hydrogens that display intermediate exchange rates (half-lives from $\approx 10^1$ to $\approx 10^3$ min) comprises five to six hydrogens for both peptides. In this intermediate exchange region, it was even possible to distinguish subpopulations of hydrogens with different exchange kinetics. This is illustrated in Figures 4 A and 4 B, which show H/D exchange data of WALP16 and WALP16(+10) in the time interval of 2 to 100 min, respectively. For WALP16, the subpopulations with the shortest half-life values correspond to lines 1 and 2 in Figure 4 A. The third subpopulation has a slightly longer half-life (not visible on the timescale of Figure 4 A). An analogous set of subpopulations was observed for WALP16(+10) (represented by lines 1, 2 and 3 in Figure 4 B). These hydrogens most likely represent the backbone hydrogens of the tryptophan residues and residues near the ends of the transmembrane helices, i.e., Gly1 and Ala16 for WALP16, and Ala6 and Ala21 for WALP16(+10). Differences between the calculated half-life values in the two peptides are ascribed to small differences in local environment at these positions.

The slowest exchanging hydrogen populations (half-lives $\approx 10^4$ min) comprise approximately ten hydrogens in both peptides and are assigned to the backbone amide hydrogens of the Leu/Ala core of the peptides. Such a protection of exchange by incorporation into a membrane is in agreement with exchange studies on other transmembrane peptides and proteins [7-9].
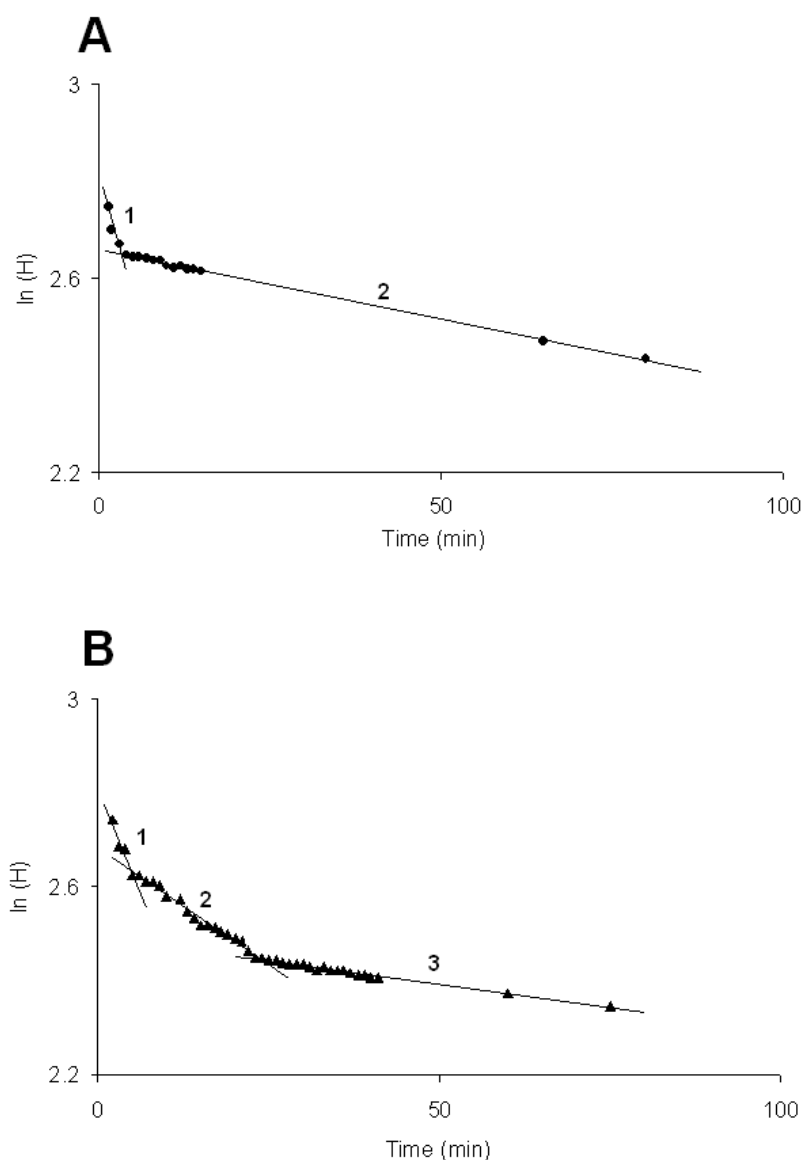
A

Figure 4 – Kinetics of hydrogen/deuterium exchange of **(A)** WALP16 and **(B)** WALP16(+10). On the y-axis the natural logarithm of the amount of protected hydrogens in the peptide (ln (H)) is shown. The time envelopes from 2-100 min for both peptides are indicated. From the slopes of the curves in the plot, the half-lives of specific hydrogen populations in this time period were calculated, and from the intercepts with the Y-axis the number of hydrogens involved. For WALP16 the intermediate exchange data are represented by the lines (1) $y = -4.9 \times 10^{-2} x + 2.81$ ($r = 0.95$), and (2) $y = -2.9 \times 10^{-3} x + 2.66$ ($r = 0.99$); for the intermediate exchange of WALP16(+10) (1) $y = -3.7 \times 10^{-2} x + 2.81$ ($r = 0.97$), (2) $y = -9.9 \times 10^{-3} x + 2.68$ ($r = 0.99$), and (3) $y = -2.0 \times 10^{-3} x + 2.49$ ($r = 0.99$).

ESI CID MS - From the results of the single-stage MS experiments, information with regard to the accessibility of exchangeable hydrogens of membrane-buried peptides could be obtained. However, from such data it is not possible to directly determine which sites have actually been exchanged. In principle this should be possible by fragmentation studies on the partly deuterated peptides. To investigate this possibility, CID MS experiments were performed on the $[M+Na]^+$ ions of WALP16 and WALP16(+10). Experiments were performed on the undeuterated peptides and partly deuterated peptides when about 12 of 22 (WALP16) and 20 of 32 (WALP16(+10)) hydrogens had been exchanged. Figure 5 shows part of a typical CID MS spectrum of partly deuterated WALP16(+10) in which series of A and Y' fragment ions can be observed, together covering almost the entire peptide. The CID MS spectra of the sodiated WALP16 and WALP16(+10) ions showed predominantly characteristic A and Y' fragment ions, corresponding to the N- and C-terminal fragments, respectively [26].
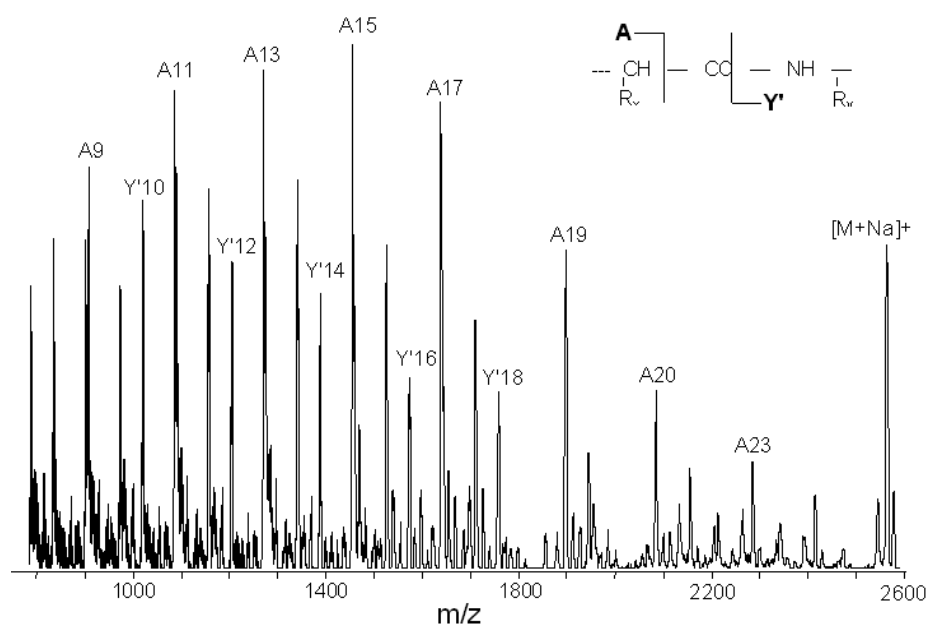
Figure 5 — Part of a nano-ESI CID MS spectrum of the [M+Na]$^+$ ion of WALP16(+10) incorporated in a DMPC bilayer 100 min after incubation in a deuterated ammonium acetate buffer. The sodiated, partly deuterated peptide parent ions as well as parts of the A fragment ion series and Y' fragment ion series are indicated (Y' is defined as [Y" – H + Na] [26]). The inset shows the fragmentation pattern; A ions correspond to N-terminal fragments and Y' ions correspond to C-terminal fragments.
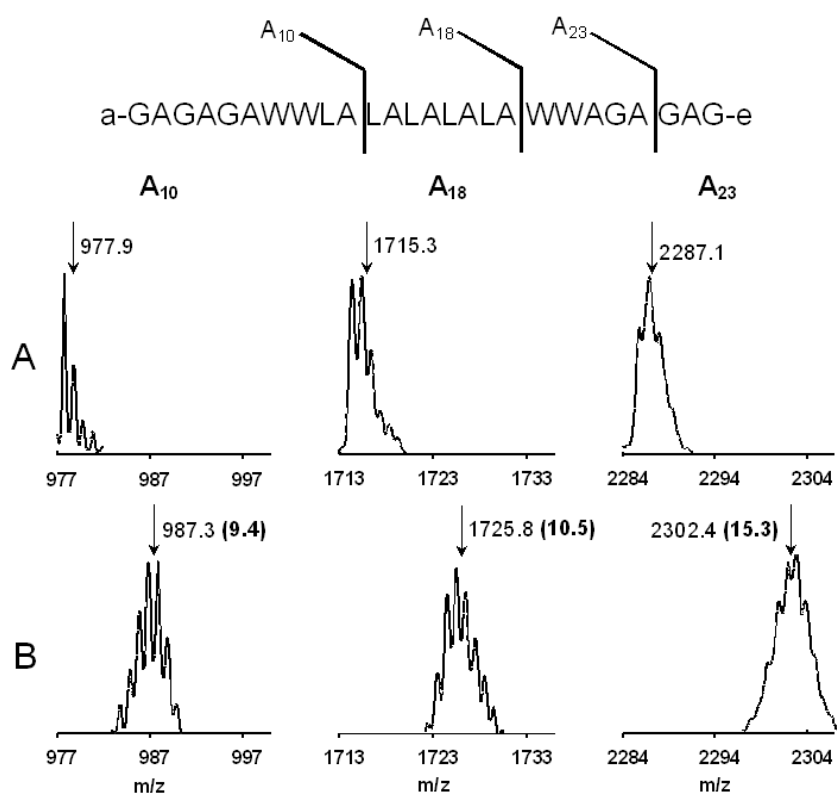
Figure 6 — Isotope envelopes of A_{10}, A_{18} and A_{23} fragment ions of WALP16(+10) incorporated in DMPC bilayers in undeuterated buffer **(A)** as opposed to the analogous fragment ions after incubation in deuterated buffer **(B)**. The arrows and numbers indicate the average m/z values for the fragment ions. The differences between the average m/z values of the undeuterated and the deuterated fragment ions are printed in bold in parentheses. These spectra were recorded when about 20 out of 32 hydrogens had exchanged. The amino acid sequence on top indicates how the A fragment ions are formed.

As an illustration of the quality of the CID MS data, isotope envelopes of A_{10}, A_{18} and A_{23} fragment ions of WALP16(+10) are shown in Figure 6. Fragment ions of WALP16(+10) in DMPC bilayers in undeuterated buffer (Figure 6 A) are compared to those in deuterated buffer when on average 20 out of 32 exchangeable hydrogens had been exchanged (Figure 6 B). The numbers in bold denote the differences between the average m/z values of the undeuterated and the deuterated fragment ions. The difference in deuterium content between the A_{10} and A_{18} fragment ions is much smaller than the difference between the A_{18} and A_{23} fragment ions, indicating that the deuterium labels were not randomly distributed over the WALP16(+10) peptide. Instead, it seems that in the partly exchanged WALP16(+10) precursor ions much less deuterium was present in the Leu/Ala core than in the other parts of the peptide.

The deuterium content of all A and Y' fragment ions as derived from the CID MS data is shown in Figures 7 A and 7 B for WALP16 and WALP16(+10), respectively (solid bars). The solid lines depicted in Figure 7 are theoretical curves using a simplified model, in which the exchanged hydrogens in the partly deuterated peptides would originate exclusively from the outermost exchangeable hydrogens. For WALP16(+10), these would be: the C-terminal and N-terminal Gly/Ala extensions, including the two exchangeable hydrogen atoms of the ethanolamine moiety (14 hydrogens), the side chains of the tryptophans (4 hydrogens) and the backbone hydrogens of the outermost tryptophans (Trp7 and Trp20) at each side of the peptide (2 hydrogens). The data collection of WALP16(+10) (shown in Figure 7 B) shows a remarkable resemblance to this hypothesized exchange kinetics.

Also WALP16 follows such a hypothetical pattern rather well. However, the observed patterns suggest in both cases the following deviations from the model. First, there appears to be a small gradient in exchange rate toward the ends of the transmembrane segments. This can be attributed to local dynamic fraying as is generally observed near the termini of α-helices [27]. Second, for both peptides the N-terminal fragments contain more deuterium than the C-terminal fragments. A possible explanation is that the C-termini are more protected from exchange, because in a right-handed α-helical conformation, amide hydrogens at the C-terminus can form hydrogen bonds with backbone carbonyl oxygens in the preceding turn, whereas the N-termini cannot form such hydrogen bonds.

It is important to note here that we cannot exclude the possibility that the measured deuterium content as depicted in Figures 7 A and 7 B has been affected by gas-phase deuterium scrambling. It is known that proton mobility within smaller protonated gas-phase peptide ions can often be sufficiently rapid to scramble deuterium labeling [28]. However, recent findings of Anderegg *et al.* [17] and Deng *et al.* [18], have shown that under certain conditions hydrogen exchange at individual peptide amide linkages can be determined by collision-induced dissociation MS. The results obtained in the present study are fully consistent with the expected exchange properties of the peptides based on the model in Figure 1. Therefore, it is suggested that CID MS as used under the conditions described here can give a reliable indication about the deuterium content in different regions of the peptide and that in our case the extent of

scrambling is limited. We believe that the fact that the investigated peptides are sodiated may hamper proton randomization.
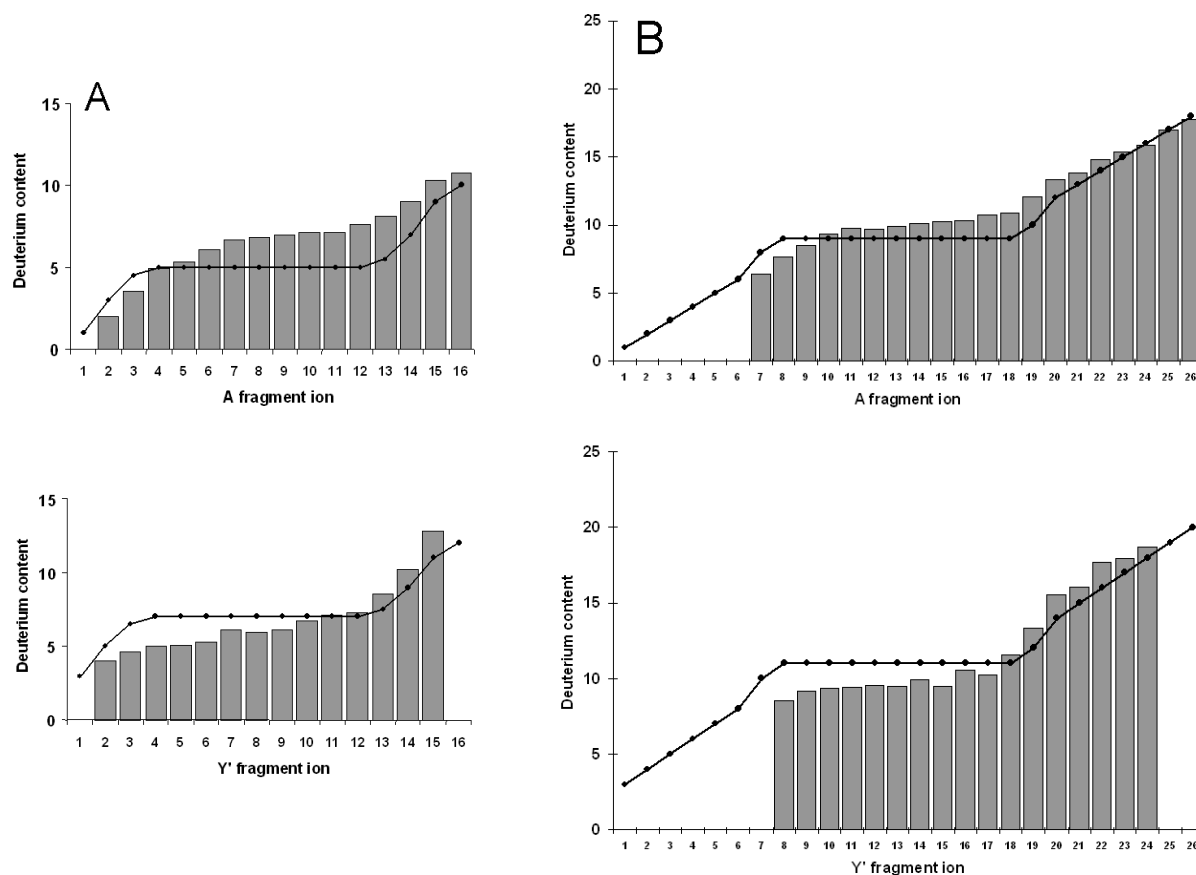

Figure 7 – Bar diagrams representing **(A, left panels)** the average deuterium content of the partly deuterated A and Y' fragment ions [26] of WALP16, and, **(B, right panels)** of WALP16(+10), as derived from nano-ESI-CID-MS measurements. The A_n fragment comprises the amide and side chain deuteriums of the N-terminal *n* amino acid residues; the Y'_n fragment comprises the amide and side chain deuteriums of the C-terminal *n* amino acid residues plus the ethanolamine terminal group. The CID MS spectrum of the $[M+Na]^+$ ion of WALP16 and WALP16(+10) were recorded when 12 out of 22 and 20 out of 32 hydrogens were exchanged, respectively. The deuterium content of the fragments as based on a simplified model (see text for explanation) is indicated by the black circles connected by a line (-●-). Data points for the fragments for which no bar is shown could not be obtained, due to poor signal-to-noise.

Conclusions - In this paper, we have described a novel direct approach to measure hydrogen/deuterium kinetics of model transmembrane peptides reconstituted in fully hydrated, dispersed phospholipid bilayers using nano-ESI-MS and CID MS. The uniqueness of this proteoliposome nano-ESI-MS technique is that the peptide-membrane system is directly introduced into the mass spectrometer without use of any membrane-mimicking detergents, 'isotropic' media, or exchange trapping techniques. The results of the experiments described here show that this method is very convenient to perform studies on the exact positioning of membrane peptides (such as the WALP peptides) in a lipid bilayer.

The method has many general advantages. It is both fast and sensitive and it allows a large flexibility in choice of environmental conditions, such as pH and ionic strength. It also allows variation in lipid as well as peptide composition, as we observed in pilot experiments with biological peptides in negatively charged phospholipid bilayers. Another advantage is the possibility to simultaneously incorporate different peptides into the membrane and subsequently monitor them independently of each other. Therefore, there is also no stringent requirement for high purity of the peptides. We propose that this relatively simple method could be equally well applied to study the positioning of larger transmembrane proteins in model or even biological membranes.

We note that other potential applications of our novel direct proteoliposome nano-ESI-MS technique lie in the field of proteomics of membrane proteins [29], which are difficult to characterize due to their inherent insolubility in aqueous solutions as well as due to the fact that membrane protein solubilizing detergents cannot easily be used in (nano-)ESI-MS. Moreover, this technique could be exploited in the investigation of lipid membrane structures, by direct introduction of, for instance, plasma membrane vesicles or detergent-resistant membrane vesicles [30].

References

1. Hvidt, A. & Nielsen, S.O. (1966) Hydrogen exchange in proteins. *Adv. Protein Sci.* **21**, 287-386.

2. Englander, S.W., Sosnick, T.R., Englander, J.J. & Mayne, L. (1996) Mechanisms and Uses of Hydrogen Exchange. *Curr. Opin. Struct. Biol.* **6**, 18-23.

3. Clarke, J. & Itzhaki, L.S. (1998) Hydrogen exchange and protein folding. Curr. Opin. Struct. Biol. 8, 112-8.

4. Goormaghtigh, E., Raussens, V. & Ruysschaert, J.M. (1999) Attenuated total reflection infrared spectroscopy of proteins and lipids in biological membranes. *Biochim. Biophys. Acta* **1422**, 105-85.

5. Sturgis, J., Robert, B. & Goormaghtigh, E. (1998) Transmembrane helix stability: the effect of helix-helix interactions studied by Fourier transform infrared spectroscopy. *Biophys. J.* **74**, 988-94.

6. Zhang, Y.P., Lewis, R.N., Henry, G.D., Sykes, B.D., Hodges, R.S. & McElhaney, R.N. (1995) Peptide models of helical hydrophobic transmembrane segments of membrane proteins. 1. Studies of the conformation, intrabilayer orientation, and amide hydrogen exchangeability of Ac-K2-(LA)12-K2-amide. *Biochemistry* **34**, 2348-61.

7. Henry, G.D., Weiner, J.H. & Sykes, B.D. (1987) Backbone dynamics of a model membrane protein: measurement of individual amide hydrogen-exchange rates in detergent-solubilized M13 coat protein using 13C NMR hydrogen/deuterium isotope shifts. *Biochemistry* **26**, 3626-34.

8. Chupin, V., Killian, J.A., Breg, J., de Jongh, H.H., Boelens, R., Kaptein, R. & de Kruijff, B. (1995) PhoE signal peptide inserts into micelles as a dynamic helix-break-helix structure, which is modulated by the environment. A two-dimensional 1H NMR study. *Biochemistry* **34**, 11617-24.

9. Pervushin, K.V., Orekhov, V., Popov, A.I., Musina, L. & Arseniev, A.S. (1994) Three-dimensional structure of (1-71)bacterioopsin solubilized in methanol/chloroform and SDS micelles determined by 15N-1H heteronuclear NMR spectroscopy. *Eur. J. Biochem.* **219**, 571-83.

10. Dempsey, C.E. & Butler, G.S. (1992) Helical structure and orientation of melittin in dispersed phospholipid membranes from amide exchange analysis in situ. *Biochemistry* **31**, 11973-7.

11. Cotten, M., Fu, R. & Cross, T.A. (1999) Solid-state NMR and hydrogen-deuterium exchange in a bilayer-solubilized peptide: structural and mechanistic implications. *Biophys. J.* **76**, 1179-89.

12. Katta, V. & Chait, B.T. (1991) Conformational changes in proteins probed by hydrogen-exchange electrospray-ionization mass spectrometry. *Rapid Commun. Mass. Spectrom.* **5**, 214-7.

13. Bai, Y., Englander, J.J., Mayne, L., Milne, J.S. & Englander, S.W. (1995) Thermodynamic parameters from hydrogen exchange measurements. *Methods Enzymol.* **259**, 344-56.

14. Benjamin, D.R., Robinson, C.V., Hendrick, J.P., Hartl, F.U. & Dobson, C.M. (1998) Mass spectrometry of ribosomes and ribosomal subunits. *Proc. Natl. Acad. Sci. U. S. A.* **95**, 7391-5.

15. Miranker, A., Robinson, C.V., Radford, S.E., Aplin, R.T. & Dobson, C.M. (1993) Detection of transient protein folding populations by mass spectrometry. *Science* **262**, 896-900.

16. Zhang, Z. & Smith, D.L. (1996) Thermal-induced unfolding domains in aldolase identified by amide hydrogen exchange and mass spectrometry. *Protein Sci.* **5**, 1282-9.

17. Anderegg, R.J., Wagner, D.S., Stevenson, C.L. & Borchardt, R.T. (1994) The Mass Spectrometry of Helical Unfolding in Peptides. *J. Am. Soc. Mass Spectrom.* **5**, 425-33.

18. Deng, Y. & Smith, D.L. (1999) Hydrogen exchange demonstrates three domains in aldolase unfold sequentially. *J. Mol. Biol.* **294**, 247-58.

19. Wimley, W.C. & White, S.H. (1996) Experimentally determined hydrophobicity scale for proteins at membrane interfaces. *Nat. Struct. Biol.* **3**, 842-8.

20. Killian, J.A., Salemink, I., de Planque, M.R.R., Lindblom, G., Koeppe, R.E., II & Greathouse, D.V. (1996) Induction of nonbilayer structures in diacylphosphatidylcholine model membranes by transmembrane alpha-helical peptides: importance of hydrophobic mismatch and proposed role of tryptophans. *Biochemistry* **35**, 1037-45.

21. de Planque, M.R.R., Kruijtzer, J.A.W., Liskamp, R.M.J., Marsh, D., Greathouse, D.V., Koeppe, R.E., II, de Kruijff, B. & Killian, J.A. (1999) Different membrane anchoring positions of tryptophan and lysine in synthetic transmembrane alpha-helical peptides. *J. Biol. Chem.* **274**, 20839-46.

22. de Planque, M.R.R., Greathouse, D.V., Koeppe, R.E., II, Schafer, H., Marsh, D. & Killian, J.A. (1998) Influence of lipid/peptide hydrophobic mismatch on the thickness of diacylphosphatidylcholine bilayers. A 2H NMR and ESR study using designed transmembrane alpha-helical peptides and gramicidin A. *Biochemistry* **37**, 9333-45.

23. Lewis, B.A. & Engelman, D.M. (1983) Lipid bilayer thickness varies linearly with acyl chain length in fluid phosphatidylcholine vesicles. *J. Mol. Biol.* **166**, 211-7.

24. Blume, A. (1983) *Biochemistry* **22**, 5436-42.

25. Liu, Y.Q. & Smith, D.L. (1994) Probing High Order Structure of Proteins by Fast Atom Bombardment Mass Spectrometry. *J. Am. Soc. Mass Spectrom.* **5**, 19-28.

26. Roepstorff, P. & Fohlman, J. (1984) Proposal for a common nomenclature for sequence ions in mass spectra of peptides. *Biomed. Mass Spectrom.* **11**, 601.

27. Wand, A.J., Roder, H. & Englander, S.W. (1986) Two-dimensional 1H NMR studies of cytochrome c: hydrogen exchange in the N-terminal helix. *Biochemistry* **25**, 1107-14.

28. Johnson, R.S. (1996) Mass Spectrometric Measurement of Changes in Protein Hydrogen Exchange Rates That Result from Point Mutations. *J. Am. Soc. Mass Spectrom.* **7**, 515-21.

29. Whitelegge, J.P., le Coutre, J., Lee, J.C., Engel, C.K., Prive, G.G., Faull, K.F. & Kaback, H.R. (1999) Toward the bilayer proteome, electrospray ionization-mass spectrometry of large, intact transmembrane proteins. *Proc. Natl. Acad. Sci. U. S. A.* **96**, 10695-8.

30. Fridriksson, E.K., Shipkova, P.A., Sheets, E.D., Holowka, D., Baird, B. & McLafferty, F.W. (1999) Quantitative analysis of phospholipids in functionally important membrane domains from RBL-2H3 mast cells using tandem high-resolution mass spectrometry. *Biochemistry* **38**, 8056-63.

CHAPTER 3

Interfacial positioning and stability of transmembrane peptides in lipid bilayers studied by combining hydrogen/deuterium exchange and mass spectrometry

Jeroen A.A. Demmers[1,2], Esther van Duijn[2], Johan Haverkamp[2], Denise V. Greathouse[3], Roger E. Koeppe II[3], Albert J.R. Heck[2] & J. Antoinette Killian[1]

[1] Department of Biochemistry of Membranes, Center for Biomembranes and Lipid Enzymology, Institute of Biomembranes, Utrecht University, Padualaan 8, 3584 CH Utrecht, The Netherlands

[2] Department of Biomolecular Mass Spectrometry, Bijvoet Center for Biomolecular Research and Utrecht Institute for Pharmaceutical Sciences, Utrecht University, Sorbonnelaan 16, 3584 CA Utrecht, The Netherlands

[3] Department of Chemistry and Biochemistry, University of Arkansas, Fayetteville, Arkansas 72701, USA

Abstract

Nano-electrospray ionization mass spectrometry (ESI-MS) was used to analyze hydrogen/deuterium (H/D) exchange properties of transmembrane peptides with varying length and composition. Synthetic transmembrane peptides were used with a general acetyl-$GW_2(LA)_nLW_2A$-ethanolamine sequence. These peptides were incorporated in large unilamellar vesicles of 1,2-dimyristoyl-*sn*-glycero-3-phosphocholine. The vesicles were diluted in buffered deuterium oxide and the H/D exchange after different incubation times was directly analyzed by means of ESI-MS. First, the influence of the length of the hydrophobic Leu-Ala sequence on exchange behavior was investigated. It was shown that longer peptide analogs are more protected from H/D exchange than expected on basis of their length with respect to bilayer thickness. This is explained by an increased protection from the bilayer environment, because of stretching of the lipid acyl chains and/or tilting of the longer peptides. Next, the role of the flanking tryptophan residues was investigated. The length of the transmembrane part that shows very slow H/D exchange was found to depend on the exact position of the tryptophans in the peptide sequence, suggesting that tryptophan acts as a strong determinant for positioning of proteins at the membrane/water interface. Finally, the influence of putative helix breakers was studied. It was shown that the presence of Pro in the transmembrane segment results in much higher exchange rates as compared to Gly or Leu, suggesting a destabilization of the α-helix. Tandem MS measurements suggested that the increased exchange takes place over the entire transmembrane segment. The results show that ESI-MS is a convenient technique to gain detailed insight into properties of peptides in lipid bilayers by monitoring H/D exchange kinetics.

Introduction

The precise manner in which membrane proteins are embedded in a lipid bilayer is essential for their structure and function. Important structural and dynamic features, such as stability of the transmembrane segments or their precise positioning at the lipid/water interface, will be determined not only by intrinsic properties of the transmembrane segments, but also by their interaction with surrounding lipids. A convenient way to gain insight into how the special characteristics of transmembrane segments and their interaction with lipids may influence the behavior of membrane proteins, is by studying model systems of artificial transmembrane peptides with desired properties in well-defined lipid bilayers.

Recently, we have described a new method using nano-ESI-MS [1] to study properties of transmembrane protein segments in model systems by analyzing the kinetics of hydrogen/deuterium (H/D) exchange. The results showed that various populations of amide hydrogen atoms can be distinguished that are characteristic for different regions of the transmembrane segments. These populations are fast exchanging amide hydrogens located in the peptide termini that are exposed to the aqueous phase, intermediately exchanging hydrogens of the residues located in the bilayer/water interface and slowly exchanging hydrogens located in

the hydrophobic core of the lipid bilayer. The results suggested that measurement of exchange properties of peptides by ESI-MS is a convenient method to investigate factors that determine interfacial positioning and/or stability of transmembrane protein segments. In the present study, we have investigated the influence of several of such factors. Hereby, special emphasis is given to the length of the α-helical hydrophobic core with respect to the bilayer thickness, the role of potential anchoring residues at the lipid/water interface, and the influence of α-helix breaking residues in the transmembrane segment.

As models for protein transmembrane segments, we have used WALP peptides that already have been used successfully to investigate various aspects of peptide/lipid interactions [2-4]. These peptides have a hydrophobic core of alternating Leu and Ala, which is flanked on both sides by Trp residues (see Table I), and they have been shown to form α-helical transmembrane helices [4]. Since in membrane proteins Trp residues are highly enriched near the membrane/water interface [5-8], they are thought to resemble a consensus sequence for transmembrane α-helical segments of intrinsic membrane proteins.

The extent to which the hydrophobic length of transmembrane segments matches the hydrophobic bilayer thickness can significantly influence membrane protein structure and function [9]. To investigate whether this is related to changes in membrane protein interfacial positioning and/or stability, we first analyzed the effects of increasing the hydrophobic length of WALP peptides on the H/D exchange kinetics of peptides with different lengths of the Leu-Ala core in bilayers of DMPC. This lipid is chosen because it forms well-defined bilayers with all peptides under the used experimental conditions [2,4,10] and has a hydrophobic thickness that approximately matches the hydrophobic length of the shortest peptide used [3].

Next, we investigated the importance of Trp as interfacial anchoring residues. It has been suggested that Trp residues prefer to be positioned at a well-defined site in the lipid headgroups [3,11-15] and that thereby they can act as membrane anchors. Their abundance at the lipid/water interface in several membrane proteins [5-7] is therefore likely to be functionally important, e.g. for stabilization of transmembrane helices or precise positioning of such helices at the interface. The present mass spectrometric method offers the opportunity to investigate these effects by analyzing the H/D exchange kinetics of peptides of identical total length in which the position of Trp residues along the sequence is varied.

Finally, besides the length of the transmembrane helices and their interfacial anchoring behavior, the stability of the transmembrane segment is also important for membrane protein structure and function. In water-soluble proteins, the stability of the backbone of regular α-helices has been found to undergo large changes when potent breakers of both α-helical and β-sheet structures, like Pro and Gly, are inserted (e.g. see [16]). However, little is known about the effect on stability of these residues in transmembrane segments. Therefore, H/D exchange kinetics in transmembrane segments containing Pro and Gly residues are compared to those of peptides without these residues.

The results of this study show that peptides that are long with respect to the hydrophobic thickness of the bilayer are protected from H/D exchange to a relatively large extent, which is explained in terms of induced adaptation (thickening) of the bilayer and/or a tilting of the peptides. Furthermore, the positions of the Trp residues in the transmembrane sequence are shown to be a critical factor for H/D exchange kinetics. These results suggest that Trp side chains interact strongly with the membrane/water interface at specific sites. Finally, it is shown that peptides containing Pro, but not Gly, show a markedly different H/D exchange pattern than peptides lacking this residue. This suggests a significant effect of Pro on the stability of the transmembrane α-helix. The results are discussed in relation to existing literature data on related peptide/lipid interactions.

Materials and methods

Chemicals - Trifluoroacetic acid (TFA) was obtained from Merck (Darmstadt, Germany), 2,2,2-trifluoroethanol (TFE) from Sigma (St. Louis, MO). Deuterium oxide (>99.9 % D) was obtained from Aldrich Chemical Company, Inc. (Milwaukee, WI, USA). D_2O was stored under nitrogen at 4°C. Sodium iodide was from OPG Farma Company (Utrecht, The Netherlands). Ammonium acetate was from Fluka (Switzerland). The phospholipid DMPC was obtained from Avanti Polar Lipids Inc. (Birmingham, AL). The peptides WALP16, WALP19, WALP21, WALP23, WALP23inner, WALP23outer, WALP23Pro and WALP23Gly were synthesized as described by Killian *et al.* [4], as modified by Greathouse *et al.* [17]. The W′ALP21 peptide was synthesized as described by De Planque *et al.* [3] for related peptides. The peptides were tested for purity by nano-ESI-MS and found to be pure.

Proteoliposome preparation - Peptide incorporation into phospholipid vesicles and mass spectrometry measurements were performed essentially as described previously [1]. Shortly, peptides were dissolved in a small volume of TFA (10 µl per mg of peptide) and dried under a nitrogen stream. To remove residual TFA, the peptides were subsequently dissolved in TFE (1 mg/ml) followed by evaporation of the solvent in a rotavapor. Peptides were then again dissolved in TFE to a final concentration of 1 mg/ml. Dry mixed films of peptide and DMPC (peptide to lipid ratio1:25) were prepared as follows. Peptide solutions in TFE (1 ml; 0.46 mM) were added to DMPC solutions in methanol (1 ml; 12 mM) and vigorously vortexed. The solvent was removed by evaporation in a rotavapor. The mixed films were then dried for 24 hrs under vacuum. The films were hydrated at about 40°C, well above the gel to liquid crystalline phase transition temperature of the phospholipid (24°C [18]) in 0.5 ml 10 mM ammonium acetate buffer (pH 7.5). Large unilamellar vesicles (LUVETs) were prepared by extrusion through a 400 nm filter at room temperature and kept at 4°C until use.

Before the start of H/D exchange, LUVETs were preincubated at 30°C for at least 30 min. For accurate comparison of the exchange data, LUVET suspensions with different peptide composition were mixed prior to the start of the exchange. LUVET suspensions were then 50

times diluted in deuterated ammonium acetate buffer at 30°C (10 mM, pH 7.5), containing ≈1 mM NaI. At selected time points, 2 μl of this diluted suspension was transferred into a gold-coated glass capillary and the measurement was started as quickly as possible, whereby the peptides were analyzed simultaneously. The dead-time between dilution and measurement was at a minimum 1 min.

MS measurements - MS measurements were performed on an ESI quadrupole time-of-flight instrument (Q-Tof; Micromass Ltd., Manchester, UK) or a an ESI time-of-flight instrument (LCT; Micromass Ltd., Manchester, UK), both operating in positive ion mode and equipped with a Z-spray nano-ESI source. Nano-ESI needles with a relatively large tip opening (several tens of μm) were prepared from borosilicate glass capillaries (Kwik-Fil™, World Precision Instruments Inc., Sarasota, Florida) on a P-97 puller (Sutter Instrument Co., Novato, CA). The needles were coated with a thin gold layer (≈500 Å) using an Edwards Scancoat sputter-coater 501 (at 40 mV, 1 kV, for 200 sec). The nano-ESI capillary was positioned ≈5 mm before the orifice of the mass spectrometer. For MS experiments, the quadrupole was set in the RF-only mode to act as an ion guide to efficiently link the ESI ion source with the reflectron time-of-flight analyzer. The potential between the nano-ESI capillary and the orifice of the mass spectrometer was typically set to 1800 V, the cone voltage was 140 V. The nanospray needle was constantly kept at ≈30°C. In CID MS (MS/MS) mode on the Q-Tof instrument, the quadrupole was used to select precursor ions, which were fragmented in the hexapole collision cell, generating product ions that were subsequently mass analyzed by the orthogonal time-of-flight mass analyzer. For CID MS measurements on the Q-Tof instrument, the collision energy was set to 150 V. Argon was used as collision gas. The quadrupole mass resolution parameters were set to a relatively large mass window to select the entire isotope envelope of the precursor ions. The reflectron time-of-flight parameters were set such that the fragment ions were detected at more than unit mass resolution, as required to obtain isotopically resolved H/D profiles. Increases in deuterium content (in Da) were calculated by using the average mass-to-charge (m/z) values of the isotope clusters of the undeuterated peptide and the (partly) deuterated peptides.

Results

To study effects of the hydrophobic length of transmembrane peptides on H/D exchange properties, a series of WALP/DMPC systems with varying peptide lengths (see Table I) were prepared for nano-ESI-MS measurements.

To allow accurate detection of small differences in exchange properties of different peptides, all experiments were performed with mixtures of two or more peptide-lipid systems synchronically. Therefore, LUVET suspensions with different peptide composition were mixed prior to the start of the exchange. Because such combination experiments are performed under identical experimental conditions, the deuterium levels can be compared directly. Figure 1
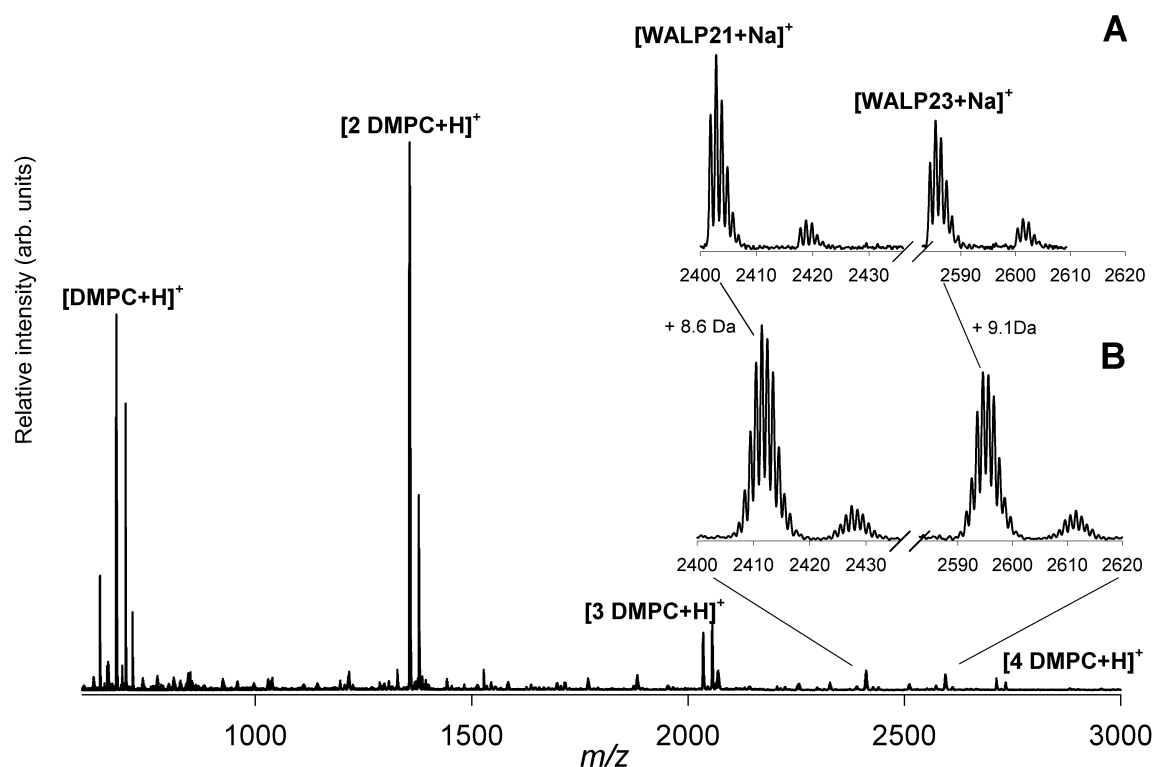
Figure 1 – Positive mode nano-ESI mass spectrum derived from WALP21/DMPC (P/L 1:25) and WALP23/DMPC (P/L 1:25) LUVETs, after incubation in 98% D_2O for 5 min. In inset **A** the isotope envelopes of both non-deuterated peptides (average mass for WALP21: 2402.95 Da; for WALP23: 2586.18 Da) are depicted. Inset **B** shows the envelopes 5 min after deuteration (average mass for WALP21: 2411.59 Da; for WALP23: 2586.18 Da). The low intensity envelopes 16 mass units higher in both insets are K^+ adducts of the peptides. For these spectra whole vesicles were directly introduced into the mass spectrometer (see "Materials and Methods"). For the recording of each spectrum (consisting of 30 scans) 10 pmoles of peptide was used.

illustrates that this method works. This figure presents, as an example, ESI mass spectra derived from simultaneously incubated and injected LUVETs of WALP21/DMPC and WALP23/DMPC dispersed in buffer, recorded by the direct proteoliposome method. The extremely hydrophobic membrane peptides are almost exclusively detected as $[M+Na]^+$ ions, whereas the monomers, dimers, trimers and tetramers of DMPC are observed as $[M+H]^+$ as well as $[M+Na]^+$ ions. The zoomed-in spectra in the inset show the isotope envelopes of the $[M+Na]^+$ ions of the non-deuterated reconstituted WALP21 and WALP23 peptides (*top*), as well as those of the WALP peptides reconstituted in bilayer dispersions that were incubated for 5 min in buffered D_2O (*bottom*). The shift in mass of the peptides indicates uptake of about 8.5-9 deuterium atoms in both cases. Moreover, the spectra indicate that the vesicles are disrupted during the ionization process in such a way that only monomers and small oligomers of phospholipid molecules are observed.

Table I – Amino acid sequences of the peptides used and their number of exchangeable hydrogens.

Peptide	Sequence	Average Mass (Da)	No. of labile H's
WALP16	[a]Ac-GWWLALALALALALAWWA-Etn[b]	1897.31	22
WALP19	Ac-GWWLALALALALALALWWA-Etn	2194.71	25
WALP21	Ac-GWWLALALALALALALALWWA-Etn	2379.95	27
WALP23	Ac-GWWLALALALALALALALALWWA-Etn	2563.18	29
W'ALP21[d]	Ac-GW'W'LALALALALALALALW'W'A-Am[c]	2391.00	23
WALP23inner	Ac-GAWLALALALALALALALALWAA-Etn	2332.91	27
WALP23outer	Ac-GWLALALALALALALALALALWA-Etn	2374.99	27
WALP23Pro	Ac-GWWLALALALALAPALALALALWWA-Etn	2547.14	28
WALP23Gly	Ac-GWWLALALALALAGALALALALWWA-Etn	2507.07	29

[a]Ac, acetyl
[b]Etn, ethanolamine
[c]Am, amide
[d]W′, Trp analog with N-methylindole side chain
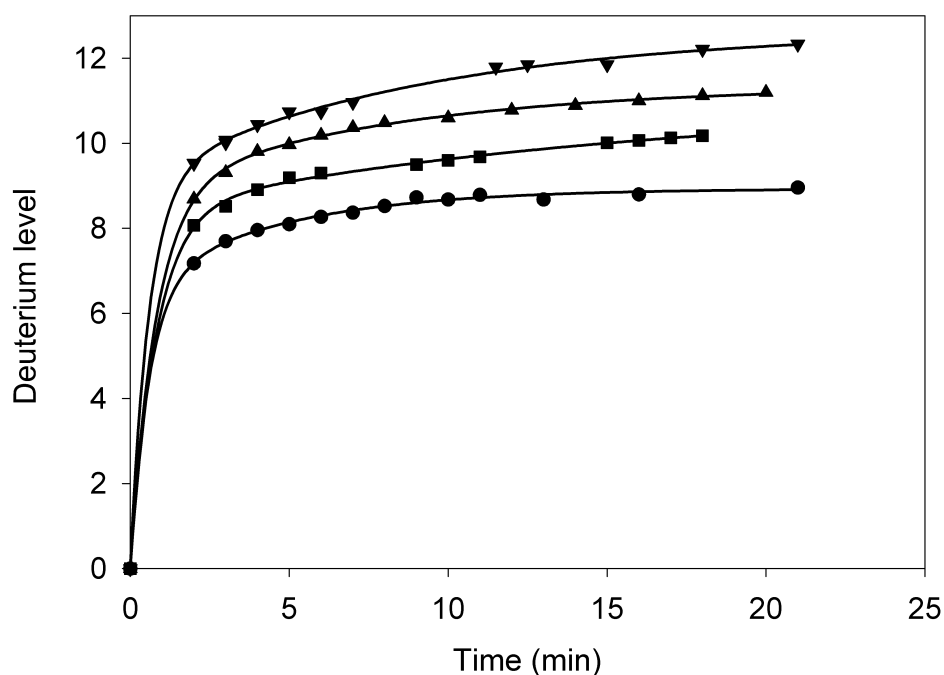
Figure 2 – Time course for deuterium uptake of WALP16 (●), WALP19 (■), WALP21 (▲) and WALP23 (▼), all incorporated in DMPC bilayers, after dilution in deuterated buffer. Experiments were performed with two peptides/lipid systems simultaneously. Data were normalized to the curve of WALP16.

The effect of increasing the hydrophobic length of the peptides with respect to the hydrophobic thickness of the bilayer was tested using a series of WALP peptides with varying hydrophobic core lengths (see Table I). Figure 2 shows the measured deuterium content as a function of incubation time in deuterated buffer. All WALP peptides incorporated in DMPC show a fast initial exchange. Within the experimental dead-time ($\approx$1.5 min) all peptides have taken up about 7-9 deuterium atoms. After this fast exchange the deuterium content continues to increase gradually with time, though at a much smaller exchange rate (defined as intermediate exchange rate, [1]). Figure 2 shows that all peptides have similar exchange kinetics curves in the first 20 min after incubation. All curves level off to a deuterium level, which is low as compared to the total number of labile hydrogens present in each peptide, which varies from 22 to 29 (see Table I). Furthermore, the deuterium content increases with increasing peptide length. However, the differences in deuterium levels are relatively small and represent only a fraction of the number of additional hydrogens that become available for exchange when the peptide length is increased.

By fitting the kinetic curves using a non-linear squares fitting to multiexponential functions in all peptides, three kinetic regions of exchange rates representing hydrogen populations were distinguished. In the short time range from 0 to 20 min, the fast and intermediate exchangeable hydrogens exchange, whereas the remaining hydrogens exchange only after $\approx$20 min. The number of hydrogens in specific populations are shown in Table II. As was shown previously [1], and will also be shown later in this work, the fast exchanging hydrogens are predominantly the hydrogens at the N- and C-termini of the peptides, sticking out of the bilayer, while the hydrogens with intermediate exchange rates are the ones close to the Trp in the interfacial region. The remaining hydrogens, including the ones in the hydrophobic core have rate constants of (much) smaller than 0.10 min^{-1}. These slow exchange rates are a result of both the extremely low partition coefficient of D_2O in a lipid bilayer [19] and the involvement of the amide protons in hydrogen bonding because of α-helix formation. The amount of fast exchanged hydrogens increases with the length of the peptides but does not increase quantitatively with the numbers of exchangeable hydrogens. For instance, only about one-third of the extra number of hydrogens of WALP23 compared to WALP16 exchanges rapidly and, therefore, the majority of the extra hydrogens of WALP23 are protected against exchange.

These results may be explained by several possible mechanisms. First, the number of protected hydrogens may be higher due to a larger core region of the α-helix in the longer peptides. Second, the longer peptides may be more protected by the bilayer itself, as a result of tilting of the longer helices, or due to adaptation of the lipids to the peptide/lipid mismatch by stretching of the acyl chains [2]. These possibilities will be discussed in more detail below. In principle, an alternative possible explanation for the protection of part of the peptides against H/D exchange, would be the formation of peptide aggregates, which would also hamper access of D_2O molecules to the amide hydrogens. However, several observations argue against this. First, no restricted component was observed in electron spin resonance (ESR) measurements

Table II - Numbers of fast, intermediate and remaining hydrogens in the investigated WALP peptides. The rates of exchange for the fast exchangeable hydrogens are all >1.2 min^{-1}, for the intermediate hydrogens between 0.16 and 0.26 min^{-1} and for the hydrogens remaining after 20 min smaller than 0.10 min^{-1}.

Peptide	No. of fast H's*	No. of intermediate H's*	No. of remaining H's*
WALP16	6.9	2.4	12.7
WALP19	8.0	2.9	14.1
WALP21	8.5	2.9	15.6
WALP23	9.1	3.5	16.4

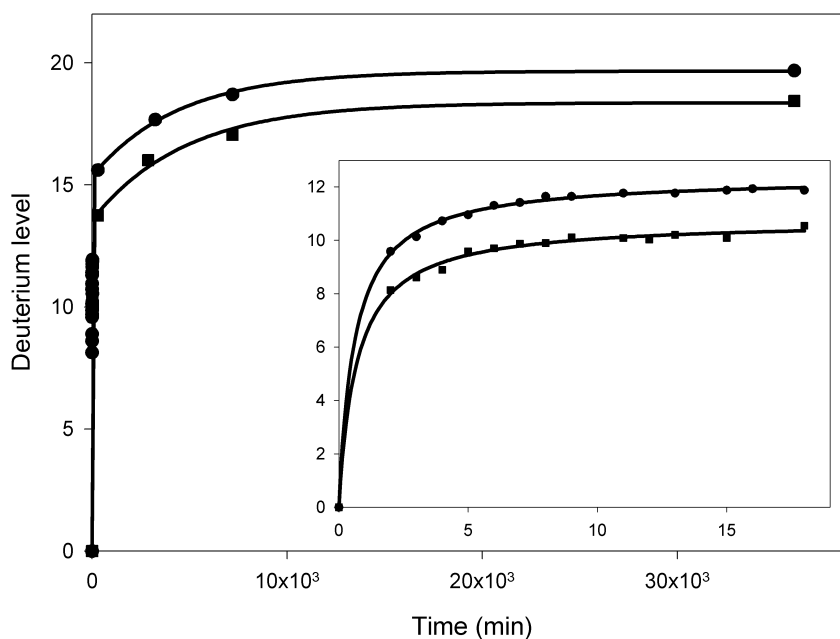*Standard errors are below 10%.

Figure 3 – Time course for deuterium uptake of WALP23inner (●) and WALP23outer (■) (see Table I for sequences) both incorporated in DMPC bilayers and simultaneously diluted in the same buffered D$_2$O. The maximum number of exchangeable hydrogens is 27 for both peptides.

in these peptide/lipid systems, suggesting that WALP peptides are most probably present as monomeric transmembrane helices [2]. Second, nano-flow ESI-MS experiments on the non-soluble WALP23 in buffer showed that when this dispersion was injected, not even a trace amount of WALP23 could be detected, not even after extensive sonication (data not shown). Remarkably, after addition of TFE (1:1; volume ratio), which presumably breaks up the aggregates, the peptide could again be easily detected in the spectrum. It is therefore concluded that it is not possible to measure aggregated peptides directly by ESI-MS, indicating that the

WALP peptides of which the mass spectra are analyzed in the present study do not originate from aggregates.

It has been proposed that Trp residues have strong interactions with the interface. To gain more insight into the potential anchoring role of the Trp residues, the positions of this aromatic amino acid were varied in peptides of invariable length. Moreover, to make the putative interaction zone less broad, the number of Trp residues was reduced to one at each terminus of the peptide (see Table I). WALP23inner has Trp residues at the 3 and 21 positions, whereas WALP23outer has Trp residues at positions 2 and 22. Figure 3 shows the deuterium incorporation of both peptides reconstituted in DMPC after synchronic dilution in deuterated buffer and subsequent mass spectrometric analysis. Although both peptides have the same number of exchangeable hydrogens, they clearly show different H/D exchange behavior. The deuterium level curve for WALP23inner lies well above the one of WALP23outer, both in the short term region as well as after longer incubation periods. Comparing the average m/z values of the isotope clusters of the peptides in both undeuterated and deuterated buffer results in a 1.6 (±0.2) Da higher deuterium content for WALP23inner. This suggests that WALP23inner has a larger population of fast exchangeable hydrogens. Consequently, WALP23inner incorporated in a DMPC bilayer seems to have a shorter protected region that could be due to a shorter inter-Trp distance. The deuteration levels of WALP23inner are also on the long term about 2 Da higher than for WALP23outer. These results suggest that the position of the Trp side chain determines the extent of protection in the bilayer environment, consistent with the idea that Trp forms a strong interfacial anchor [3,12,14,15].

The time course for exchange of WALP23inner appears to match that of WALP23, when comparing the data in Figures 2 and 3. However, if one assumes that the tryptophan side chain hydrogens exchange fast, then WALP23inner and WALP23outer would have two fast exchangeable hydrogens less than WALP23, and therefore the data would suggest that it is the backbone exchange of WALP23outer that matches well that of WALP23. Measurements with W′ALP21, which contains methylated Trp residues (see Table I), and thus has no exchangeable hydrogen atom in the indole side chain moiety, suggested that these indole hydrogens indeed exchange rapidly. It was found that the H/D exchange curve of this peptide lies close to 4 Da lower than that of WALP21 after both short and longer incubation times (data not shown). The apparent similarity in backbone exchange kinetics of WALP23 and WALP23outer is consistent with the idea that in the unfavorable case when the peptide is long with respect to the hydrophobic thickness of the bilayer (as is the case for the WALP23/DMPC system), the outer Trp will be furthest away from the favorable interaction site and therefore will be more important for determining the interfacial positioning of the peptide.

As shown previously, the proteoliposome spraying technique enables study of not only H/D exchange of the fast and intermediate exchangeable hydrogens, but also extremely slowly exchanging transmembrane amide hydrogens [1]. The stability of the backbone of regular α-helices has been found to undergo large changes when potent breakers of α-helical structures in
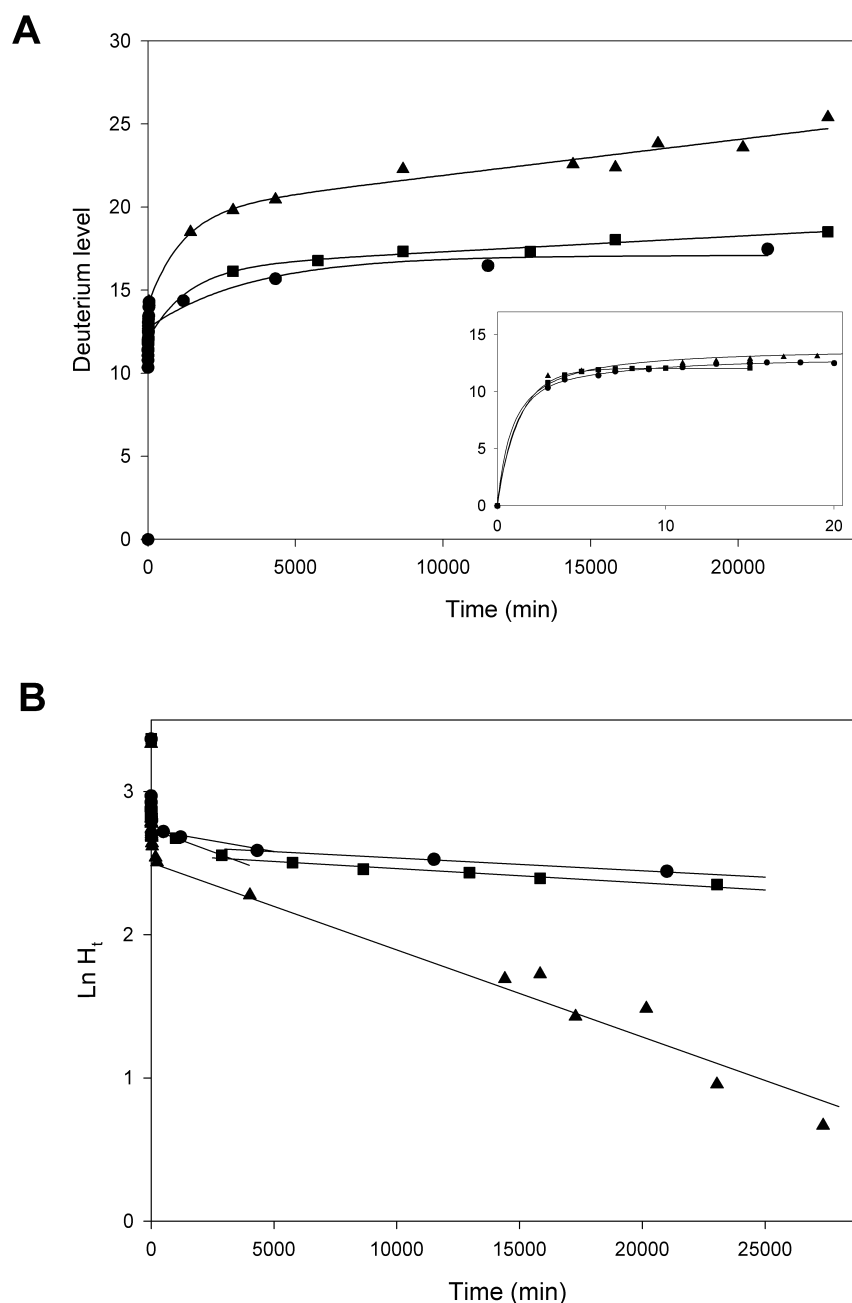
A

B

Figure 4 − **(A)** Time dependent change in deuterium contents of WALP23 (●),WALP23Pro (▲) and WALP23Gly (■), all incorporated in a DMPC bilayer after exposure to deuterated buffer. The insert shows the uptake in the time region between 0 and 20 min. The plot in **(B)** shows the converted data in which the time dependent decrease in the natural logarithm of the number of protected hydrogens is shown. Best-fit regression lines are shown, and hydrogen populations with similar exchange rates were probed from these plots (see text for details).

soluble (globular) proteins, like Pro and Gly, are inserted (e.g. [16]). In order to investigate the effect of such amino acids on the stability of transmembrane α-helices, modified WALP23 peptides with a Pro or Gly residue in the middle of the peptide (see Table I) were incorporated in DMPC model membranes, and peptide mass increase was monitored. Generally, the time

Table III – H/D exchange data for the sets of hydrogens exchanging after 100 min of WALP23, WALP23Gly and WALP23Pro.

Peptide	No. of hydrogens	Exchange rate $\times\, 10^7\, s^{-1}$
WALP23	13.8	1.5
WALP23Gly	13.0	1.7
WALP23Pro	13.3	10

courses for exchange of WALP23, WALP23Gly and WALP23Pro shown in the inset in Figure 4 A are quite similar at short incubation times (fast and intermediate exchange). This indicates that the positioning of the termini and the residues located in the interfacial region of all peptides is similar. However, after longer incubation times the deuterium level of WALP23Pro increases at a higher rate than that of WALP23 and WALP23Gly. In this time period, the amide hydrogens in the transmembrane region exchange [1]. In order to probe H/D exchange rate constants the data were converted to plots of the natural logarithm of the number of remaining exchangeable hydrogens (H_t) with time, showing linear segments representing populations of hydrogens exchanging at the same rate (see Figure 4 B). The rate of exchange for the remaining 13 hydrogens in WALP23Pro as determined from these logarithmic plots is about seven times higher than in WALP23 (Table III), but for WALP23Gly this rate is almost similar to that of WALP23. This suggests that the amide hydrogens in the transmembrane helix of WALP23Pro are more accessible to exchange and thus less protected, probably due to destabilization of the α-helix. In our studies Gly does not significantly disturb the α-helix character of the transmembrane part.

To further investigate the differences in exchange kinetics between WALP23Pro and WALP23, fragmentation studies were performed, which allow determination of the sites of the exchanged hydrogens [1]. Collision-induced fragmentation (CID) of Na^+ cationized hydrophobic peptides generates mostly N-terminal A_n fragment ions and C-terminal Y'_n fragment ions (see Figure 5 A). The deuterium levels in series of fragments were determined from differences in the centroids of the isotope envelopes and are represented by bar diagrams (Figures 5 B & C). Briefly, the smaller the slope in these bar diagrams, the less deuterium uptake takes place in this part of the peptide. Figure 5 B & C show a series of deuterium content plots of the fragment ions of WALP23 and WALP23Pro, respectively, both incorporated in DMPC and after various incubation times in deuterated buffer. WALP23 (as well as WALP16, WALP19 and WALP21 – not shown) has a transmembrane part that is quite stable against exchange even after very long incubation times, indicated by the flat region in the bar diagrams, while both the C-terminal ends
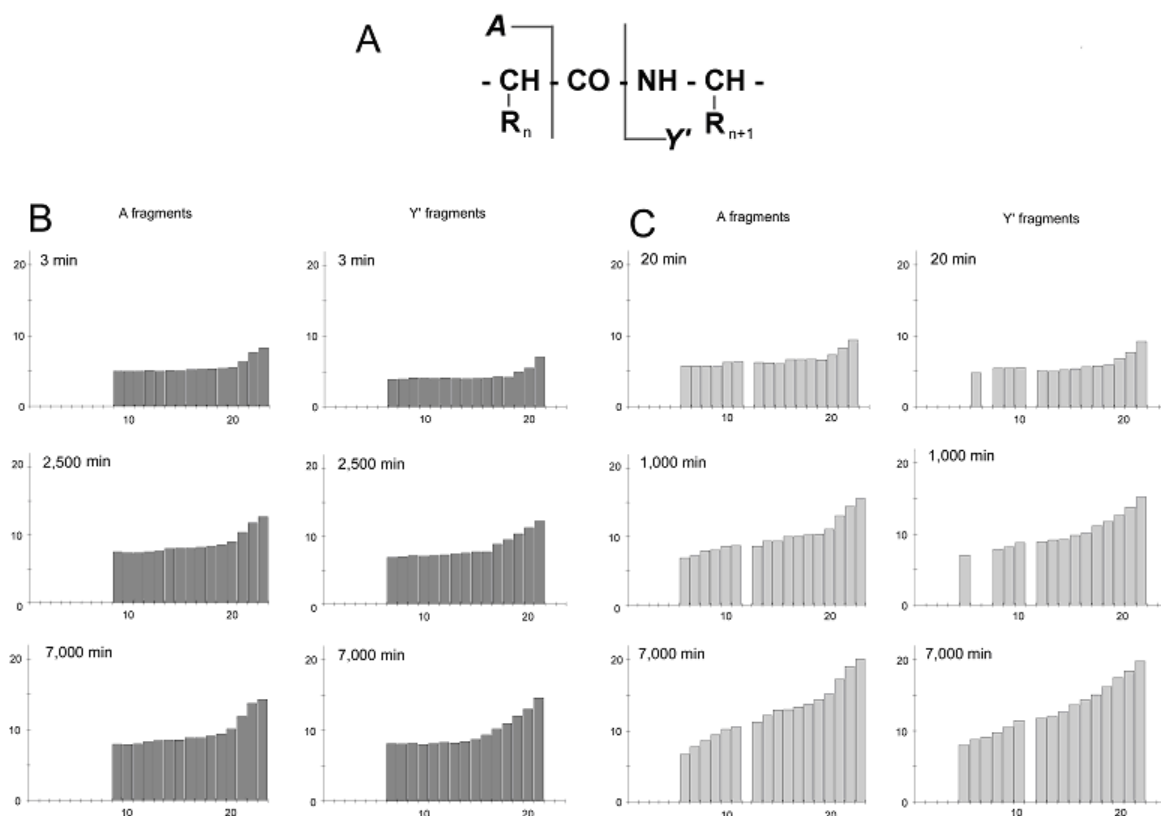
Figure 5 — Bar diagrams representing the deuterium levels of the partly deuterated A and Y' fragment ions [20] of **(B)** WALP23 and **(C)** WALP23Pro. The A_n fragment (**panel A**) comprises the amide and side chain deuteriums of the N-terminal n amino acid residues; the Y'_n fragment comprises the amide and side chain deuteriums of the C-terminal n amino acid residues plus the ethanolamine terminal group. These bar plots were constructed using CID MS spectra of the sodium cationized ion $[M+Na]^+$ of the membrane peptides incorporated in DMPC bilayers incubated in buffered D_2O for the indicated time periods. Blank entries indicate potential fragments whose signal-to-noise ratios were too weak to be analyzed accurately, except for Y'_{11} and A_{12} in WALP23Pro, which corresponds to the presence of Pro.

(higher A fragments) and the N-terminal ends (higher Y' fragments) of the peptide exchange fast. Also the termini of WALP23Pro (Figure 5 C) exchange fast, and, like in WALP23, after short incubation times there is no exchange in the segment corresponding to the transmembrane part. However, after longer incubation times the flat region in the center of WALP23Pro disappears, indicating that a significant part of the H/D exchange also takes place in the transmembrane part.

These results suggest that Pro destabilizes the α-helical structure. From the CID MS experiments it then can be concluded that destabilization is not centered around the Pro residue, but that it takes place over the entire transmembrane region.

Discussion

In this study the recently developed proteoliposome nano-flow ESI-MS technique [1] has been exploited to study the H/D exchange kinetics of a series of synthetic transmembrane peptides. These peptides were designed to gain insight into several crucial factors that can influence the positioning and stability of transmembrane peptides in lipid bilayers.

First, the effect of elongation of the hydrophobic part of transmembrane peptides with respect to the hydrophobic thickness of the bilayer was investigated. The peptides were incorporated in a DMPC bilayer and deuterium exchange kinetics of peptides that were only differing in the hydrophobic core length were studied. The hydrophobic thickness of a DMPC bilayer in the fluid phase is ≈23 Å [21]. This is close to the estimated length of the backbone of WALP16, which would be 24 Å if one assumes that it forms an ideal α-helix with a net length of 1.5 Å per amino acid. WALP23 on the other hand, would be too long for this relatively thin bilayer and would extend into the aqueous phase. If it is assumed that the part that extends out of the hydrophobic part of the bilayer exchanges fast, as was shown to occur for polar extensions on both sides of a WALP16 analog [1], then peptides that are longer than WALP16 should have a larger population of fast exchangeable hydrogens. This indeed was found to be the case. However, the number of fast exchangeable hydrogens in the longer peptides was much less than the total number of additional exchangeable hydrogens, suggesting that longer peptides somehow are more protected against exchange. There are several possibilities to explain this observation. A likely explanation is that the membrane environment itself provides increased protection, for instance by increasing its hydrophobic thickness by stretching of the phospholipid acyl chains. Such an interpretation would be in agreement with earlier results from ^{2}H-NMR experiments [2], which show that the phospholipid acyl chains are more ordered in the presence of relatively long peptides. This interpretation is schematically depicted in Figure 6 A. An alternative or additional mechanism by which the membrane environment could provide increased protection of longer peptides would be by accommodating the peptides in a tilted orientation. Infrared experiments [10] indicated that such a tilt may indeed occur, albeit only to a minor extent. Finally, one might argue that the longer core region is responsible for the larger extent of protection in longer α-helices, because more backbone amide protons will be involved in hydrogen bonding. However, the results with peptides of identical total length, but with the Trp at different positions, argue against this possibility. These peptides, WALP23inner and WALP23outer (see Table I), are expected to have an equal length of the stable core region, yet they show distinct differences in H/D exchange kinetics. It was found that the part that exhibits extremely slow exchange corresponds closely to the Trp-Trp distance in these peptides. Because tryptophans have a strong interaction with the lipid/water interface [3,11-15], these results suggest that it is the position of the helix with respect to the interface that determines the extent of exchange. Thus, it is likely that the affinity of Trp for the lipid/water interface causes the larger protection from exchange for WALP23outer as compared to WALP23inner, by inducing the bilayer to adapt at least partially to the Trp-Trp distance by either stretching of the acyl
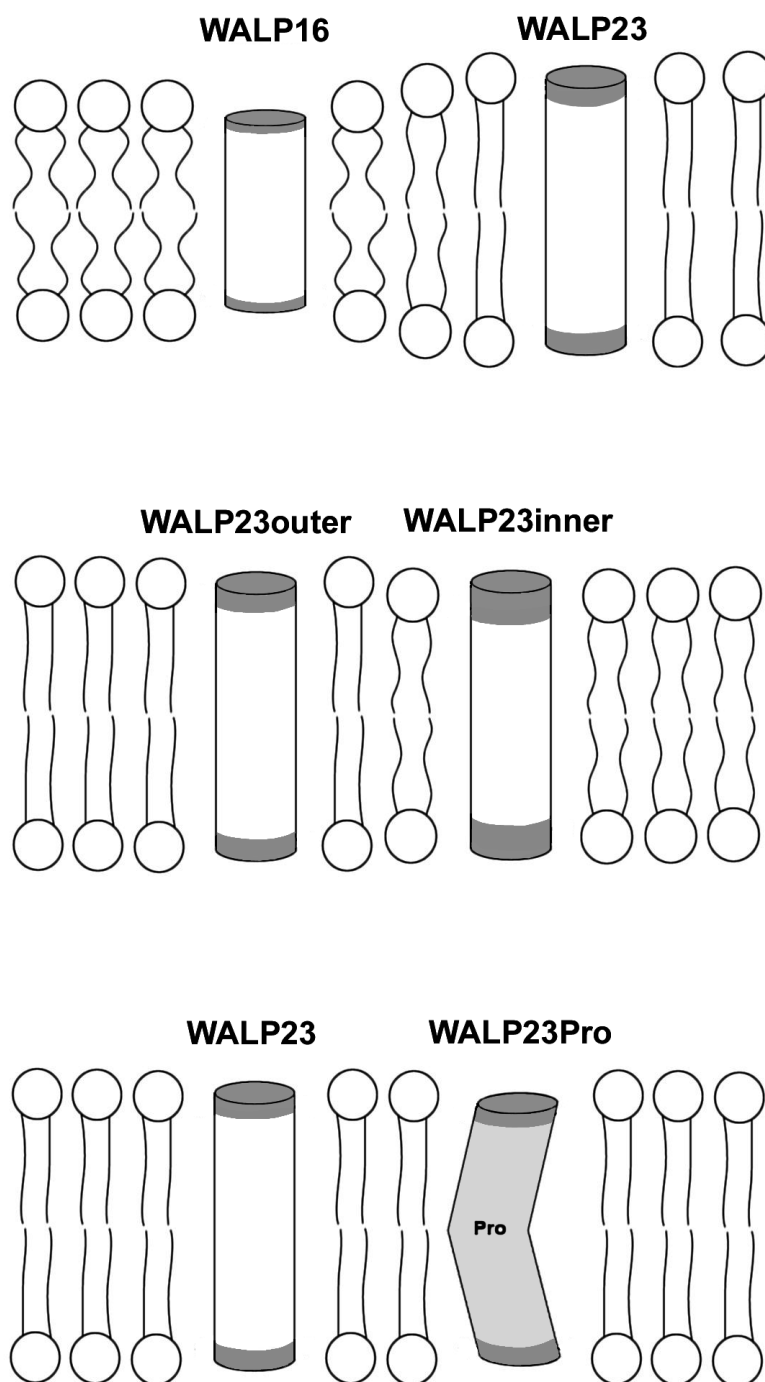
Figure 6 – Model for the incorporation of different peptides in a DMPC bilayer, depicting adaptation of the bilayer thickness as one of the possible mechanisms to explain the observed data. When a too long peptide is incorporated in the bilayer, the lipid acyl chains are able to partially adapt their hydrophobic thickness **(A)**. The gray areas indicate the parts of the peptide that are exchanging fast. Tryptophans are likely to be important for positioning in the interface region, since WALP23inner exhibits more H/D exchange than does WALP23outer **(B)**. Amide hydrogens in a transmembrane segment with a Pro residue are involved in hydrogen bonding to a lesser extent, and show faster exchange over the whole transmembrane region. Therefore, the regular transmembrane α-helix is destabilized, perhaps involving introduction of a kink in the helix **(C)**.

chains, as schematically depicted in Figure 6 B, or by accommodating the peptide in a tilted orientation.

Remarkably, WALP23 which contains two Trp residues at each side of the peptide, showed similar backbone amide exchange kinetics as WALP23outer. This suggests that the outer Trp residues are the determinants for interfacial positioning of this relatively long peptide and hence that localization of Trp residues further away from the interface towards the aqueous phase is unfavorable. Together, the results show that Trp has strong membrane anchoring properties and interacts with a well-defined region in the bilayer interface. This supports the idea that Trp residues, which have shown to be clustered at the border between the hydrophilic and hydrophobic zones both in single-spanning [8] and multispanning integral membrane proteins (e.g. [5,7]) are important for stabilizing integral membrane proteins in a lipid bilayer [3,11-15]. The observation that Trp residues may determine the precise interfacial position of transmembrane segments of proteins also is functionally relevant, since the interfacial positioning of for instance receptor proteins or channel-forming proteins can determine their accessibility to enzymes, substrates or ligands [22].

Finally, the effect of inserting specific amino acid residues that are generally known to destabilize a regular α-helix in water-soluble proteins, like Pro and Gly, was studied. The frequent occurrence of Pro in the putative transmembrane helices of integral membrane proteins, particularly transport proteins and G-coupled receptors, has led to the suggestion that the presence of this conserved amino acid residue might play a role in folding and/or assembly of integral membrane proteins in general and that it may be essential for functional activity of transport proteins and ion channels [16,23,24], because of its supposed ability to introduce kinks into transmembrane α-helices. Our results show that the presence of a Pro residue in the transmembrane helix of WALP23 leads to a significant increase in exchange after longer incubation times, whereas CID MS measurements demonstrated that exchange in the transmembrane helix region is increased. The similar exchange kinetics in the short term region of WALP23 peptides with and without Pro suggest that the peptides are anchored in the lipid bilayer interface in a similar way. Therefore, it is suggested that the presence of a Pro residue may cause a less stable helix fold of the hydrophobic core of WALP23, as schematically depicted in Figure 6 C.

There may be some other possibilities to interpret the increased H/D exchange rates for WALP23Pro as compared to WALP23. One such possibility would be that because of a Pro-induced kink in the peptide the lipid acyl chains in the vicinity of the transmembrane helix may be perturbed. This would allow an increase of water permeation in the bilayer, and, therefore, could lead to somewhat higher exchange rates specifically in the transmembrane region. In principle, an alternative possibility could be that the peptide does not have a transmembrane orientation, but instead is located on the surface of the bilayer, which also would result in higher exchange rates. However, in this case one would expect much faster exchange rates than the ones observed, because the peptide would be in direct contact with bulk deuterated water.

Indeed, control measurements on WALP23 in TFE/D$_2$O buffer (1:1; volume ratio), in which the peptide forms an α-helix (data not shown), demonstrated that under these conditions H/D exchange was already complete within less than 60 min at 30°C. Another argument against a surface localization of WALP23Pro would be the observed similarity between the numbers of fast exchangeable protons with those in WALP23, which by various techniques has been shown to adopt a transmembrane orientation [3,10]. Hence we exclude this possibility. Finally, one might consider the possibility of a slow equilibrium between surface and bound states of WALP23Pro. In this case, however, several populations of deuterated WALP23Pro (i.e. fast and slowly exchanging) should be present in the mass spectra at the same time. Since this is not observed, we exclude this latter possibility as well.

In contrast to WALP23Pro, WALP23Gly shows similar exchange kinetics as WALP23, indicating that Gly does not have a strong effect on the stability of the transmembrane helix, at least in the systems studied here. Gly has been suggested to play a role in environment-dependent α-helix modulation [25] and to mediate helix-helix interactions in membrane proteins [26]. Conformational studies on model peptides in a membrane mimetic environment [25] and analysis of dihedral backbone angles in crystal structures of several membrane proteins [27] suggested that Gly does not disrupt the secondary structure of α-helical transmembrane segments. The results of the present study support this. In summary, our results show that insertion of a Pro residue but not of Gly results in significant destabilization of a transmembrane α-helix in a lipid bilayer. The structural changes in Pro-containing transmembrane segments might be important for functional properties of membrane proteins.

This study has shown that the effect of variations in hydrophobic length, in the positions of flanking residues and of insertion of putative helix breakers in transmembrane peptides, can be studied in great detail by H/D exchange combined with mass spectrometry, whereby the positions of the exchanged hydrogens can be derived from CID MS experiments. Moreover, it was shown that it is possible to measure H/D exchange in two or more peptides simultaneously, allowing determination of very small differences in deuterium levels. Detailed information about helix stability and interfacial positioning, as obtained in the present study, not only provides insight into the factors that determine the way in which membrane proteins are integrated into a lipid bilayer, but also may be useful for predictions of transmembrane segments from amino acid sequences. In future studies we plan to extrapolate the method to larger integral membrane proteins and membrane-bound proteins.

References

1.   Demmers, J.A.A., Haverkamp, J., Heck, A.J.R., Koeppe, R.E., II & Killian, J.A. (2000) Electrospray ionization mass spectrometry as a tool to analyze hydrogen/deuterium exchange kinetics of transmembrane peptides in lipid bilayers. *Proc. Natl. Acad. Sci. U. S. A.* **97**, 3189-94.

2.   de Planque, M.R.R., Greathouse, D.V., Koeppe, R.E., II, Schafer, H., Marsh, D. & Killian, J.A. (1998) Influence of lipid/peptide hydrophobic mismatch on the thickness of diacylphosphatidylcholine bilayers. A

2H NMR and ESR study using designed transmembrane alpha-helical peptides and gramicidin A. *Biochemistry* **37**, 9333-45.

3. de Planque, M.R.R., Kruijtzer, J.A.W., Liskamp, R.M.J., Marsh, D., Greathouse, D.V., Koeppe, R.E., II, de Kruijff, B. & Killian, J.A. (1999) Different membrane anchoring positions of tryptophan and lysine in synthetic transmembrane alpha-helical peptides. *J. Biol. Chem.* **274**, 20839-46.

4. Killian, J.A., Salemink, I., de Planque, M.R.R., Lindblom, G., Koeppe, R.E., II & Greathouse, D.V. (1996) Induction of nonbilayer structures in diacylphosphatidylcholine model membranes by transmembrane alpha-helical peptides: importance of hydrophobic mismatch and proposed role of tryptophans. *Biochemistry* **35**, 1037-45.

5. Doyle, D.A., Cabral, J.M., Pfuetzner, R.A., Kuo, A.L., Gulbis, J.M., Cohen, S.L., Chait, B.T. & MacKinnon, R. (1998) The Structure of the Potassium Channel   Molecular Basis of K+ Conduction and Selectivity. *Science* **280**, 69-77.

6. Kovacs, F., Quine, J. & Cross, T.A. (1999) Validation of the single-stranded channel conformation of gramicidin A by solid-state NMR. *Proc. Natl. Acad. Sci. U. S. A.* **96**, 7910-5.

7. Iwata, S., Ostermeier, C., Ludwig, B. & Michel, H. (1995) Structure at 2.8 A resolution of cytochrome c oxidase from Paracoccus denitrificans. *Nature* **376**, 660-9.

8. Landolt Marticorena, C., Williams, K.A., Deber, C.M. & Reithmeier, R.A. (1993) Non-random distribution of amino acids in the transmembrane segments of human type I single span membrane proteins. *J. Mol. Biol.* **229**, 602-8.

9. Killian, J.A. (1998) Hydrophobic mismatch between proteins and lipids in membranes. *Biochim. Biophys. Acta* **1376**, 401-15.

10. de Planque, M.R.R., Goormaghtigh, E., Greathouse, D.V., Koeppe, R.E., II, Kruijtzer, J.A.W., Liskamp, R.M.J., de Kruijff, B. & Killian, J.A. (2001) Sensitivity of single membrane-spanning alpha-helical peptides to hydrophobic mismatch with a lipid bilayer: effects on backbone structure, orientation, and extent of membrane incorporation. *Biochemistry* **40**, 5000-10.

11. Persson, S., Killian, J.A. & Lindblom, G. (1998) Molecular ordering of interfacially localized tryptophan analogs in ester- and ether-lipid bilayers studied by 2H-NMR. *Biophys. J.* **75**, 1365-71.

12. Braun, P. & von Heijne, G. (1999) The aromatic residues Trp and Phe have different effects on the positioning of a transmembrane helix in the microsomal membrane. *Biochemistry* **38**, 9778-82.

13. Ridder, A.N.J.A., Morein, S., Stam, J.G., Kuhn, A., de Kruijff, B. & Killian, J.A. (2000) Analysis of the role of interfacial tryptophan residues in controlling the topology of membrane proteins. *Biochemistry* **39**, 6521-8.

14. Yau, W.M., Wimley, W.C., Gawrisch, K. & White, S.H. (1998) The preference of tryptophan for membrane interfaces. *Biochemistry* **37**, 14713-8.

15. Wimley, W.C. & White, S.H. (1996) Experimentally determined hydrophobicity scale for proteins at membrane interfaces. *Nat. Struct. Biol.* **3**, 842-8.

16. Eyles, S.J. & Gierasch, L.M. (2000) Multiple roles of prolyl residues in structure and folding. *J. Mol. Biol.* **301**, 737-47.

17. Greathouse, D.V., Goforth, R.L., Crawford, T., van der Wel, P.C.A. & Killian, J.A. (2001) Optimized aminolysis conditions for cleavage of N-protected hydrophobic peptides from solid-phase resins. *J. Peptide Res.* **57**, 519-27.

18. Blume, A. (1983) *Biochemistry* **22**, 5436-42.

19. Jansen, M. & Blume, A. (1995) A comparative study of diffusive and osmotic water permeation across bilayers composed of phospholipids with different head groups and fatty acyl chains. *Biophys. J.* **68**, 997-1008.

20. Roepstorff, P. & Fohlman, J. (1984) Proposal for a common nomenclature for sequence ions in mass spectra of peptides. *Biomed. Mass Spectrom.* **11**, 601.

21. Lewis, B.A. & Engelman, D.M. (1983) Lipid bilayer thickness varies linearly with acyl chain length in fluid phosphatidylcholine vesicles. *J. Mol. Biol.* **166**, 211-7.

22. Killian, J.A. & von Heijne, G. (2000) How proteins adapt to a membrane-water interface. *Trends Biochem. Sci.* **25**, 429-34.

23. Eilers, M., Shekar, S.C., Shieh, T., Smith, S.O. & Fleming, P.J. (2000) Internal packing of helical membrane proteins. *Proc. Natl. Acad. Sci. U. S. A.* **97**, 5796-801.

24. Schiffer, M., Ainsworth, C.F., Deng, Y.L., Johnson, G., Pascoe, F.H. & Hanson, D.K. (1995) Proline in a transmembrane helix compensates for cavities in the photosynthetic reaction center. *J. Mol. Biol.* **252**, 472-82.

25. Li, S.C. & Deber, C.M. (1992) Glycine and beta-branched residues support and modulate peptide helicity in membrane environments. *FEBS Lett.* **311**, 217-20.

26. Russ, W.P. & Engelman, D.M. (2000) The GxxxG motif: a framework for transmembrane helix-helix association. *J. Mol. Biol.* **296**, 911-9.

27. Javadpour, M.M., Eilers, M., Groesbeek, M. & Smith, S.O. (1999) Helix packing in polytopic membrane proteins: role of glycine in transmembrane helix association. *Biophys. J.* **77**, 1609-18.

CHAPTER 4

Factors affecting gas-phase deuterium scrambling
in peptide ions and their implications for protein
structure determination

Jeroen A.A. Demmers[1,2], Dirk T.S. Rijkers[3], Johan Haverkamp[1], J. Antoinette Killian[2]
& Albert J.R. Heck[1]

[1] Department of Biomolecular Mass Spectrometry, Bijvoet Center for Biomolecular Research and Utrecht Institute
for Pharmaceutical Sciences, Utrecht University, Sorbonnelaan 16, 3584 CA Utrecht, The Netherlands
[2] Department of Biochemistry of Membranes, Center for Biomembranes and Lipid Enzymology, Institute of
Biomembranes, Utrecht University, Padualaan 8, 3584 CH Utrecht, The Netherlands
[3] Department of Medicinal Chemistry, Utrecht Institute for Pharmaceutical Sciences, Utrecht University,
Sorbonnelaan 16, 3584 CA Utrecht, The Netherlands

Abstract

In this report, we evaluate the validity of using hydrogen/deuterium exchange in combination with collision-induced dissociation mass spectrometry (CID MS) for the detailed structural and conformational investigation of peptides and proteins. This methodology, in which partly deuterated peptide ions are subjected to collision-induced dissociation in the vacuum of a mass spectrometer, has emerged as a useful tool in structural biology. It may potentially provide quantitatively the extent of deuterium incorporation per individual amino acid in peptides and proteins, thus providing detailed structural information related to protein structure and folding. We report that this general methodology has limitations caused by the fact that the incorporated deuterium atoms migrate prior or during the CID MS analysis. Our data are focused on a variety of transmembrane peptides, incorporated in a lipid bilayer, in which the near-terminal amino acids that anchor at the lipid-water interface are systematically varied. Our findings suggest that, under the experimental conditions we use, the extent of intramolecular hydrogen scrambling is strongly influenced by experimental factors, such as the exact amino acid sequence of the peptide, the nature of the charge carrier, and therefore most likely by the gas-phase structure of the peptide ion. Moreover, the observed scrambling seems to be independent of the nature of the peptide fragment ions (i.e., protonated B and Y'' ions, and sodiated A and Y' ions). Our results strongly suggest that scrambling may be reduced by using alkali metal cationization instead of protonation in the ionization process.

Introduction

Solution phase hydrogen/deuterium (H/D) exchange in combination with electrospray ionization mass spectrometry (ESI-MS) has become a useful tool to study protein structure and conformation [1-6], protein-protein interactions and protein-membrane interfacial regions [7-10]. By determination of mass increases because of the uptake of deuterium atoms in time, global exchange kinetics can be derived. To reveal the sites of deuterium incorporation at a higher resolution, the protein can be cleaved enzymatically, and the resulting peptides can subsequently be fragmented by gas-phase collision-induced dissociation (CID) to get isotopic information. However, interpretation of CID MS data on partly deuterated peptide ions can, in principle, be hampered by both intermolecular and intra-molecular migration of hydrogens or deuteriums. Obviously, for detailed structural analysis both migration processes are undesirable and need to be addressed in detail.

Intermolecular exchange can take place when peptide ions in the gas phase undergo collisions with gaseous H_2O or D_2O in the relatively high-pressure region at the interface. Such bimolecular H/D exchange reactions of peptides and proteins in the gas phase have been studied extensively (e.g. [11-14]), and exchange rates have been proposed to be dependent on a number of factors, like gas-phase proton affinity, accessibility of exchangeable sites at the surface, and the structure of the molecule.

In addition, isotopic information can be depleted by intramolecular migration of hydrogens or deuteriums (a process also referred to as 'scrambling'), which involves the redistribution of hydrogen isotopes over the peptide ion as a consequence of high hydrogen mobility. Under what conditions the process of hydrogen migration within peptides takes place is not fully understood [15,16]. It may be that scrambling occurs induced by the numerous collisions with neutral gas molecules during the collisional activation and, therefore, would be a direct consequence of the peptide fragmentation process. Alternatively, it could be that scrambling occurs earlier in the analysis process, for example, somewhere during the ionization process or in between the ionization and collisional activation.

In the literature, conflicting results have been reported about scrambling in peptide ions. In several studies, it has been shown that hydrogen mobility within peptide ions is sufficiently rapid to scramble their position even prior to collisional activation [11,17,18], whereas in other studies, it has been claimed that intramolecular migration of amide hydrogens is minor or even negligible [8,10,16,19-22]. As H/D exchange in combination with CID MS is used more and more for structural and conformational investigations of proteins and peptides, it is very important to understand the factors underlying deuterium scrambling and to find ways to control or prevent this process.

In our research, we aim to use H/D exchange in combination with CID MS to study in detail the structural interactions of transmembrane proteins and peptides within the membrane. We showed before [9,10] that H/D exchange in hydrophobic transmembrane peptides can be measured by mass spectrometry by direct introduction of these (normally insoluble) peptides using vesicular structures of phospholipid bilayers dispersed in aqueous buffer. To obtain more detailed information on the architecture of the transmembrane peptides in the bilayer, we performed CID MS experiments on the partly deuterated peptides [9,10]. In these previous studies no significant amount of deuterium scrambling was observed, which allowed us to determine the nature of peptide-model membrane interactions. However, in these experiments, only transmembrane peptides consisting of a Leu-Ala sequence of variable length and flanked by Trp residues were used. Because these peptides could hardly be protonated because of their hydrophobicity and lack of charged residues, all experiments in these previous studies were performed on sodiated peptide species. To test whether this CID MS based method is also valid for protonated peptide species, as well as for peptides containing different flanking residues, we decided to address this issue in more detail. The goal of the present study was therefore to systematically investigate the possible occurrence of deuterium scrambling and to elucidate the influence of several crucial experimental factors on scrambling during CID MS.

In our experiments, we make use of peptides with a general acetyl-$GX_2(LA)_nLX_2A$-ethanolamine/amide sequence (where X is a variable residue and $n = 7$ or 8), which are incorporated in phospholipid bilayers in an α-helical manner and in a transmembrane orientation, as verified by oriented circular dichroism, polarized Fourier transform infrared spectroscopy, and nuclear magnetic resonance spectroscopy measurements [23-25]. All

experiments were performed at neutral pH. Both the protonated and the sodium cationized species were then subjected to CID MS. This system is very suitable to study the extent of deuterium scrambling during CID MS for several reasons. First, the time window in which the peptides remain only partly deuterated is very long as the exchange rates in the hydrophobic core of the peptide are extremely low in contrast with water-soluble peptides of similar length [9,10]. As a consequence, it is possible to perform CID MS experiments on the full length peptides at time points when the deuterium content is relatively constant with respect to the time it takes to perform such an experiment. Consequently, there is no need for lowering the pH in order to quench H/D exchange, which might introduce unwanted side effects. Second, as we may get full sequence coverage over the transmembrane peptides in the CID MS fragmentations, there is no need for prior digestion of the protein into smaller peptides, which may complicate the interpretation of the data. Finally, a set of transmembrane peptides is available, which vary only in the near-terminal amino acid residues. The hydrophobic core and the terminal residues are kept invariant. Because of these reasons, we believe that this experimental system provides a unique opportunity to study the influence of specific factors on the extent of scrambling.

Materials and methods

Chemicals - The peptides WALP21, WALP23, KALP23, HALP23, FALP21, YALP21 (see Table I) were synthesized as described previously [23,24]. K*ALP23 (see Table I) was obtained by reductive methylation of KALP23. Reductive methylation was performed using a modified procedure based on previously published methods [26,27]. Briefly, 10 μmol of KALP23 peptide was dissolved in 25 ml dioxane/methanol/0.6 M $NaHCO_3$ (14:5:1, v/v/v) and the pH was raised by addition of 100 μl of a 20 g NaOH/L solution. Subsequently, 320 μmol of 37% formaldehyde diluted with dioxane/methanol (1:1, v/v) was added, giving an 8-fold excess of formaldehyde over the numbers of lysine residues present. $NaBH_3CN$ dissolved in acetonitrile/water (1:1, v/v) was added in small portions to a final concentration of 20 mM. The reaction mixture was stirred for 18 h at room temperature. The identity of the peptide after methylation was determined by ESI MS/MS, which showed that each of the lysine side-chain nitrogens was dimethylated.

Trifluoroacetic acid (TFA) was obtained from Merck (Darmstadt, Germany), and 2,2,2-trifluoroethanol (TFE) from Sigma (St. Louis, MO). Deuterium oxide (>99.9 % D) was obtained from Aldrich Chemical Company, Inc. (Milwaukee, WI, USA) and was stored under nitrogen at 4°C. Sodium iodide was from OPG Farma Company (Utrecht, The Netherlands). Ammonium acetate was from Fluka (Switzerland). The phospholipid dimyristoylphosphatidylcholine (DMPC) was obtained from Avanti Polar Lipids Inc. (Birmingham, AL).

Proteoliposome preparation - Peptide incorporation into phospholipid vesicles and ESI MS measurements were performed essentially as described previously [9,10]. Briefly, peptides were dissolved in TFE (1 mg/ml). The peptide solutions in TFE were added to a DMPC solution in

Table I — Sequences of transmembrane peptides used (variable flanking residues are bold-faced).

Peptide	Sequence
FALP21	Ac-G**FF**LALALALALALALAL**FF**A-Am
HALP23	Ac-G**HH**LALALALALALALAL**HH**A-Am
KALP23	Ac-G**KK**LALALALALALALAL**KK**A-Am
K*ALP23	Ac-G**K*K***LALALALALALALAL**K*K***A-Am
WALP21	Ac-G**WW**LALALALALALALAL**WW**A-Etn
WALP23	Ac-G**WW**LALALALALALALAL**WW**A-Etn
YALP21	Ac-G**YY**LALALALALALALAL**YY**A-Am
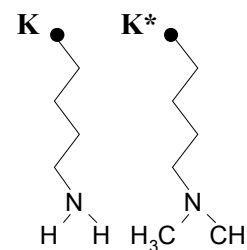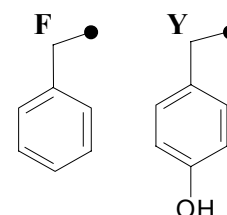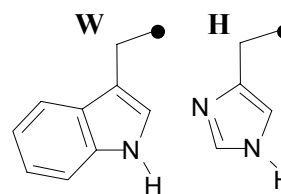
Abbreviations: Ac: acetyl; Am: amide; Etn: ethanolamide; A: alanine; F: phenylalanine; G: glycine; H: histidine; K: lysine; L: leucine; W: tryptophan; Y: tyrosine, K*: lysine with di-methylated side-chain nitrogen. For chemical structure of amino acid side-chains: see panel on the right.

methanol (1 ml; 12 mM) and vigorously vortexed. The solvent was removed by evaporation in a rotary evaporator. The mixed films were then dried for 24 h under vacuum. The films were hydrated in 0.5 ml 10 mM ammonium acetate buffer (pH 7.5). Large unilamellar vesicles (LUVETs) were prepared by extrusion through a 200 nm filter. H/D exchange was initiated by diluting the LUVET suspensions 50 times in 20 mM ammonium acetate deuterated buffer (pD 7.5). The final concentration of the peptides was approximately 10 µM. When sodium-cationized species were studied, sodium iodide was added to a final concentration of 1 mM. At selected time points, 2 µl of this diluted suspension was transferred into a gold-coated glass capillary, and the measurement was started as quickly as possible. The deadtime between dilution and measurement was 1 min.

ESI MS measurements - ESI MS measurements were performed on a quadrupole time-of-flight instrument (Q-Tof; Micromass Ltd., Manchester, UK) operating in positive ion mode and equipped with a Z-spray nano-ESI source, or an LCQ ion trap instrument (ThermoQuest), equipped with a Protana source setup. Nano-ESI capillaries were prepared as described before [9]. The nano-ESI capillary was positioned approximately 5 mm before the orifice of the mass spectrometer. For MS experiments on the Q-Tof instrument the quadrupole was set in the RF-only mode to act as an ion guide to efficiently link the ESI ion source with the reflectron time-of-flight analyzer. The potential between the nano-ESI capillary and the orifice of the mass

spectrometer was typically set to 1.8 kV, and the cone voltage to 80 V. The source temperature was 80°C. In MS/MS mode, the quadrupole was used to select precursor ions, which were fragmented in the hexapole collision cell, generating product ions that were subsequently mass analyzed by the orthogonal time-of-flight mass analyzer. For MS/MS measurements on the Q-Tof instrument, the collision energy was set to values between 80 and 100 V for sodiated peptides, and between 40 and 60 V for protonated peptides. Argon was used as collision gas at a pressure of 25 psi. The quadrupole mass resolution parameters were set to a relatively large mass window in order to select the entire isotope envelope of the precursor ions. The reflectron time-of-flight parameters were set such that the fragment ions were detected at more than unit mass resolution, as required to obtain isotopically resolved (fragment) ion peaks.

For MS experiments on the LCQ, the capillary temperature was set to 150°C. The capillary voltage and spray voltage were set to 20 V and 0.90-1.20 kV, respectively. The tube lens offset was 50 V. In the ion optics, the octapoles were set to –3.90 and –19.0 V, and the lens voltage was –40 V. The maximum injection time was chosen to be 1000 ms. For MS/MS measurements on the LCQ, the collision energy was set to 80% for Na^+-cationized parent ions. The entire isotope envelopes were selected for CID MS analysis.

Deuterium uptake calculations - The increases in deuterium content of the peptide fragments (in Da) was calculated by using the average mass-to-charge (m/z) values of the isotope clusters of the nondeuterated peptide (fragments) and the partly deuterated peptide (fragments), as described more detailed previously [9].

Results

Global H/D exchange profiles - Global H/D exchange profiles of the peptides given in Table 1 were determined to verify their incorporation in a transmembrane orientation in the phospholipid bilayer. These peptides vary primarily in the flanking residues (bold-faced in Table I). Global H/D exchange of the transmembrane peptides was measured by diluting the vesicle dispersions 1:50 in buffered D_2O. A mass spectrum obtained after introducing vesicles of KALP23/DMPC directly into a Q-Tof mass spectrometer (Figure 1) was dominated by intense signals of phospholipid monomers and small oligomers. Still the protonated (and to a lesser extent) the sodiated KALP23 were visible and isotopically resolved. The inset shows at the top the nondeuterated peptide ions and at the bottom the partly deuterated peptide ions following dilution of the vesicle dispersion in D_2O.

All peptides investigated show a similar distinct exchange pattern when the number of protected hydrogens is plotted versus incubation time in D_2O (Figure 2 A). The fast initial global exchange of approximately 2/3 of all exchangeable hydrogen atoms for all vesicle-incorporated XALP peptides studied reveals that these hydrogens are easily accessible to the deuterated solvent. For all peptides, the deuterium uptake levels off after approximately 10 min, although there is still a substantial amount of exchangeable hydrogen atoms left. This indicates that the
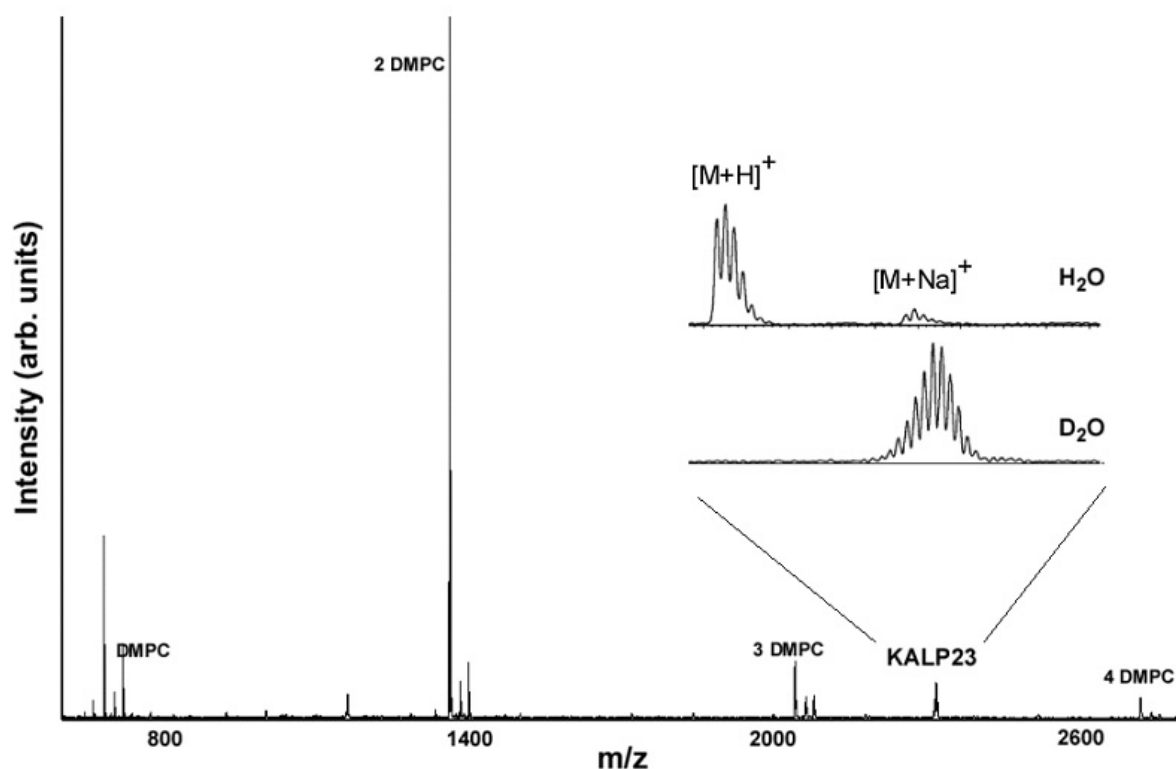
Figure 1 – Mass spectrum obtained after introducing KALP23/DMPC vesicles (ratio 1:25) directly from ammonium acetate buffer solution (no extra sodium iodide added) into a Q-Tof mass spectrometer. The DMPC monomers, as well as dimers, trimers and tetramers (2 DMPC, 3 DMPC and 4 DMPC, respectively), are clearly visible. KALP23 is observed mainly as a protonated species (m/z 2288), although some sodium ionized ions can be observed as well at m/z values 22 Da higher than the protonated species. The inset shows the non-deuterated peptide sprayed from vesicles dispersed in H_2O buffer, as well as the partly deuterated peptide sprayed from vesicles dispersed in D_2O buffer after an incubation time of 24 h. The mass increase was in this case about 25 Da.

peptides have a protected part in which the hydrogens exchange only at extremely low rates. The number of protected amide hydrogens was found to be in agreement with the number of amino acid residues in the hydrophobic core of the peptide, as has been shown before for a somewhat shorter WALP peptide analog [9]. It is therefore believed that the region of the peptide that is well protected from H/D exchange must be embedded in the hydrophobic core of the bilayer (see Figure 2 B). Moreover, additional protection from exchange could be caused by the involvement of these amide hydrogens in hydrogen bonding in the transmembrane α-helical structure [9,10]. Several complementary experiments confirm this hypothesis. Circular dichroism measurements have revealed that all WALP peptides and KALP23 (as well as FALP21, YALP21 and HALP23, unpublished data), are soluble in phosphatidylcholine-systems and form stable α-helices [25]. The shorter protected region in KALP23 with respect to the other peptides can be

explained by the different anchoring behavior of a lysine residue in the lipid bilayer headgroup region [24].

Control experiments with fully deuterated peptides indicated that no back-exchange of either backbone or side-chain hydrogens took place during MS and CID MS analysis.
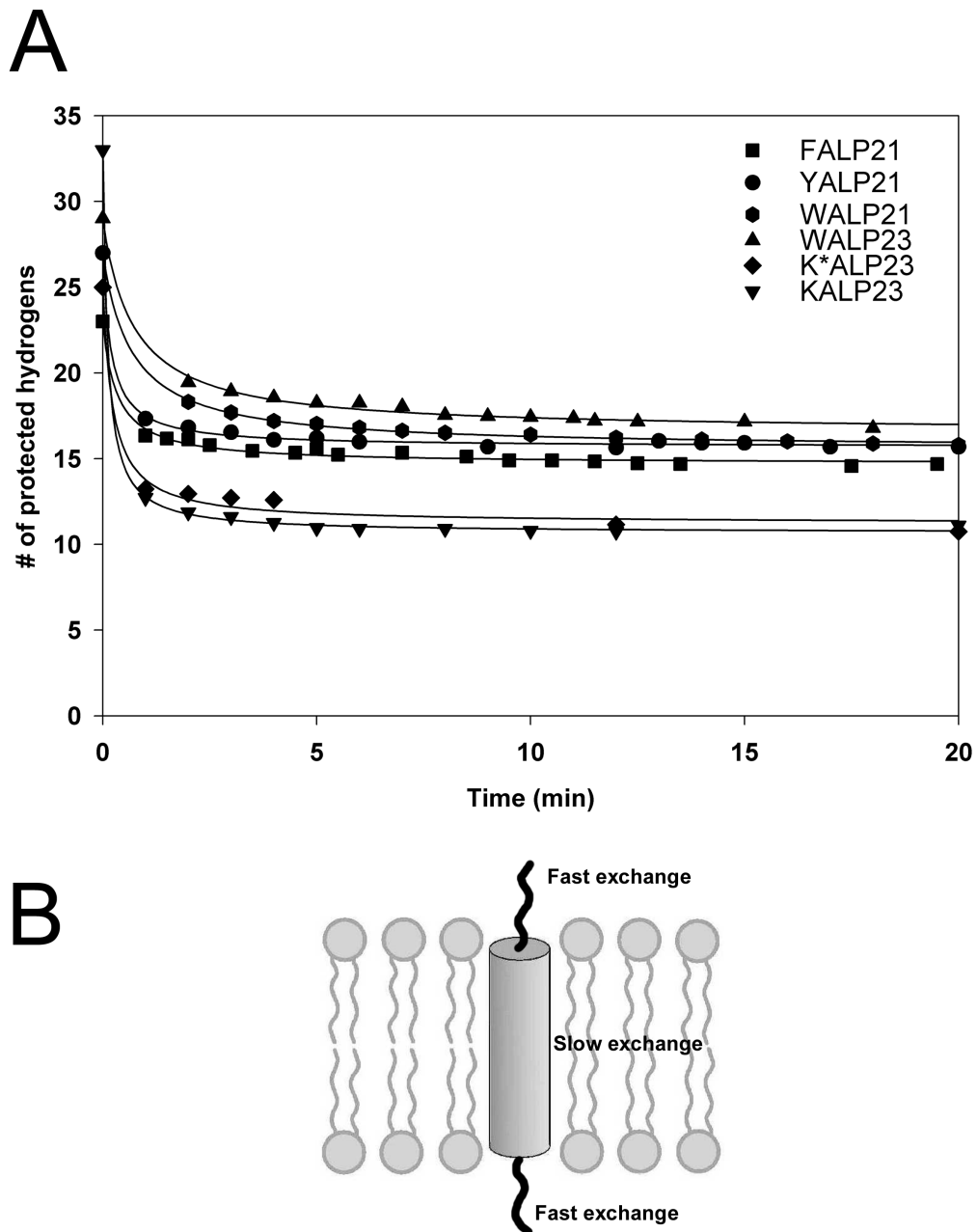

Figure 2 – (A) Global H/D exchange curves of several transmembrane peptides. All peptides were reconstituted in phospholipid bilayers and subsequently incubated in D$_2$O buffer and sprayed directly from buffer solution. **(B)** Proposed incorporation model of transmembrane peptides in a phospholipid bilayer.

Effect of selected amino acid mutations on deuterium scrambling - In our earlier work on WALP peptides, we showed by using CID MS that specifically the transmembrane parts of the peptides were protected from H/D exchange, as nearly no deuteriums were incorporated in these parts of the peptides [9,10]. To illustrate this further, Figure 3 A shows the average deuterium content for all detected fragment ions of sodiated WALP23 precursor ions. In all experiments described in this section, CID MS was performed on the sodiated peptide ion, approximately 20 min after dilution in D_2O, allowing only easily accessible hydrogens to be exchanged. In the N-terminal A fragment ion series (for nomenclature, see ref. [28]) going from A_9 to A_{20}, the deuterium content increases only very little (plateau in the plot), suggesting that there is no significant deuterium uptake in the sequence region from Ala9-Leu20. The small increase in deuterium content might indicate (1) a very limited amount of scrambling, possibly involving the tryptophan side chains, or (2) a limited amount of H/D exchange in the peptide core. Because A_9 was the smallest fragment ion observed in the CID MS spectrum, only information about the C-terminal part of the peptides could be derived from this fragment ion series. However, the complementary Y' fragment ion series gave similar information about the deuterium uptake in the N-terminal region (data not shown). The results in Figure 3 D show the deuterium content profile for the A fragment ions of sodiated KALP23 precursor ions derived from CID MS experiments. In sharp contrast with the pattern for WALP23, the nearly linearly increasing curve suggests that the hydrogen and deuterium atoms have scrambled randomly over all available sites. For K*ALP23 (Figure 3 B), in which the lysine side-chains were dimethylated, the deuterium content profile is quite different from that of KALP23. Instead of a random distribution of deuterium over the available sites as observed for KALP23, there is clearly a less steep gradient in the middle region of the diagram, indicating less deuterium incorporation in the transmembrane part. On the other hand, HALP23 (Figure 3 C) and FALP21 (Figure 3 E), like WALP23, seem to show a partly protected region. The plateau, however, is less pronounced than in the case of WALP23, revealing more scrambling in these cases. Finally, YALP21 shows a deuterium incorporation pattern resembling more KALP23 than WALP23.

The observations described here indicate that the scrambling is heavily dependent on the nature of the amino acid in the flanking residues. This dependence will be discussed in more detail below.

Effect of cationization on deuterium scrambling - All data shown above were obtained from sodium-cationized peptides, since in general these hydrophobic peptides were rather difficult to protonate. To determine the influence of the nature of the charge carrier on the extent of scrambling, protonated as well as sodium-, potassium- and cesium-cationized transmembrane peptides were subjected to CID MS. Both the $[M+H]^+$ and $[M+Na]^+$ species of FALP21, HALP23, KALP23, K*ALP23, and WALP23 could be generated and subjected to CID MS, although the spectra of the protonated ions of the latter two were of relatively poor quality due to low signal-to-noise ratios. In general, CID MS spectra of protonated species predominantly
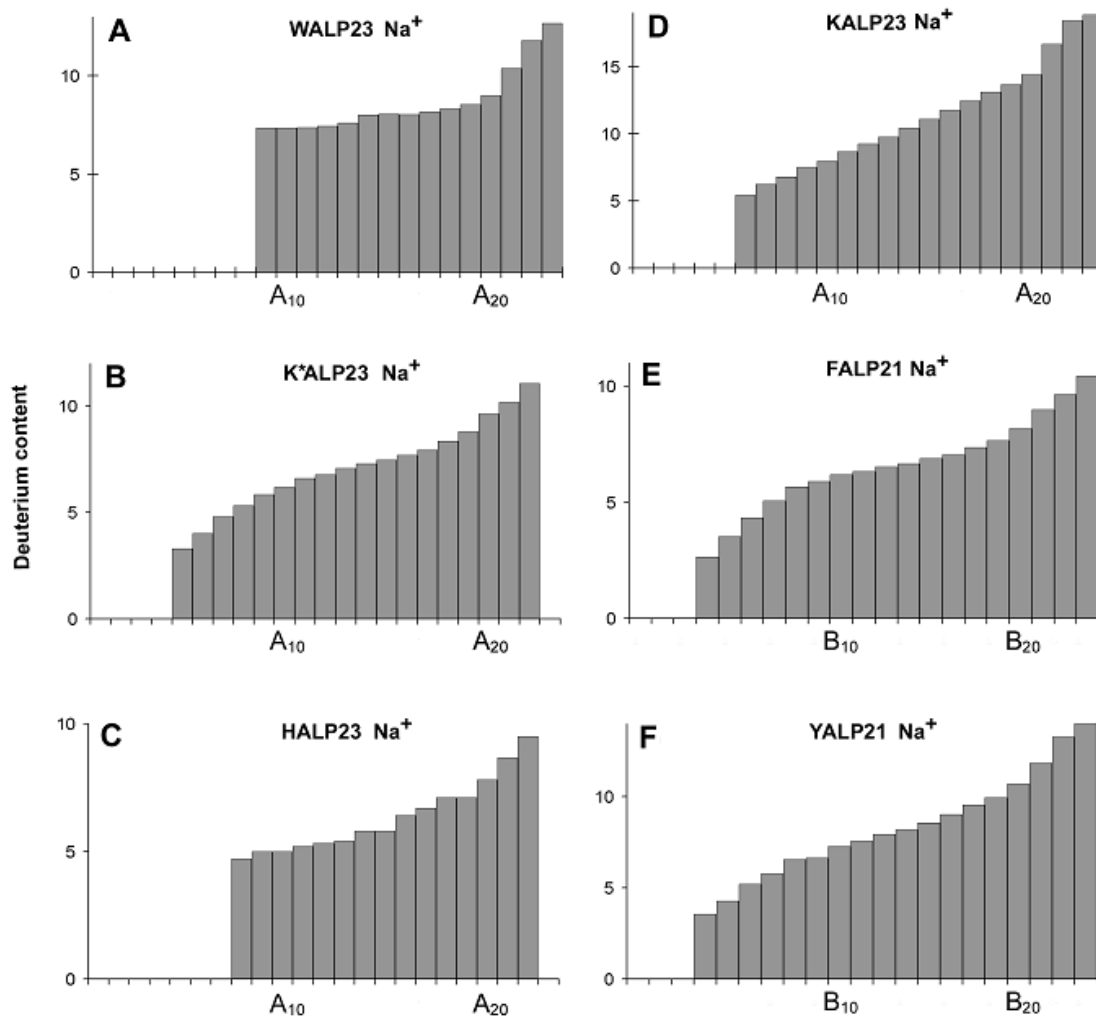
Figure 3 – Deuterium content profiles of A fragment ions of partly deuterated sodium cationized **(A)** WALP23, **(B)** K*ALP23, **(C)** HALP23, **(D)** KALP23, **(E)** FALP21, **(F)** YALP21. Although only deuterium content profiles for the A ion series are shown here, the sodiated Y' fragment gave similar patterns.

showed B and Y'' ions, whereas the sodium-, potassium- and cesium-cationized species gave rise primarily to A and Y' fragment ions (nomenclature according to ref. [28]).

In Figure 4, the resulting deuterium content profiles for the fragment ions of protonated WALP23, K*ALP23 and HALP23 are given. The protonated ion pairs were generated from the same solution as the sodiated ones and studied under identical conditions, so they are directly comparable to the sodiated ones in Figures 3 A-C. The bar diagrams indicate that there are clear differences in deuterium content profiles between CID fragments of protonated and sodium-cationized peptides. In general, fragmentation of sodium-cationized peptides results in profiles, indicating little deuterium uptake in the hydrophobic core. In contrast, CID MS on the complementary protonated peptides resulted in most cases in deuterium distributions randomly distributed over all exchangeable sites.
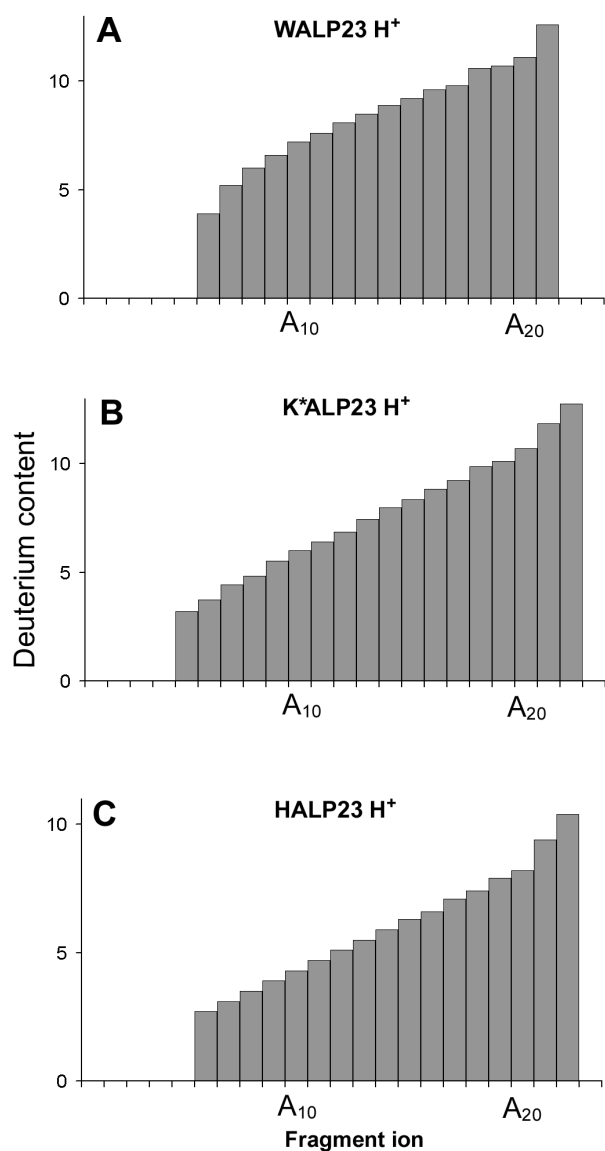
Figure 4 – Deuterium content profiles of B fragment ions of partly deuterated protonated **(A)** WALP23, **(B)** K*ALP23, **(C)** HALP23. Although only deuterium content profiles for the B ion series are shown here, the protonated Y" fragment gave similar patterns.

Even WALP23, which did not show much scrambling for the sodium cationized species, shows a deuterium distribution pattern that indicates substantial scrambling when the protonated ions are studied. Also, the other protonated peptides showed a more random distribution of deuterium atoms over all exchangeable sites. Apparently, under the conditions used here fragmentation of protonated peptide ions does not result in deuterium profiles that are useful for the analysis of protected parts in the transmembrane peptide.

To investigate whether the sodium cationized ion was unique in generating such deuterium profiles, or whether the size of the charge carrier also can influence the extent of scrambling, experiments were performed with potassium- and cesium-cationized peptide ions. Fragmentation of both K^+-and Cs^+-cationized HALP23, KALP23 and K*ALP23 peptides resulted in the formation of mainly A and Y' fragment ions, comparable to Na^+ cationized species, although the amount of collision energy had to be increased. The deuterium patterns for

K$^+$- and Cs$^+$-cationized peptides were similar to those of the Na$^+$ cationized peptides (data not shown).

Effect of the instrumental set-up on deuterium scrambling - To study whether the observed behavior could be an artifact of the used instrument (Q-Tof), CID MS experiments on a representative set of sodiated WALP peptides were also performed on a LCQ ion trap. Not only is the interface different, also the collisional activation process, including the reaction time, is somewhat different from the process as it occurs in the Q-Tof. Our data revealed that, in general, very similar deuterium uptake patterns could be extracted from the CID MS data taken on the hybrid Q-ToF and the LC-Q ion trap (data not shown).

Additionally, using the Q-Tof, in-source fragmentation experiments were performed as an alternative to CID MS in the quadrupole collision cell. We performed these experiments to test whether the time window for ion fragmentation might have an influence on the observed deuterium scrambling. K*ALP23 and WALP23 were measured using relatively high cone- and extraction voltages in the absence of collision gas. The disadvantage of this "nozzle-skimmer" dissociation is that there is no precursor ion selection. Still, the spectra recorded under these harsh conditions revealed many B and Y" fragment ions of both K*ALP23 and WALP23, indicating that mostly the [M+H]$^+$ species of these peptide ions were fragmented. Although the signal-to-noise ratio was poor, the deuterium content plot obtained from this data showed a similar pattern as the one obtained from the protonated ions that were subjected to CID in the collision cell (data not shown).

Discussion

Comparison to other H/D exchange CID MS studies - H/D exchange in combination with gas-phase sequencing by CID MS of proteolytic peptide ions has become a frequently used method to probe structural properties of peptides and proteins [8,10,16,19-22]. The CID MS fragment ion data are used to resolve deuterium incorporation per amino acid in the protein. This interpretation of the CID MS data is only valid if deuterium scrambling prior to and during ion fragmentation can be excluded. In the present study, we have investigated parameters that influence the extent of deuterium scrambling in model transmembrane peptides. We do observe extensive scrambling, which seems to be in contrast to several of the above-mentioned studies. Therefore, we first consider some differences in experimental conditions between our and the more conventional studies and the influence they may have on the scrambling process.

Solution-phase conditions, such as pH, temperature, and nature of the solvent, are important parameters in H/D exchange. In the conventional studies mentioned above, the peptide/protein sample is incubated in a buffered D$_2$O solution at physiological pH. This is similar to our studies with the addition that the transmembrane peptides are now embedded in a phospholipid bilayer. In the analysis stage, in the conventional studies, a pH and temperature drop (pH = 2-3, T = 0 °C) are introduced, which "freeze" the exchange (and/or back-exchange). We do not introduce such a step as our data reveal that after a few minutes of incubation the

exchange rates in the lipid membrane environment are already close to 0. Therefore, the ionization process starts in our case from an aqueous solution at neutral pH, with the peptides embedded in the phospholipid bilayer. In the conventional studies the peptide/protein ionization process starts from a cold, acidic, often aqueous/organic mixed solution. It cannot be excluded that these differences have an effect on possible H/D scrambling during the ionization process. As in our case, the ionization process is performed from a solution at a more physiological pH, and the rates for possible exchange are expected to be higher. Additionally, the presence of the phospholipid molecules may influence H/D scrambling during the ionization process. We should therefore be careful in directly comparing our results to those obtained in more conventional studies. Still, we envisage that scrambling mostly occurs in the gas-phase during the activation and fragmentation step in the CID process. We note that extensive scrambling has been reported in some conventional studies as well for C-terminal ions [16,21,22], albeit not for the complementary N-terminal ions. Our data reveal similar extents of scrambling for both types of ions. As the applied CID MS procedure is identical in all studies, we suggest that H/D scrambling is a process that should be properly addressed in all studies that combine H/D exchange with CID MS.

Quantification of deuterium scrambling - To quantify the extent of scrambling in our system, we define two limiting cases. In the first case, which we term the *statistical state*, the total deuterium content of the peptide is assumed to be statistically distributed over all available exchangeable sites in the peptide. This model therefore predicts that the subsequent fragment ions show a regular increase of deuterium content, which is only dependent on the number of exchangeable hydrogens present on each particular amino acid. The second limiting case we define as the *core-protected state*. In this model, we assume that the hydrophobic core region of the peptide is completely protected from exchange. In this *core-protected state*, the total number of deuterium atoms is first distributed over the terminal amino acids, which are not part of the inner hydrophobic core, whereas the remaining deuterium atoms are then added to the core region starting from the termini. This model would be in agreement with the expected positioning of transmembrane peptides in a lipid bilayer.

We can calculate the deuterium content for each peptide fragment generated by CID MS predicted by both models. This was done taking a 23-residue peptide with one exchangeable hydrogen in its flanking residues as an illustration. The resulting deuterium profiles are depicted schematically in Figure 5.

The results indicate that all experimental deuterium distributions of the different peptides can be classified using these limiting case models. When the patterns in Figure 3 are compared, it is evident that the deuterium distribution in the fragment ions of WALP23 follows to a large extent the core-protected state model, whereas the distribution for KALP23 closely follows the statistical state model.
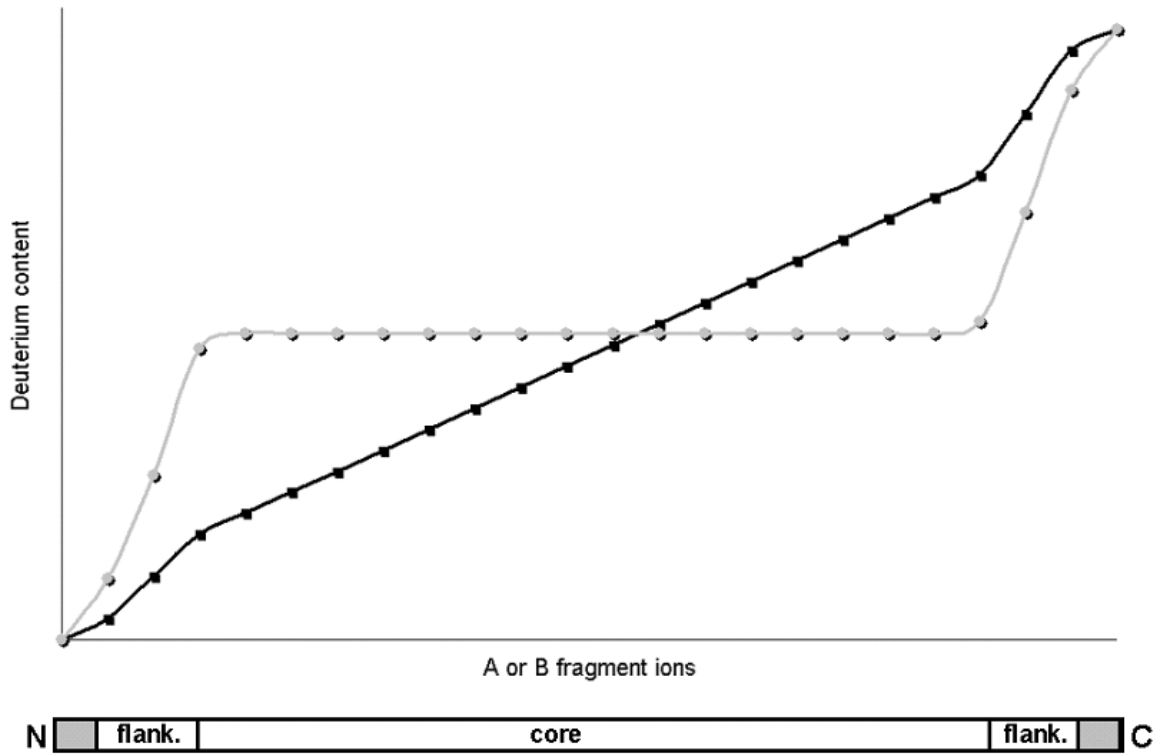
Figure 5 – Schematic representation of the deuterium content in each fragment ion in the two limiting hypothetical cases of deuterium distribution over a 23-residue peptide, with flanking residues that have one exchangeable hydrogen in the side chain. The calculated deuterium content per fragment ions according to the *statistical state* model, in which full scrambling occurs, is depicted as a black line. The *core-protected* model, characterized by its slope of zero in the middle region, is represented by a gray line (see text for detailed description). For peptides with flanking amino acids that do not contain exchangeable hydrogens, the curves are somewhat different and the calculations were adjusted.

For a more quantitative description of the extent of scrambling in the studied peptides, the deviations between the experimental and predicted deuterium content of the peptide fragments according to both models were compared using Eq. **(1)**. From these deviations a scrambling factor (SF) was determined for each different peptide ion.

$$
\textbf{(1)} \qquad \textbf{SF} = \frac{\sum\limits_{i}^{N} \left| \Delta (D_{st} - D_{co}) \right| - \sum\limits_{i}^{N} \left| \Delta (D_{st} - D_{ex}) \right|}{\sum\limits_{i}^{N} \left| \Delta (D_{st} - D_{co}) \right|}
$$

In this formula $\Delta(D_{st}-D_{co})$ is the deviation between the deuterium content per fragment ion in the *statistical state* model and the *core-protected* model, $\Delta(D_{st}-D_{ex})$ is the deviation between the

deuterium content per fragment ion in the statistical state model and the experimental values, i is the individual subsequent fragment ions, and N is the total number of fragment peaks of which the mass increase could be determined from the CID MS spectra. The scrambling factor is thus defined as between 0 (indicating no scrambling) and 1 (representing a state with a statistical distribution of all deuterium atoms). The calculated scrambling factors are graphically shown in Figure 6, as a function of the charge carrier (H^+ or Na^+) and flanking amino acid. Some interesting features may be extracted from these data. The smallest scrambling factor observed is 0.23 for sodium cationized WALP23. On the other end of the scale, protonated KALP23 reveals a scrambling factor of nearly 1. Of all transmembrane peptides studied here, these peptides represent the most extreme cases. From the calculated scrambling factors, it can be concluded not only that the variation in the charge carrier has a dramatic effect on the extent of deuterium scrambling, but also that different amino acids can induce various degrees of scrambling. This is in agreement with results reported by Buijs *et al.* [15] on the role of different amino acids on the extent of hydrogen migration in peptide ions. From the data presented, it can be concluded that the overall order of scrambling-inducing capacity of the studied flanking residues is the same for both the protonated and sodium cationized peptide ions, that is, K > Y > H > K* > F > W.
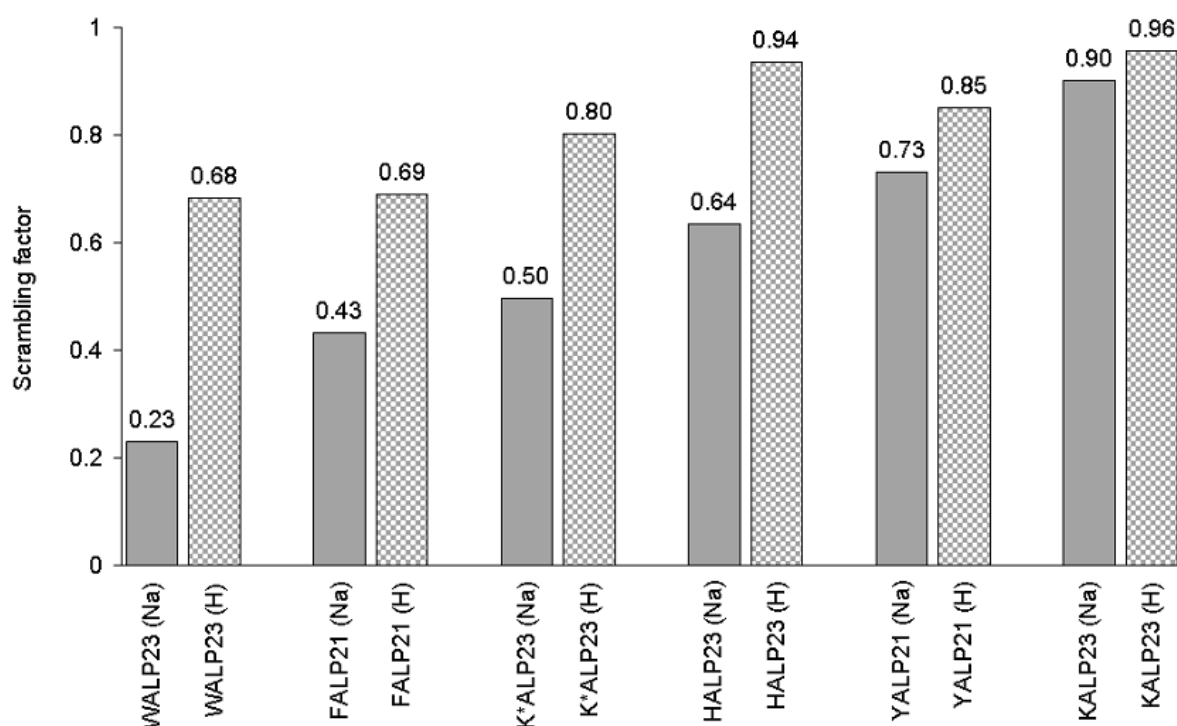

Figure 6 — Scrambling factors for sodium-cationized and protonated peptides with variable flanking residues. The numbers were calculated using Eq. (1) with two extreme hypothetical cases as reference values (see text for details). Scrambling factors of sodium-cationized species are given as solid bars, and those of protonated species as block patterned bars.

The most direct indication that suggests the importance of the presence of exchangeable hydrogens at the flanking residues in the scrambling process comes from the substantial difference between sodium cationized KALP23 (SF_{Na+} 0.90) and K*ALP23 (SF_{Na+} 0.50). However, as Phe does not have exchangeable side-chain hydrogens, this reasoning cannot be used to explain the observation that there is less scrambling in WALP23 (SF_{Na+} 0.23) than in FALP21 (SF_{Na+} 0.43). Moreover, significant differences are even observed between Trp-, His- and Tyr-flanked transmembrane peptides, which all have one exchangeable side-chain hydrogen. Also, YALP21 (SF_{Na+} 0.73) showed more scrambling than both FALP21 and HALP23 (SF_{Na+} 0.64), although Tyr is more polar than Phe, and less polar than His. Therefore, the polarity of the amino acid cannot directly be correlated with the extent of scrambling. Also, there does not seem to be a direct relationship between the gas phase proton affinity of the flanking residues and the extent of scrambling, since HALP23 and WALP23 have similar scrambling factors although their gas phase proton affinities are quite different (see Table II). Finally, the length of the hydrophobic stretch between the flanking residues does not seem to affect the amount of scrambling significantly, since a much longer KALP peptide (31 residues) revealed as much scrambling as KALP23 (not shown), and a shorter WALP peptide (16 residues) was similar to WALP23 [9,10].

The differences observed resulting from the different charge carriers are probably easier to interpret. The extent of scrambling seems to be highly dependent on the charge carrier being a proton or an alkali metal ion. In all cases, fragmentation of the sodium-cationized species resulted in (far) less scrambling when compared to the protonated species. Interestingly, much more collision energy has to be transferred into the peptide ions to induce fragmentation in the sodium-cationized peptides when compared to the protonated species. The higher activation energy in sodium-cationized does not seem to lead to increase in the extent of scrambling. Our results suggest that the *less* activated protonated ions are more prone to hydrogen migration than the *more* activated sodiated ions. We therefore hypothesize that in the gas-phase the sodium ion is more fixed into a specific position, whereas the proton may more easily migrate between the different basic sites available in the peptide ion. This hypothesis is in agreement with the mobile proton model [29,30]. Our findings may suggest that the proton in the protonated species acts as a catalyst for deuterium scrambling.

Ion mobility studies [31-33] have revealed that gas-phase structures of ions may be very different from the solution-phase structures of their neutral counterparts and that they are highly dependent on the sequence of the peptides. For instance, in studies on poly-Ala derived peptides the position of only one incorporated Lys residue spectacularly changed the gas-phase conformation [31,32]. On the other hand, peptide ion conformations in the gas-phase are dependent on the nature of the charge carrier [13,34]; there are several indications that sodium-cationized peptides adopt in the gas-phase a more compact structure than their protonated counterparts, which may render them less prone to hydrogen migration. We therefore propose that the observed trends in deuterium scrambling could be caused by differences in gas-phase

structures and energetics of the studied system. It is difficult to speculate about the possible structures the ions may adopt in the gas-phase and about how these structures relate to the observed scrambling. To get a better view on this subject, it would be interesting to perform ion mobility studies on these ions, possibly in combination with theoretical structure and dynamics calculations.

Table II – Gas-phase proton affinity (according to ref. [35]) and number of exchangeable hydrogens for each flanking amino acid residue.

Residue	Gas phase proton affinity (kcal/mol)	# of exchangeable side-chain hydrogens
H	230.5	1
K	228.7	2
W	223.5	1
Y	220.7	1
F	219.9	0
K*	n.d.	0

General conclusion - The results obtained in this study indicate that intramolecular deuterium migration (scrambling) can occur during CID MS analysis. The extent of scrambling was found to be highly dependent on the nature of the charge carrier and the exact amino acid sequence, whereas it was independent of the type of mass spectrometer, as well as on the type of fragment ions studied. In general, alkali ion-cationized peptide ions revealed much less scrambling when compared to their protonated counterparts. It would therefore be advisable to implement this observation in structure and dynamics calculations. Moreover, the amino acid sequence of the peptide drastically influences the extent of deuterium scrambling, but it was difficult to correlate the observed trends directly to the molecular composition of the amino acid.

We conclude that although in general some detailed information on peptide and protein structural elements may be obtained by combining H/D exchange and CID MS, care has to be taken in the interpretation of the data as deuterium scrambling may influence the outcome of such measurements.

References

1. Smith, D.L., Deng, Y. & Zhang, Z. (1997) Probing the non-covalent structure of proteins by amide hydrogen exchange and mass spectrometry. *J. Mass Spectrom.* **32**, 135-46.

2. Engen, J.R. & Smith, D.L. (2001) Investigating protein structure and dynamics by hydrogen exchange MS. *Anal. Chem.* **73**, 256A-65A.

3. Tito, P., Nettleton, E.J. & Robinson, C.V. (2000) Dissecting the hydrogen exchange properties of insulin under amyloid fibril forming conditions: a site-specific investigation by mass spectrometry. *J. Mol. Biol.* **303**, 267-78.

4. Wood, T.D., Chorush, R.A., Wampler, F.M., 3rd, Little, D.P., O'Connor, P.B. & McLafferty, F.W. (1995) Gas-phase folding and unfolding of cytochrome *c* cations. *Proc. Natl. Acad. Sci. U. S. A.* **92**, 2451-4.

5. Maier, C.S., Schimerlik, M.I. & Deinzer, M.L. (1999) Thermal denaturation of Escherichia coli thioredoxin studied by hydrogen/deuterium exchange and electrospray ionization mass spectrometry: monitoring a two-state protein unfolding transition. *Biochemistry* **38**, 1136-43.

6. Wagner, D.S., Melton, L.G., Yan, Y., Erickson, B.W. & Anderegg, R.J. (1994) Deuterium exchange of alpha-helices and beta-sheets as monitored by electrospray ionization mass spectrometry. *Protein Sci.* **3**, 1305-14.

7. Mandell, J.G., Baerga-Ortiz, A., Akashi, S., Takio, K. & Komives, E.A. (2001) Solvent accessibility of the thrombin-thrombomodulin interface. *J. Mol. Biol.* **306**, 575-89.

8. Akashi, S. & Takio, K. (2000) Characterization of the interface structure of enzyme-inhibitor complex by using hydrogen-deuterium exchange and electrospray ionization Fourier transform ion cyclotron resonance mass spectrometry. *Protein Sci.* **9**, 2497-505.

9. Demmers, J.A.A., Haverkamp, J., Heck, A.J.R., Koeppe, R.E., II & Killian, J.A. (2000) Electrospray ionization mass spectrometry as a tool to analyze hydrogen/deuterium exchange kinetics of transmembrane peptides in lipid bilayers. *Proc. Natl. Acad. Sci. U. S. A.* **97**, 3189-94.

10. Demmers, J.A.A., van Duijn, E., Haverkamp, J., Greathouse, D.V., Koeppe 2nd, R.E., Heck, A.J.R. & Killian, J.A. (2001) Interfacial positioning and stability of transmembrane peptides in lipid bilayers studied by combining hydrogen/deuterium exchange and mass spectrometry. *J. Biol. Chem.* **276**, 34501-8.

11. McLafferty, F.W., Guan, Z.Q., Haupts, U., Wood, T.D. & Kelleher, N.L. (1998) Gaseous Conformational Structures of Cytochrome-C. *J. Am. Chem. Soc.* **120**, 4732-40.

12. Cassady, C.J. (1998) Gas-phase reactivity and molecular modeling studies on triply protonated dodecapeptides that contain four basic residues. *J. Am. Soc. Mass Spectrom.* **9**, 716-23.

13. Kaltashov, I.A., Doroshenko, V.M. & Cotter, R.J. (1997) Gas phase hydrogen/deuterium exchange reactions of peptide ions in a quadrupole ion trap mass spectrometer. *Proteins* **28**, 53-8.

14. Heck, A.J.R., Jorgensen, T.J.D., O'Sullivan, M., von Raumer, M. & Derrick, P.J. (1998) Gas-phase noncovalent interactions between vancomycin-group antibiotics and bacterial cell-wall precursor peptides probed by hydrogen/deuterium exchange. *J. Am. Soc. Mass Spectrom.* **9**, 1255-66.

15. Buijs, J., Hagman, C., Hakansson, K., Richter, J.H., Hakansson, P. & Oscarsson, S. (2001) Inter- and intra-molecular migration of peptide amide hydrogens during electrospray ionization. *J. Am. Soc. Mass Spectrom.* **12**, 410-9.

16. Deng, Y.Z., Pan, H. & Smith, D.L. (1999) Selective Isotope Labeling Demonstrates That Hydrogen Exchange at Individual Peptide Amide Linkages Can Be Determined by Collision Induced Dissociation Mass Spectrometry. *J. Am. Chem. Soc.* **121**, 1966-7.

17. Harrison, A.G. & Yalcin, T. (1997) Proton Mobility in Protonated Amino-Acids and Peptides. *Int. J. Mass Spectrom.* **165**, 339-47.

18. Johnson, R.S., Krylov, D. & Walsh, K.A. (1995) Proton Mobility Within Electrosprayed Peptide Ions. *J. Mass Spectrom.* **30**, 386-7.

19. Eyles, S.J., Speir, J.P., Kruppa, G.H., Gierasch, L.M. & Kaltashov, I.A. (2000) Protein conformational stability probed by Fourier transform ion cyclotron resonance mass spectrometry. *J. Am. Chem. Soc.* **122**, 495-500.

20. Akashi, S., Naito, Y. & Takio, K. (1999) Observation of hydrogen-deuterium exchange of ubiquitin by direct analysis of electrospray capillary-skimmer dissociation with courier transform ion cyclotron resonance mass spectrometry. *Anal. Chem.* **71**, 4974-80.

21. Anderegg, R.J., Wagner, D.S., Stevenson, C.L. & Borchardt, R.T. (1994) The Mass Spectrometry of Helical Unfolding in Peptides. *J. Am. Soc. Mass Spectrom.* **5**, 425-33.

22. Kim, M.Y., Maier, C.S., Reed, D.J. & Deinzer, M.L. (2001) Site-Specific Amide Hydrogen/Deuterium Exchange in E. coli Thioredoxins Measured by Electrospray Ionization Mass Spectrometry. *J. Am. Chem. Soc.* **123**, 9860-6.

23. Killian, J.A., Salemink, I., de Planque, M.R.R., Lindblom, G., Koeppe, R.E., II & Greathouse, D.V. (1996) Induction of nonbilayer structures in diacylphosphatidylcholine model membranes by transmembrane alpha-helical peptides: importance of hydrophobic mismatch and proposed role of tryptophans. *Biochemistry* **35**, 1037-45.

24. de Planque, M.R.R., Kruijtzer, J.A.W., Liskamp, R.M.J., Marsh, D., Greathouse, D.V., Koeppe, R.E., II, de Kruijff, B. & Killian, J.A. (1999) Different membrane anchoring positions of tryptophan and lysine in synthetic transmembrane alpha-helical peptides. *J. Biol. Chem.* **274**, 20839-46.

25. de Planque, M.R.R., Goormaghtigh, E., Greathouse, D.V., Koeppe, R.E., II, Kruijtzer, J.A.W., Liskamp, R.M.J., de Kruijff, B. & Killian, J.A. (2001) Sensitivity of single membrane-spanning alpha-helical peptides to hydrophobic mismatch with a lipid bilayer: effects on backbone structure, orientation, and extent of membrane incorporation. *Biochemistry* **40**, 5000-10.

26. Jentoft, N. & Dearborn, D.G. (1979) Labeling of proteins by reductive methylation using sodium cyanoborohydride. *J. Biol. Chem.* **254**, 4359-65.

27. Dottavio-Martin, D. & Ravel, J.M. (1978) Radiolabeling of proteins by reductive alkylation with [14C]formaldehyde and sodium cyanoborohydride. *Anal. Biochem.* **87**, 562-5.

28. Roepstorff, P. & Fohlman, J. (1984) Proposal for a common nomenclature for sequence ions in mass spectra of peptides. *Biomed. Mass Spectrom.* **11**, 601.

29. Dongre, A.R., Jones, J.L., Somogyi, A. & Wysocki, V.H. (1996) Influence of peptide composition, gas-phase basicity, and chemical modification on fragmentation efficiency: Evidence for the mobile proton model. *J. Am. Chem. Soc.* **118**, 8365-74.

30. Wysocki, V.H., Tsaprailis, G., Smith, L.L. & Breci, L.A. (2000) Special feature: Commentary - Mobile and localized protons: a framework for understanding peptide dissociation. *J. Mass Spectrom.* **35**, 1399-406.

31. Hudgins, R.R., Ratner, M.A. & Jarrold, M.F. (1998) Design of helices that are stable *in vacuo*. *J. Am. Chem. Soc.* **120**, 12974-5.

32. Kinnear, B.S., Hartings, M.R. & Jarrold, M.F. (2001) Helix unfolding in unsolvated peptides. *J. Am. Chem. Soc.* **123**, 5660-7.

33. Wyttenbach, T., von Helden, G. & Bowers, M.T. (1996) Gas-phase conformation of biological molecules: Bradykinin. *J. Am. Chem. Soc.* **118**, 8355-64.

34. Reyzer, M.L. & Brodbelt, J.S. (2000) Gas-phase H/D exchange reactions of polyamine complexes: (M + H)+, (M + alkali metal+), and (M + 2H)2+. *J. Am. Soc. Mass Spectrom.* **11**, 711-21.

35. Bojesen, G. & Breindahl, T. (1994) On the Proton Affinity of Some Alpha-Amino-Acids and the Theory of the Kinetic Method. *J. Chem. Soc.-Perkin Trans. 2* **5**, 1029-37.

CHAPTER 5

Interaction of the K+ channel KcsA with membrane phospholipids as studied by ESI mass spectrometry

Jeroen A.A. Demmers[1,2], Annemieke van Dalen[1], Ben de Kruijff[1], Albert J.R. Heck[2] & J. Antoinette Killian[1]

1. Department of Biochemistry of Membranes, Center for Biomembranes and Lipid Enzymology, Institute of Biomembranes, Utrecht University, The Netherlands
2. Department of Biomolecular Mass Spectrometry, Bijvoet Center for Biomolecular Research and Utrecht Institute for Pharmaceutical Sciences, Utrecht University, The Netherlands

Abstract

In this study we have used electrospray ionization mass spectrometry (ESI-MS) to investigate interactions between the bacterial K⁺ channel KcsA and membrane lipids. KcsA was reconstituted into lipid vesicles of variable lipid composition. These vesicles were directly analyzed by ESI-MS or mixed with trifluoroethanol (TFE) before analysis. In the resulting mass spectra non-covalent complexes of KcsA and phospholipids were observed with an interesting lipid specificity. The anionic phosphatidylglycerol (PG), and, to a lesser extent, the zwitterionic phosphatidylethanolamine (PE), which both are abundant bacterial lipids, were found to preferentially associate with KcsA as compared to the zwitterionic phosphatidylcholine (PC). We hypothesize that these preferred phospholipids represent lipids that directly interact with the protein in the phospholipid bilayer and remain attached to the protein during the analysis.

Introduction

An important characteristic of integral membrane proteins is the presence of hydrophobic membrane spanning segments, which are compatible for interactions with membrane lipids. In order to understand functioning of membrane proteins at the molecular level, it is necessary to gain knowledge about the interactions between these proteins and the lipids which surround them. The enormous diversity of membrane lipids, comprising zwitterionic phospholipids (e.g. phosphatidylcholine (PC) and phosphatidylethanolamine (PE)), anionic phospholipids (e.g. phosphatidylglycerol (PG), phosphatidic acid (PA) and phosphatidylinositol), sphingolipids and sterols suggests a specific involvement of such lipids in particular cellular processes. Indeed, for several membrane lipid classes, roles in functioning, oligomerization and assembly of membrane proteins have been established. Whether such effects are caused by direct interactions between lipids and proteins, or whether they are indirect effects on the proteins involved, is unclear.

A large array of experimental biophysical techniques is available to study interactions between integral membrane proteins and lipids. However, electrospray ionization mass spectrometry (ESI-MS) has to our knowledge never been used for this purpose, even though it has been proven to be a suitable technique to study non-covalent interactions between proteins [1-3] and between soluble proteins and phospholipids [4]. We have shown before that it is possible to perform direct ESI-MS experiments on phospholipid membrane vesicles containing transmembrane peptides [5,6]. This method may also be suitable for investigation of interactions between integral membrane proteins and phospholipids. Here we explore this possibility using KcsA as a model protein.

KcsA is a homotetrameric K⁺ channel from *Streptomyces lividans* [7]. The crystal structure is known, as well as many aspects of its channel function [8-13]. It is a predominantly α-helical integral membrane protein with each monomer containing two transmembrane segments. The protein can be expressed with an N-terminal His-tag in *E. coli*, which after purification can be functionally reconstituted into lipid bilayers [7]. It has been found recently that specific lipids can

significantly promote assembly and oligomerization of newly synthesized KcsA and that they also can increase the stability of KcsA reconstituted in model membranes [14].

Using KcsA reconstituted in lipid vesicles of varying composition we show here that non-covalent interactions between KcsA and phospholipids can be detected by ESI-MS. It is shown that anionic lipids as well as PE have an increased affinity for KcsA as compared to PC. This specificity is very similar to that observed in membrane assembly and tetramer stability, suggesting that direct and specific lipid-KcsA interactions are involved in those processes [14].

Experimental

Materials - The phospholipids 1,2-dioleyl-*sn*-glycero-3-phosphocholine (DOPC), 1,2-dipalmitoleoyl-*sn*-glycero-3-phosphocholine (DPoPC), 1,2-dioleyl-*sn*-glycero-3-phosphoethanolamine (DOPE), 1,2-dioleyl-*sn*-glycero-3-phosphate (DOPA), 1,2-dioleyl-*sn*-glycero-3-phosphoglycerol (DOPG) and 1,2-dieicosenoyl-*sn*-glycero-3-phosphocholine (DEiPC) were supplied by Avanti Polar Lipids Inc. (Birmingham, AL). n-Dodecyl-β-D-maltoside (DDM) was from Anatrece Inc. Bio-Beads SM-2 Adsorbent from Bio-Rad Laboratories. KcsA was expressed and purified with an N-terminal His-tag as described [14].

Preparation of LUVETs - Dry films of mixtures of phospholipids were prepared by mixing the appropriate amounts of lipids dissolved in chloroform and evaporation of the solvent under a stream of nitrogen. These films were dried overnight under vacuum to remove all solvent. They were then rehydrated at room temperature in 50 mM Tris-Cl (pH 7.4) to a final concentration of 10 mM phospholipid. The resulting multilamellar vesicles were vortexed and freeze–thawed (10 cycles). Finally, the vesicle suspensions were extruded 10 times through 0.2 µm polycarbonate filters, resulting in the formation of unilamellar vesicles (LUVETs).

Reconstitution of KcsA - Reconstitution of KcsA in lipid bilayer vesicles was performed as described [14]. Briefly, LUVETs were solubilized with Triton X-100 and mixed with KcsA in 1 mM DDM in 1:150 protein:lipid molar ratio. The detergent was removed using BioBeads, according to the manufacturer's procedure, which resulted in the formation of proteoliposomes. The proteoliposomes were collected by centrifugation for 1 h at 100 krpm at 4°C (TLA 120.2 rotor) and subsequently resuspended in the desired volume of 50 mM Tris-Cl buffer (pH 7.4).

Mass spectrometry - MS measurements were performed on an electrospray ionization time-of-flight (ESI-ToF) instrument (LC-T; Micromass Ltd., Manchester, UK), operating in positive ion mode and equipped with a Z-spray nano-flow ESI source. Nano-flow ESI capillaries with a relatively large tip opening were prepared from borosilicate glass capillaries (Kwik-Fil™, World Precision Instruments Inc., Sarasota, Florida) on a P-97 puller (Sutter Instrument Co., Novato, CA). The capillaries were coated with a thin gold layer (approx. 500 Å) using an Edwards Scancoat sputter-coater 501 (at 40 mV, 1 kV, for 200 sec). Basically, three different MS experiments were performed. For measuring the molecular mass of the KcsA monomer, the protein was first extracted from detergent solution with organic solvents, primarily according to

[15]. The KcsA solution in 90% formic acid was sprayed using a capillary voltage of 1500 V and a cone and extraction voltage of 50 and 0 V, respectively. When proteoliposome dispersions with reconstituted KcsA at neutral pH were directly introduced into the mass spectrometer (according to [5]), voltages were set to relatively high values to allow detection of protein signals. Typically, the capillary voltage was set to 2800 V, and the cone and extraction cone to 200 and 50 V, respectively. Finally, by mixing these proteoliposome suspensions with the organic solvent TFE in a 1:1 or 1:5 ratio, protein ions could be observed using more gentle experimental parameters (i.e., capillary voltage 1800 V, cone voltage 80 V; the extraction cone voltage was varied between 0 and 50 V).

Results

For characterization of KcsA, first the exact mass of the protein was measured. Figure 1 shows the mass spectrum of purified KcsA including the His-tag in 90% formic acid. The numbers indicate the charge states. The deconvoluted spectrum (inset) reveals a major peak with a total mass of 19274.33 ± 0.13 Da, which is in agreement with the theoretical value for KcsA of 19274.43 Da and with earlier measurements [15], indicating that the majority of the protein is not
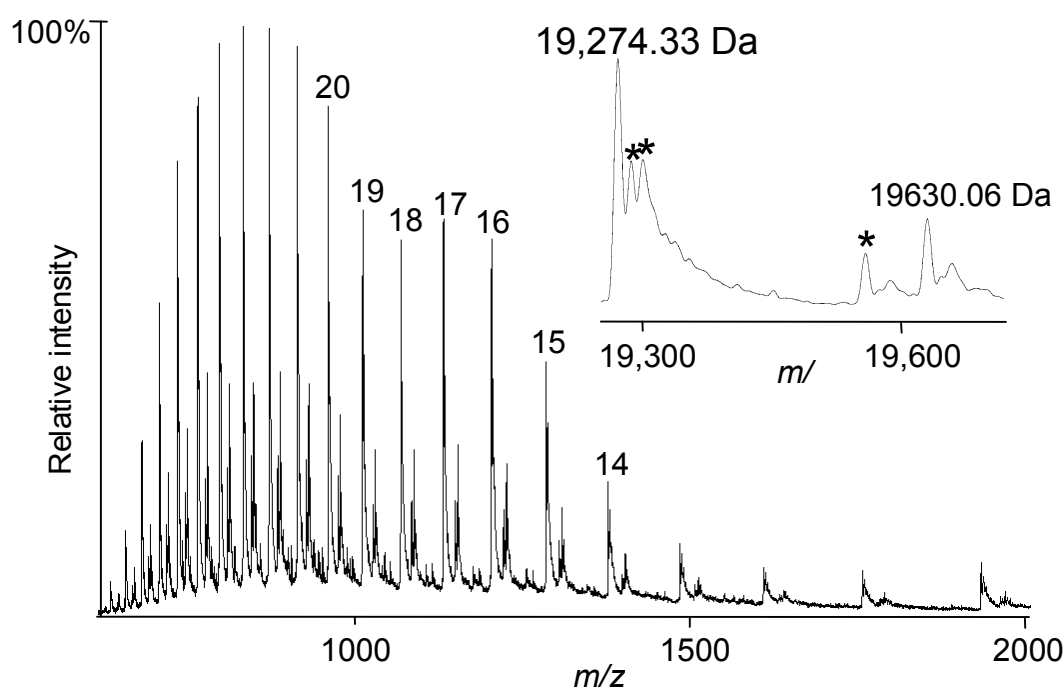
Figure 1 – ESI-ToF mass spectrum of KcsA in 90% formic acid. The deconvoluted spectrum (inset) gives a total mass for KcsA of 19274.33 ± 0.13 Da. The extra peaks indicated by asterisks were only observed when the protein was sprayed from formic acid and may represent formylation products of the protein. The second series of peaks in the spectrum with an average intensity of about one fourth of the KcsA peaks represents a compound with a mass of 19630.06 ± 0.93 Da (see text for details).

post-translationally modified when overexpressed in *E. coli*. Besides the peak series representing KcsA, there is a series representing a minor compound with a mass of 19630.06 ± 0.9 Da. This compound most likely represents a covalently modified KcsA protein. The identity of this modification (≈355 Da) will be subject of a forthcoming study. Here we focus only on the full-length KcsA protein.

Figure 2 – ESI-ToF mass spectrum of KcsA reconstituted in lipid vesicles (DOPC/DOPG, 1:1) sprayed directly from an aqueous 50 mM Tris-Cl buffer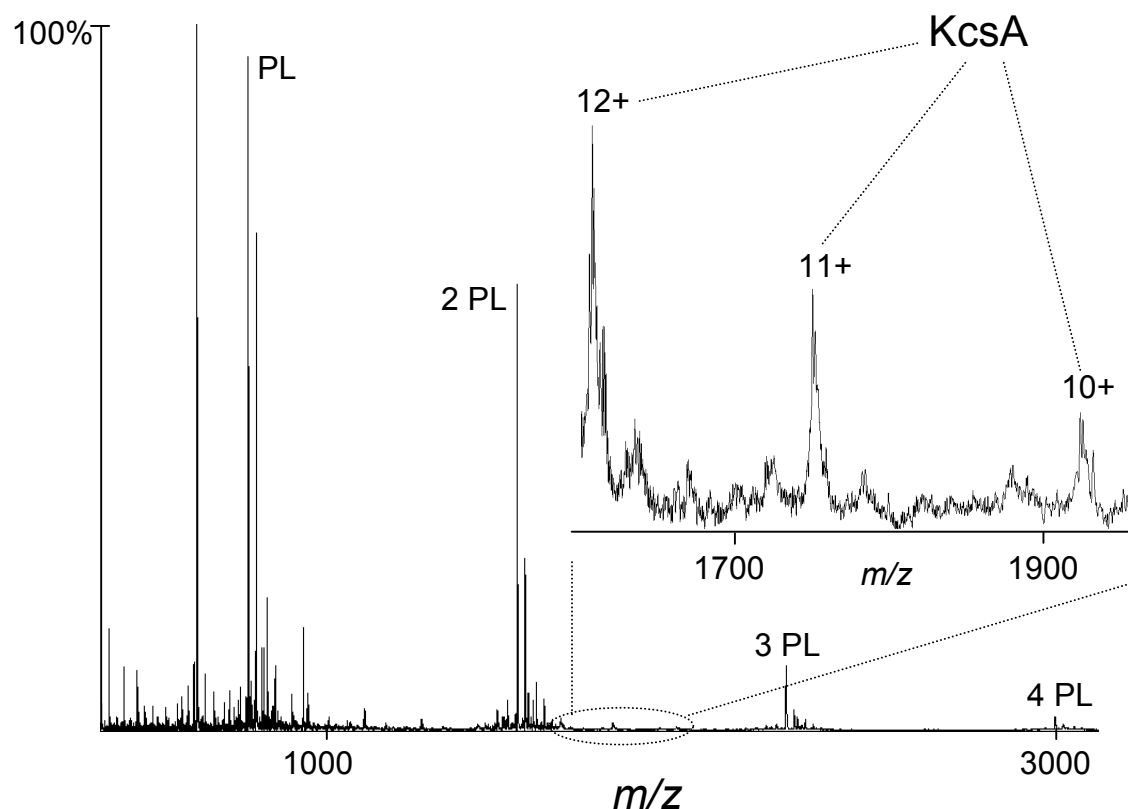 solution (pH 7.4). The most intense peaks are from phospholipid (PL) ions and singly or multiply charged oligomers of phospholipids. KcsA is visible by its 10+, 11+ and 12+ charge states (inset). The intensity of the KcsA peaks is only about 1-2 % of that of the base peak in the spectrum, but still the signal-to-noise ratio is substantial.

In order to study possible interactions of KcsA with specific phospholipid classes, KcsA was first reconstituted in proteoliposomes of DOPC and DOPG, in which the KcsA tetramer is highly stable. Figure 2 shows the spectrum of DOPC/DOPG (1:1) vesicles with reconstituted KcsA directly introduced into the mass spectrometer by ESI from an aqueous buffer solution. The major peaks represent phospholipid multimers. In addition, several low-intensity peaks around *m/z* 1800 representing charge states of KcsA are clearly visible. Only monomeric KcsA was detected in the mass spectrum, although under the used conditions KcsA is present as a tetramer in the bilayer [16]. A likely explanation is that the settings were too harsh to allow non-

covalent interactions to stay intact (see 'Discussion'). Also, no protein-phospholipid complexes could be detected.

Because the proteoliposome spraying technique required harsh conditions and because it was difficult to obtain reproducible protein signals of sufficient intensity with this technique, dispersions were mixed with TFE, which is often used as a membrane-mimicking solvent. Spectra of vesicle dispersions with TFE, using more gentle experimental conditions, showed much higher signal-to-noise ratios than obtained for the direct proteoliposome approach (see for example Figure 3). Nevertheless, again only ions of the KcsA monomer could be detected. However, under these conditions satellite peaks of KcsA signals were observed, which were assigned to non-covalent complexes of the protein and phospholipid molecules. Figure 3 shows a mass spectrum of KcsA, reconstituted in vesicles of DPoPC/DOPG (1:1), with the inset showing the satellite peaks. Comparison of insets A and B reveals that increasing the extraction cone voltage results in a decrease in the relative intensities of these satellite peaks as compared to the KcsA peaks, demonstrating that these satellite peaks indeed represent non-covalent complexes.
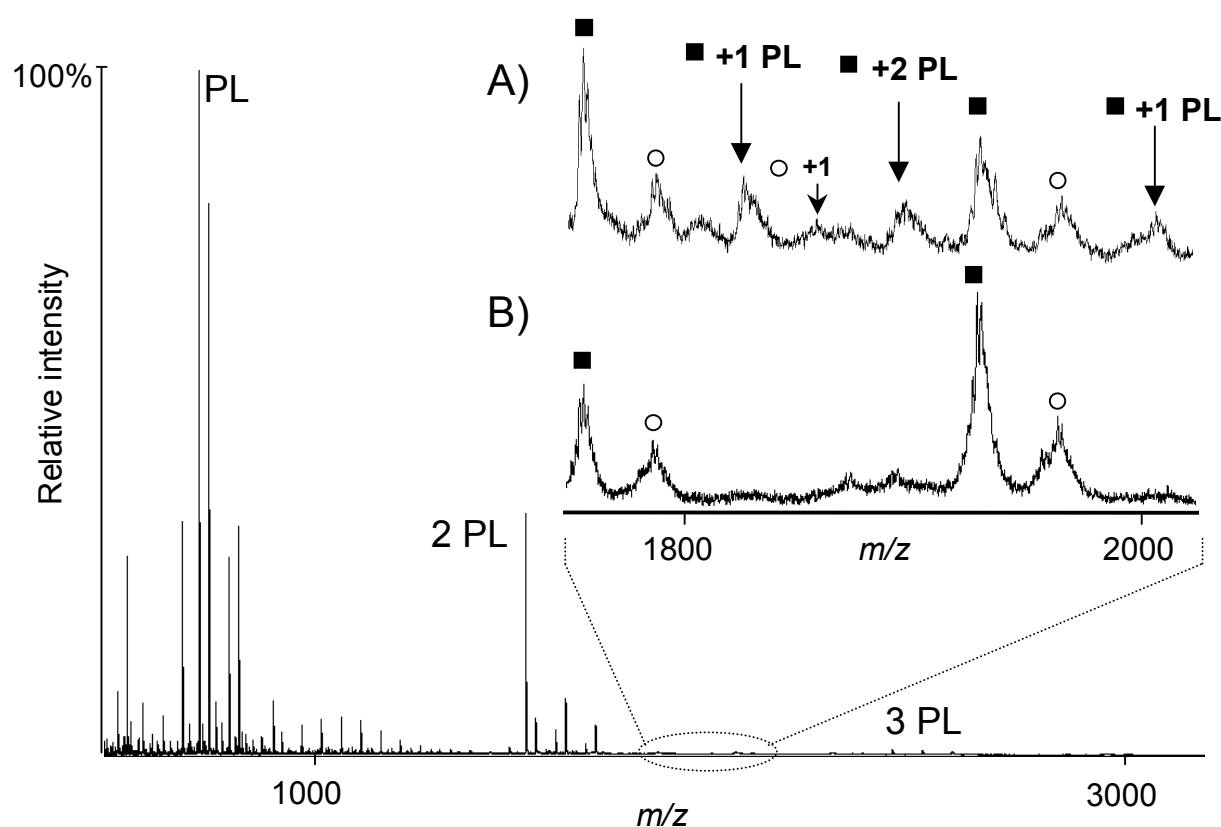
Figure 3 – ESI-ToF mass spectra of KcsA reconstituted vesicles of DPoPC/DOPG sprayed from an aqueous buffer/TFE mixture: effect of the extraction cone voltage on detection of non-covalently bound KcsA-phospholipid complexes. At low extraction cone voltage (panel A) the charge states 10+ and 11+ of KcsA (black squares), as well as KcsA-phospholipid complexes (arrows) are visible. Increasing the extraction cone voltage results in disappearance of these non-covalently bound complexes (panel B). The peaks indicated by the open circles represent the modified protein (see Figure 1).
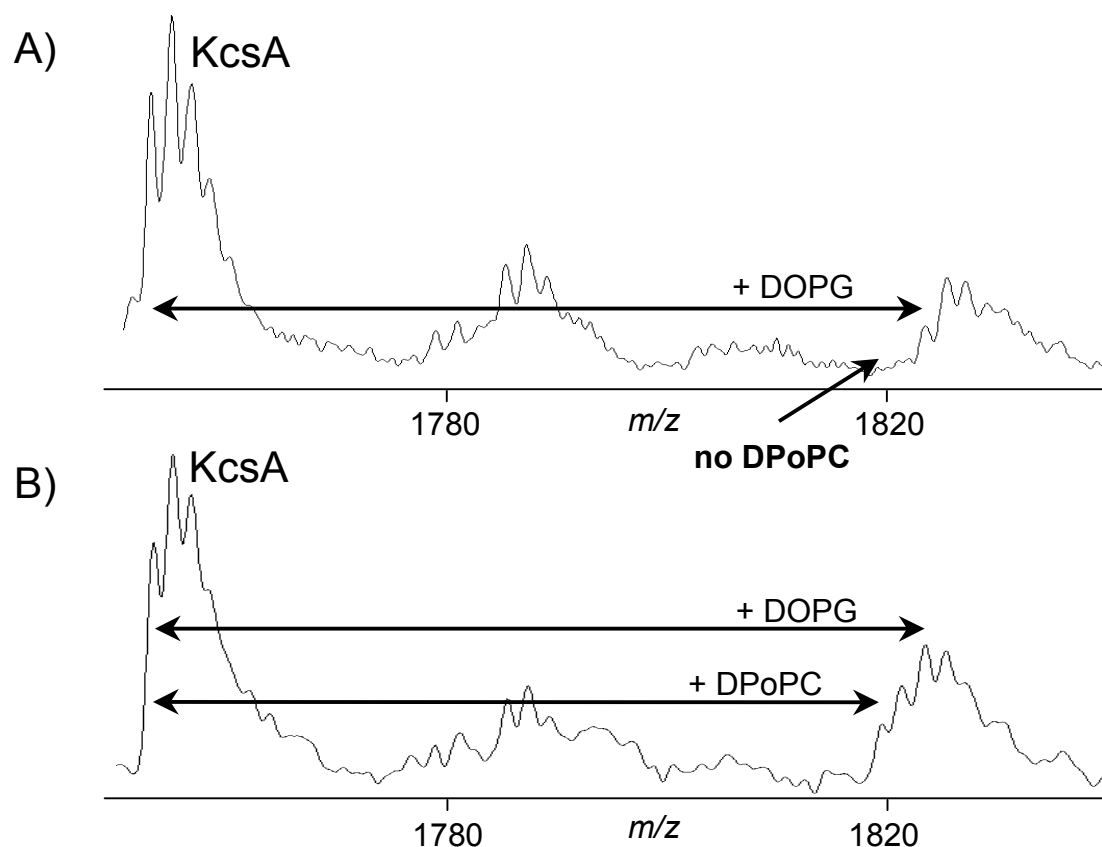
Figure 4 – (A) ESI-ToF mass spectra of KcsA reconstituted in equimolar DPoPC/DOPG vesicles sprayed from a buffer/TFE mixture. Only KcsA-DOPG complexes are detected, whereas KcsA-DPoPC complexes are completely absent. A similar peak shape is visible in the KcsA-phospholipid complexes, indicating that only one phospholipid molecule is present in the complex. The extra peaks at the KcsA charge states is due to Na^+- and K^+-adducts. **(B)** When KcsA is reconstituted in vesicles enriched in PC (DPoPC/DOPG, 5:1), some KcsA-DPoPC adducts are visible, although the major adduct complex is represented by KcsA-DOPG.

The presence of non-covalent protein/lipid complexes in principle allows analysis of preferential binding of specific phospholipid species by KcsA. To discriminate between binding of PC and PG, the combination of DPoPC (molecular mass: 730.1 Da) and DOPG (molecular mass: 774.0 Da) was used to ensure a sufficiently large difference in mass in order to characterize the observed complex and to avoid overlapping peaks in the mass spectrum. A closer look at the KcsA-phospholipid complexes that are formed in these mixtures (Figure 4) shows that the fine structure of the peaks due to Na^+- and K^+-adducts is similar to that of the protein peak. Strikingly, only the KcsA-PG complex at m/z 1823.6 and not the KcsA-PC complex, which would be at m/z 1819.6, is observed, although the protein was reconstituted in vesicles of PC/PG in a 1:1 ratio. Only when KcsA is reconstituted in vesicles enriched in PC (DPoPC/DOPG ratio = 5:1), KcsA-PC complexes were detected, as observed in Figure 4B. Nevertheless, the KcsA-PG complex is also in this case the predominant complex, indicating preferential binding of PG. These results are quantified in Figure 5.

The lipid specificity of binding to KcsA was also tested in a variety of other lipid mixtures (see Figure 5). First, to test whether preferential binding was specific for PG only or general for anionic phospholipids, KcsA was reconstituted in vesicles of the anionic lipid DOPA (molecular mass: 698.9 Da) and DPoPC (1:1 ratio). The relative intensities of the KcsA-PA complex were similar to those observed in PG binding experiments and again no PC binding to the protein was observed, suggesting that the preferential binding indeed is general for anionic lipids. Next, in order to test whether the abundant zwitterionic bacterial lipid PE shows a similar low affinity for KcsA as the eukaryotic zwitterionic lipid PC, the protein was reconstituted in vesicles of DOPE (molecular mass: 744.0 Da) and DOPG (1:1 ratio) and analyzed by ESI-MS. In this case, about 90% of the lipid associated to KcsA represented PG. Surprisingly, when KcsA in vesicles containing both DOPA and DOPE was analyzed, it showed a similar affinity towards both of the phospholipids. Since no PC association at all was observed in PC/PG and PC/PA vesicles, these results suggest that the affinity of KcsA for PE is significantly higher than for PC. This could be confirmed by analysis of KcsA reconstituted in mixtures of DEiPC (molecular mass: 842.2) and DOPE (1:1 ratio), which showed that indeed binding of PE is favored over PC. However, some PC binding was also observed. Together, the results suggest that the affinity of KcsA for PE is higher than for PC, but that the affinity for PG is higher than for PE.
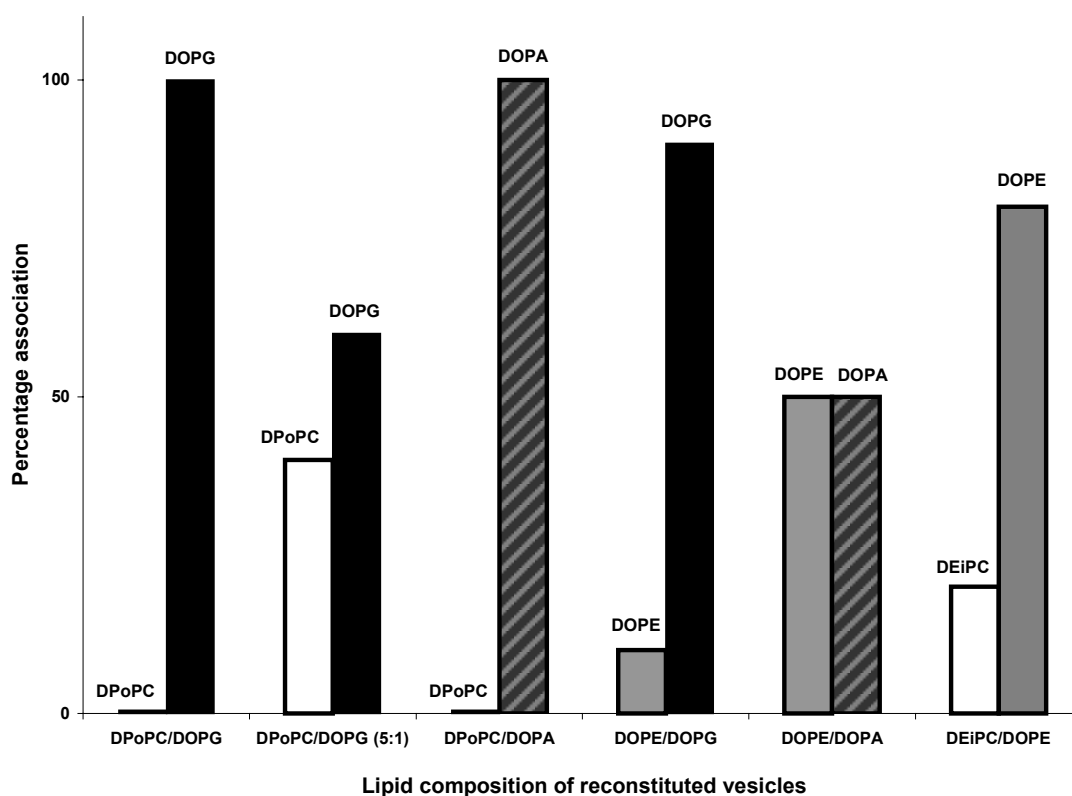
Figure 5 – Quantification of phospholipid binding to KcsA in vesicles composed of the indicated phospholipid mixtures (1:1 ratio, except for the second entry, where the DPoPC/DOPG ratio is 5:1), as derived from KcsA-phospholipid complex peak intensities in the mass spectra. The phospholipid composition of the vesicles is given on the x-axis. The sum of the binding percentages for two classes of phospholipids is in every case 100%. The error in the measurements was estimated to be about 10%.

Discussion

We show in this paper that ESI-MS can be used to detect non-covalent complexes of KcsA, reconstituted in lipid vesicles, and phospholipid molecules. These complexes were not observed when vesicles were sprayed directly, but could be observed after mixing with TFE, which allowed analysis of lipid vesicles under more gentle conditions. Most probably, these bound lipids are those that directly interact with the protein when incorporated in a lipid bilayer. Indeed, control experiments showed that protein-lipid complexes cannot be observed when mixtures of lipid vesicles and the water-soluble protein cytochrome c are analyzed by direct ESI-MS (data not shown). Interestingly, ESI-MS of reconstituted vesicles from aqueous buffer solution resulted in the detection of only the monomeric species of KcsA in the mass spectrum, although in lipid bilayer vesicles the protein is solely present as a tetramer, as detected by SDS-PAGE analysis [14]. An explanation for this could be that the high voltages applied during analysis do not allow non-covalent protein-protein interactions to stay intact. SDS-PAGE analysis suggested that when vesicles are mixed with TFE, KcsA is present as a monomer (not shown). This may be the reason why also under the less harsh experimental conditions that can be used after mixing of the vesicles with TFE only monomeric KcsA was detected by ESI-MS, .

Our data show that the order of preference of KcsA to associate with a phospholipid species was PG ≈ PA > PE > PC. We hypothesize that the preferential binding of KcsA to the phospholipids PG, PA and, to a lesser extent, PE, as analyzed by ESI-MS, reflects the order of affinity of KcsA to these lipids in the phospholipid bilayer. We do not believe that there is a large difference in interaction energies between KcsA and the various phospholipids in the gas-phase. In that case, significant variations in the cone voltage threshold needed for dissociation of the protein-lipid complex due to variable interaction energies should have been observed for the different lipids, which was clearly not the case in our experiments. It should be noted though, that the nature of interactions in the gas-phase can be different from that in solution phase.

Interestingly, complexes of KcsA and more than one phospholipid molecule were also observed, even though the voltages that had to be applied to achieve sufficient sensitivity were rather high, which normally results in a lower amount of non-covalently bound complexes detected. The observation that under conditions of complete detergent-mediated delipidation no phospholipids are bound to the channel protein [13] supports our notion that no specific, co-factor type lipid interaction takes place.

For practical reasons we have used combinations of phospholipids with variable acyl chain lengths. Since the variation in chain length was only small, we assumed that this did not affect the affinity of KcsA for the different classes of lipids. However, in some cases it was possible to use a combination of lipid species with equal chains, e.g. DOPE and DOPG. The large difference in affinity of KcsA for these lipids, suggests that it is indeed the nature of the phospholipid headgroup that governs the interaction of the phospholipid with KcsA. This is supported by preliminary results of an SDS-PAGE assay, which indicate that there is no

significant difference in KcsA tetramer stability in bilayers of PC species with acyl chains ranging from $C_{14:1}$ to $C_{20:1}$ (S. Hegger and A. van Dalen, unpublished results).

Our results indicate that KcsA has the highest affinity for anionic lipids. Anionic lipids have been found to be important for integration of membrane proteins into the membrane in general [17,18] and PG has been suggested to be needed for correct folding of the KcsA monomer [14]. Furthermore, anionic lipids have been shown to be important for KcsA channel activity [19] and stability [14]. Our observation of a preferential interaction of KcsA monomers with anionic lipids correlates well with these findings. An obvious possibility to explain the preferred affinity of KcsA for anionic lipids is that these lipids interact with positively charged residues in the interfacial region. For instance, the N-terminal amphipathic α-helix, which is situated in the membrane-water interface according to a model by Cortes *et al.* [20], contains several positively charged amino acid residues. Limited proteolysis studies with trypsin on reconstituted KcsA and subsequent separation between membrane fraction and water fraction, have shown that the tryptic fragment peptide containing the N-terminal α-helix associates with the membrane fraction (data not shown). This demonstrates that the N-terminal part of the protein indeed has a strong interaction with lipids Alternatively, or additionally, the positively charged residues in the KcsA loop region may interact with negatively charged phospholipids.

The preferred interaction of KcsA to PE may be explained by the capacity of this phospholipid for hydrogen bonding to the protein, which is not possible for PC. Alternatively, PE might preferentially surround KcsA because its relatively small headgroup may result in different and perhaps more favorable packing properties at the protein-lipid interface, as compared to PC. Interestingly, both PG and PE have been found to increase the efficiency of tetramer formation of newly synthesized KcsA in a lipid bilayer as compared to PC alone [14]. Based on the results in this paper, we hypothesize that the roles of PG and PE in KcsA assembly and stability are a consequence of direct, preferential interactions of KcsA with these lipids.

In conclusion, this study shows that the binding affinities of certain classes of membrane lipids to an integral membrane protein can be investigated by ESI-MS. The possibility to visualize such interactions opens perspectives for a better understanding of the association of proteins and surrounding lipids in biological membranes. A future challenge will be to improve experimental measurement conditions sufficiently to enable the detection of intact protein assemblies (e.g. the tetrameric form of KcsA) and complexes with phospholipids at physiological concentration levels.

References

1.   Robinson, C.V., Chung, E.W., Kragelund, B.B., Knudsen, J., Aplin, R.T., Poulsen, F.M. and Dobson, C.M. (1996). Probing the Nature of Noncovalent Interactions by Mass Spectrometry: A Study of Protein CoA Ligand Binding and Assembly. *J. Am. Chem. Soc.* **118**, 8646-53.

2.   van Berkel, W.J., van den Heuvel, R.H.H., Versluis, C. and Heck, A.J.R. (2000). Detection of intact megaDalton protein assemblies of vanillyl-alcohol oxidase by mass spectrometry. *Protein Sci.* **9**, 435-9.

3. Loo, J.A. (2000). Electrospray ionization mass spectrometry: a technology for studying noncovalent macromolecular complexes. *Int. J. Mass Spectrom.* **200**, 175-86.

4. de Brouwer, A.P.M., Versluis, C., Westerman, J., Roelofsen, B., Heck, A.J.R. and Wirtz, K.W.A. (2002). Determination of the stability of the noncovalent phospholipid transfer protein-lipid complex by electrospray time-of-flight mass spectrometry. *Biochemistry* **41**, 8013-8.

5. Demmers, J.A.A., Haverkamp, J., Heck, A.J.R., Koeppe, R.E., II and Killian, J.A. (2000). Electrospray ionization mass spectrometry as a tool to analyze hydrogen/deuterium exchange kinetics of transmembrane peptides in lipid bilayers. *Proc. Natl. Acad. Sci. U. S. A.* **97**, 3189-94.

6. Demmers, J.A.A., van Duijn, E., Haverkamp, J., Greathouse, D.V., Koeppe 2nd, R.E., Heck, A.J.R. and Killian, J.A. (2001). Interfacial positioning and stability of transmembrane peptides in lipid bilayers studied by combining hydrogen/deuterium exchange and mass spectrometry. *J. Biol. Chem.* **276**, 34501-8.

7. Schrempf, H., Schmidt, O., Kummerlen, R., Hinnah, S., Muller, D., Betzler, M., Steinkamp, T. and Wagner, R. (1995). A prokaryotic potassium ion channel with two predicted transmembrane segments from Streptomyces lividans. *EMBO J.* **14**, 5170-8.

8. Doyle, D.A., Cabral, J.M., Pfuetzner, R.A., Kuo, A.L., Gulbis, J.M., Cohen, S.L., Chait, B.T. and Mackinnon, R. (1998). The Structure of the Potassium Channel: Molecular Basis of K+ Conduction and Selectivity. *Science* **280**, 69-77.

9. Roux, B. and MacKinnon, R. (1999). The cavity and pore helices in the KcsA K+ channel: electrostatic stabilization of monovalent cations. *Science* **285**, 100-2.

10. Morais-Cabral, J.H., Zhou, Y. and MacKinnon, R. (2001). Energetic optimization of ion conduction rate by the K+ selectivity filter. *Nature* **414**, 37-42.

11. Jiang, Y., Lee, A., Chen, J., Cadene, M., Chait, B.T. and MacKinnon, R. (2002). The open pore conformation of potassium channels. *Nature* **417**, 523-6.

12. Le Coutre, J., Kaback, H.R., Patel, C.K.N., Heginbotham, L. and Miller, C. (1998). Fourier transform infrared spectroscopy reveals a rigid alpha- helical assembly for the tetrameric Streptomyces lividans K+ channel. *Proc. Natl. Acad. Sci. U. S. A.* **95**, 6114-7.

13. Tatulian, S.A., Cortes, D.M. and Perozo, E. (1998). Structural dynamics of the Streptomyces lividans K+ channel (SKC1): secondary structure characterization from FTIR spectroscopy. *FEBS Lett.* **423**, 205-12.

14. van Dalen, A., Hegger, S., Killian, J. and de Kruijff, B. (2002). Influence of lipids on membrane assembly and stability of the potassium channel KcsA. *FEBS Lett.* **525**, 33-8.

15. Le Coutre, J., Whitelegge, J.P., Gross, A., Turk, E., Wright, E.M., Kaback, H.R. and Faull, K.F. (2000). Proteomics on full-length membrane proteins using mass spectrometry. *Biochemistry* **39**, 4237-42.

16. van Dalen, A., van der Laan, M., Driessen, A.J., Killian, J.A. and de Kruijff, B. (2002). Components required for membrane assembly of newly synthesized K+ channel KcsA. *FEBS Lett.* **511**, 51-8.

17. de Kruijff, B. (1994). Anionic phospholipids and protein translocation. *FEBS Lett.* **346**, 78-82.

18. van Klompenburg, W. and de Kruijff, B. (1998). The role of anionic lipids in protein insertion and translocation in bacterial membranes. *J. Membr. Biol.* **162**, 1-7.

19. Heginbotham, L., Kolmakova-Partensky, L. and Miller, C. (1998). Functional reconstitution of a prokaryotic K+ channel. *J. Gen. Phys.* **111**, 741-749.

20. Cortes, D.M., Cuello, L.G. and Perozo, E. (2001). Molecular architecture of full-length KcsA: role of cytoplasmic domains in ion permeation and activation gating. *J. Gen. Physiol.* **117**, 165-80.

CHAPTER 6

Summarizing discussion

The work described in this thesis was aimed at exploring the possibilities provided by mass spectrometry (MS) to study interactions of transmembrane peptides and proteins with biological model membranes, either by analyzing hydrogen/deuterium exchange kinetics or by investigating non-covalent interactions between proteins and lipids. New methodologies were developed, tested and applied in various model peptide- and protein-lipid systems. In this chapter, the results will be summarized and critically discussed.

Global hydrogen/deuterium exchange kinetics and mass spectrometry in studying peptide-membrane interactions

We have developed an approach to measure hydrogen/deuterium (H/D) kinetics of membrane peptides in lipid bilayers by use of nano-flow electrospray ionization (ESI-) MS. In this approach, dispersions of fully hydrated lipid bilayers with reconstituted peptides of proteins are directly introduced into the mass spectrometer ('proteoliposome nano-flow ESI-MS'). No use is made of any membrane-mimicking detergents, 'isotropic' media or exchange trapping techniques. Membrane peptides and proteins are characterized by an intrinsic hydrophobicity and insolubility in aqueous solvent, which make analysis by conventional ESI-MS difficult. Until recently, spraying such hydrophobic proteins was only performed from organic solvents, in which they are fully denatured. The twofold advantage of our novel method is that (1) the lipid bilayer acts as 'matrix' to bring hydrophobic, membrane-associated components from the aqueous buffer solution in the gas-phase, and (2) membrane peptides and proteins can be studied in their natural habitat, the phospholipid bilayer membrane.

In Chapter 2, we have shown that this method in combination with H/D exchange is convenient to study a variety of properties of transmembrane peptides in lipid bilayers, such as the positioning in the bilayer interface and the conformational stability of an α-helix. In general, we measured the uptake of deuterium atoms in the peptides while they were incorporated in lipid bilayers in time upon incubation in heavy water. We used 'WALP' peptides, which are designed, synthetic peptides with a hydrophobic core of variable length of leucine and alanine, flanked on both sides by Trp residues, that adopt a transmembrane orientation in lipid bilayers. Experiments were performed with WALP16, which fits well in a bilayer of DMPC (a lipid containing $C_{14:0}$ acyl chains), and WALP16(+10), which contains putative water-soluble extensions that stick out of the lipid bilayer. It was shown that the exchanging hydrogens could be divided into several populations, which had different exchange rates. These hydrogen populations were assigned to different regions of the peptides according to the model, as shown in Figure 1. In this model, the hydrophobic Leu-Ala sequence is supposed to be deeply embedded in the hydrophobic core of the bilayer and the flanking Trp residues are located in the interface close to the lipid headgroups. Based on the model, fast exchanging hydrogens were assigned to the terminal regions of both peptides and the water-soluble extensions in WALP16(+10), and the side-chain hydrogens of the Trp residues. The intermediate exchange rates were assigned to amide hydrogens in the interfacial regions, whereas the extremely slowly exchanging hydrogens were

assigned to the amide hydrogens in the transmembrane regions of both peptides. The slow exchange rates in the transmembrane region are due to (1) the involvement of the amide hydrogens in an α-helical structure, and (2) protection by the lipid bilayer, because of the low permeability coefficient of the bilayer hydrophobic inner core for water.
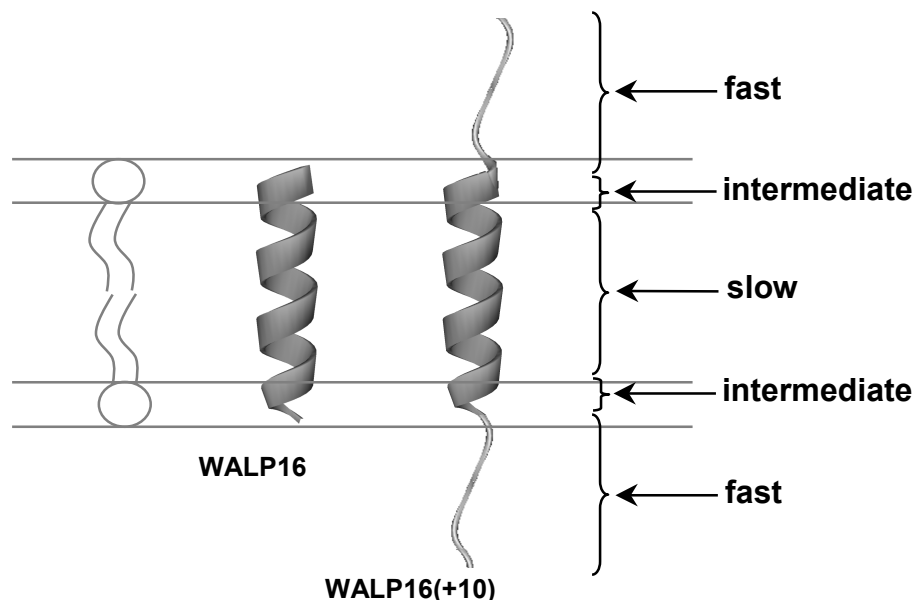

Figure 1 – Models of WALP16 and WALP16(+10) embedded in a phospholipid bilayer. The arrows indicate parts of the peptides that were found to exhibit fast, intermediate and slow exchange.

In Chapter 3, we have described the application of this method to a large set of membrane incorporated WALP-like peptides, which were varied in sequence length, in positions of the Trp residues, and in amino acid composition of the transmembrane sequence. The effects of these modifications could be studied in detail. First, the effect of elongating the hydrophobic part of transmembrane peptides with respect to the hydrophobic thickness of the bilayer was investigated. When we compared the exchange of two 'extreme' peptides, one that fits well in a DMPC lipid bilayer (WALP16), and one that is expected to be much too long with respect to the hydrophobic thickness (WALP23), the effects were quite remarkable. Instead of an increase in deuterium content of seven (this is the number of 'extra' backbone amide hydrogens in WALP23, compared to WALP16), the increase was just two deuteriums after short incubation times. This suggests that the longer peptide is relatively more protected from exchange. One explanation is the membrane environment itself providing increased protection by increasing its hydrophobic thickness because of stretching of the phospholipid acyl chains, as described in the 'mattress model' of Mouritsen and Bloom [1]. This would be in agreement with earlier results on similar peptide-membrane systems from ^{2}H-NMR experiments [2,3]. However, there may be other or additional factors that are responsible for an increased protection of longer peptides from deuterium incorporation. An alternative explanation could be the increased stability of α-

helicity in longer peptides in general, since more amide hydrogens are involved in hydrogen bonding. In principle, increased protection could also be established by tilting of the helices. However, recent ^{2}H-NMR experiments on ^{2}H-alanine labeled WALP peptides have shown that tilting occurs only to a very minor extent in these systems [4].

Results from ^{31}P-NMR and ^{2}H-NMR experiments on the effects of peptides on lipid phase behavior and acyl chain ordering, suggest that both the nature and position of the flanking residues determine the effective hydrophobic length of a transmembrane protein segment [5]. The experiments described in Chapter 3 for the first time provided direct evidence that Trp residues indeed act as determinant for effective hydrophobic length and positioning of transmembrane helices in the membrane interface. This was demonstrated by experiments with WALP peptides of identical length, but in which the sites of the flanking Trp residues were changed by one position (WALP23inner, with Trp-residues 18 residues apart, and WALP23outer, with Trp-residues 20 residues apart). This difference in Trp-positioning was found to result in a difference in deuterium content of about 2, both after short and long incubation times, suggesting that the bilayer thickness adapts to the Trp-Trp distance. These results fit well with the hypothesis that Trp is important for stabilizing integral membrane proteins in the membrane-water interface [6-8].

Insight into the role of Gly and Pro, which are often found in naturally occurring transmembrane α-helices, was obtained in Chapter 3. Gly did not have any effect on H/D exchange rates compared to the regular α-helical WALP23 peptide, although it is considered to be an α-helix breaker in helices in soluble proteins. This is in agreement with earlier studies on the role of Gly in transmembrane segments [9,10]. In contrast, the observed increased deuterium exchange rate in the transmembrane region of WALP23Pro, suggests that the presence of a Pro residue has a destabilizing effect on the helix fold in a regular transmembrane α-helical peptide.

Pro is found often in transmembrane segments in especially transport proteins, ion channels and G-protein-coupled receptors and this appeared to be an important characteristic in functioning [11-17]. Pro has been supposed to be involved in protein dynamic processes, where the *cis-trans* isomerization of an X-Pro (X is any amino acid) peptide bond buried within the membrane, and the resulting redirection of the protein chain, is proposed to be required as the reversible conformational change for the regulation of transport channels [18,19] and G-protein-coupled receptors [14]. Molecular dynamics (MD) simulations have shown that a kinked α-helix is the most favorable conformation when a Pro is present [20]. The effect found in our studies is consistent with such a Pro-induced kinked conformation.

In an effort to compare the results on synthetic transmembrane peptides with those on real membrane proteins, we also performed some pilot experiments on the M13 major coat protein (not described in previous chapters). The three-dimensional structure of this 5.3 kDa single-spanning integral membrane protein in micelles [21] shows an amphipathic N-terminal α-helix, that is connected by a hinge region to a putative transmembrane helix (Figure 2). H/D exchange kinetics of the membrane-incorporated M13 major coat protein were studied in order

to (1) determine whether the N-terminal helix shows increased protection by its supposed location on the surface of the membrane, and (2) compare H/D exchange rates of the transmembrane segment to those found for model peptides (as described in Chapters 2 and 3). It was found that after several minutes a large part (about 65%) of the hydrogens had exchanged, probably including the amide hydrogens in the amphipathic α-helix. Within several hours, almost 80% (corresponding to a population of more than 60 hydrogens) had exchanged, leaving a population of 20% (16 hydrogens) that exchanged at very slow rates. These hydrogens most probably represent the amide hydrogens in the transmembrane α-helix. This amount of extremely slowly exchanging hydrogens would be consistent with the amount found in WALP23, which has a comparable transmembrane length (Figure 2).

We can conclude that H/D exchange in combination with MS can give useful information on the properties of small integral membrane proteins in a lipid bilayer. Although the method has many advantages over existing methods, it clearly also has some drawbacks. These will be discussed in the next section.

A

M13

WALP23

N

C

B

```
 1   AEGDDPAKAA FDSLQASATE
21   YIGYAWAMVV VIVGATIGIK
41   LFKKFTSKAS
```
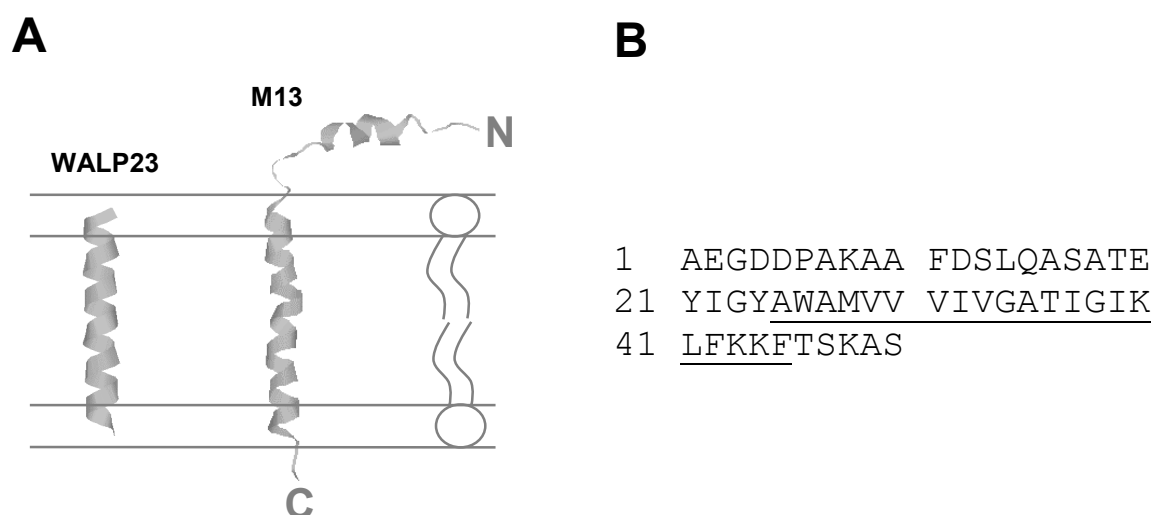
Figure 2 – (A) Model of the α-helical WALP23 peptide and M13 major coat protein (PDB accession code: 2CPB) incorporated in a phospholipid bilayer. The transmembrane segment lengths of the peptide and the protein are comparable. **(B)** Amino acid sequence of M13 major coat protein. The putative transmembrane segment is underlined.

General remarks on H/D exchange combined with nano-flow ESI-MS

General advantages of MS are the high speed of analysis, the high sensitivity and the large flexibility in choice of environmental conditions, such as pH, ionic strength, variety of lipid mixtures, and peptide composition. Another advantage is the possibility to simultaneously incorporate different peptides into the membrane, and subsequently monitor them independently of each other. In contrast to other techniques that are used for monitoring H/D exchange of membrane peptides and proteins, such as Fourier-transformed infrared (FTIR) (e.g.

[22-24]) and nuclear magnetic resonance (NMR) spectroscopy (e.g [24-28]), which cannot differentiate between the amide hydrogens of one peptide or the other, mass spectrometry allows detection of amide hydrogen exchange in each of the peptides separately. Therefore, there is no stringent requirement for high purity of the peptides.

Although MS has been used since a decade or so to monitor H/D exchange, before the start of the studies described in this thesis it had never been applied to membrane incorporated peptides. One difference between our H/D exchange procedure and some that are conventionally used, is the absence of a quenching step by lowering the pH and temperature in order to virtually stop the exchange reaction. In our procedure, a pH drop could not be used, since the vesicular dispersions could not be sprayed at low pH, possibly because of aggregate formation. In our case however, this was not a critical issue: there was no necessity to quench the reaction, since we did not study very fast exchange rates. In cases where monitoring of such very fast rates is required, a problem would be the long experimental dead-time of about one minute in our case. This problem may be solved by stopped-flow H/D exchange labeling to decrease the experimental dead-time (e.g. [29]). Furthermore, miniaturization of the experimental setup could offer interesting improvements in future experiments.

Another potential complication is the back-exchange phenomenon, which is an issue that is not yet elaborated in H/D exchange studies using MS. Exchangeable deuteriums could in principle exchange back to hydrogens, for instance by H_2O from air. Pilot experiments with a KALP23 peptide that was freshly dissolved in pure deuterated methanol (MeOD; 99+ atom % deuterium), showed that there is an inverse proportional dependence in the amount of retained deuteriums and the distance between the tip opening of the ESI capillary and the mass spectrometer sample cone inlet. An increase in the length of the trajectory of the ionized peptide through this region by several tens of millimeters, results in an observed mass decrease of 1.5 to 2 Da (approximately 5 % of the total deuterium amount). It should be noted however, that when experiments were set up to minimize back-exchange, more than 95% of the deuterium labels in fully deuterated KALP23 in control experiments were retained during analysis. All experiments described in this thesis were carried out under the same conditions of minimal back-exchange and were therefore comparable.

Use of collision-induced dissociation MS to localize deuterium atoms

Besides the possibility of direct introduction of vesicle dispersions into the mass spectrometer and monitoring global H/D exchange rates, an additional feature of our methodology is the ability to determine the deuterium content of individual amide bonds in the peptides by collision-induced dissociation (CID) MS. CID MS on membrane incorporated model peptides in all cases revealed almost complete sequences of the peptides. Even CID MS on a 50-residue membrane protein (M13 major coat protein) resulted in almost complete coverage.

In Chapter 2, experiments were described that were performed on both the undeuterated and partly deuterated sodium cationized model peptides. The resulting CID MS spectra showed

series of Na^+-cationized N-terminal A_n and C-terminal Y'_n fragment ions, together covering almost the entire peptide. The difference in masses between fragment ions of the undeuterated peptides and those of the partly deuterated peptides indicated that the deuterium labels were not randomly distributed over the peptides.

The measurement of the deuterium content of the fragment ions of bilayer incorporated WALP16 and WALP16(+10) as measured by CID MS, could be used to analyze which regions of the peptides are protected from deuterium exchange. For both peptides, it was shown that after short incubation times in the transmembrane region no deuterium exchange took place, whereas in the flanking regions (and in addition in case of WALP16(+10) the extensions), exchange did take place. The results supported the model presented in Figure 1. As expected, and as exemplified by WALP23 in Chapter 3, the exchange gradually 'moved' in time from the flanking regions to the inner hydrogens in the transmembrane part, showing that indeed the amide hydrogens closest the bilayer center were most protected from exchange.

In Chapter 3, this CID MS method was also successfully applied to partly deuterated WALP23 and WALP23Pro, both incorporated in lipid bilayers in deuterated buffer. In both cases, the terminal regions of the peptide contained deuterium already after short incubation times and therefore exchanged fast, and the transmembrane region did not contain deuteriums. However, after longer incubation times, large differences in H/D exchange between WALP23 and WALP23Pro were found in the transmembrane parts. From these CID MS data, it was concluded that destabilization is not centered around the Pro residue, but that it takes place over a larger part of the transmembrane region.

The CID MS analyses described in Chapters 2 and 3 were successfully applied, and presented viable information additional to the global H/D exchange data. However, subsequent studies, reported in Chapter 4, revealed that this may not always be the case. Although H/D exchange in combination with gas-phase sequencing by CID MS of proteolytic peptide ions has become a frequently used method to probe structural properties of peptides and proteins [30-35], the interpretation of CID MS data clearly is only valid if deuterium inter- and/or intramolecular deuterium migration ('scrambling') prior to and during ion fragmentation can be excluded. Scrambling may result in loss of isotopic information. Since this is an unwanted effect, it is important to investigate by which experimental factors scrambling is influenced. In Chapter 4, it is shown that scrambling indeed could occur in model transmembrane peptides and the influence of some practical parameters on the extent of deuterium scrambling in model transmembrane peptides was investigated.

The amount of scrambling determined for various peptides and various charge carriers indicated that the nature of the charge carrier has a dramatic effect on the extent of deuterium scrambling. The extent of scrambling was relatively low when an alkali metal ion was present as the charge carrier, as compared to a proton. There is evidence that in the gas-phase a sodium ion is more fixed to a specific position, whereas a proton may more easily migrate between the different basic sites available in the peptide ion, which would be in agreement with the mobile

proton model [36,37]. Our findings may suggest that the proton in the protonated species acts as a catalyst for deuterium scrambling. In addition, different amino acids could induce various degrees of scrambling. This is in agreement with previous results on the role of different amino acids on the extent of hydrogen migration in peptide ions [38]. It was concluded that the overall order of scrambling-inducing capacity of the studied flanking residues was the same for both the protonated and sodium cationized peptide ions, i.e. K > Y > H > F > W. This order could not easily be explained. Neither the polarity, nor the gas phase proton affinity of the variable amino acids could be correlated with the extent of scrambling. One factor that did not influence the extent of scrambling was the type of fragment ions studied: in our case, both the sodiated C-terminal Y_n' and N-terminal A_n ions showed a similar extent of scrambling, in contrast to other studies [31,34,35]. We propose that the observed trends in deuterium scrambling can be caused by differences in gas-phase structures. In order to study gas-phase structures of these peptide ions, it could be useful to perform ion mobility studies [39].

We have also performed pilot CID MS experiments on membrane incorporated, partly deuterated M13 major coat protein (data not shown). This protein contains a substantial amount of Lys residues (see Figure 2). However, no completely sodium cationized M13 major coat protein could be generated to subject to CID MS. According to the results presented in Chapter 4, these conditions can provoke scrambling. Indeed, deuterium atoms seemed to be present all over the peptide sequence, indicating the occurrence of extensive scrambling. This is the major reason why our studies on M13 major coat protein were not further pursued.

In conclusion, care has to be taken in the interpretation of the data in CID MS experiments, as deuterium scrambling may influence the outcome of such measurements. Although in general some detailed information on peptide and protein structural elements may be obtained by combining H/D exchange and CID MS, the results in Chapter 4 indicate that this method is not applicable in every case.

MS as a tool to study non-covalent interactions between proteins and phospholipids

The goal of the study presented in Chapter 5 was to investigate the potassium channel KcsA and its interactions with lipid membranes by MS. At the same time, we wanted to find out whether direct proteoliposome ESI MS could be exploited in studying large and multimeric integral membrane proteins. As such, this study served as an extension of the study presented in Chapter 2. An additional challenge would be to be able to analyze non-covalent protein-protein complexes in a lipid membrane environment. In this respect, KcsA seems a good model protein, since it forms a stable tetramer in lipid bilayers.

We have shown in Chapter 5 that reconstituted KcsA in lipid vesicles could be analyzed by a direct ESI-MS approach when sprayed from aqueous buffer solutions. However, only the monomeric species of KcsA was detected in the mass spectrum, although in lipid bilayer vesicles the protein is present as a tetramer [40]. An explanation for this could be that the high voltages

applied during analysis do not allow non-covalent protein-protein interactions to stay intact. When the reconstituted vesicles were first mixed with TFE prior to analysis, protein signals with much higher signal-to-noise ratios were obtained and analysis was performed under relatively gentle conditions. Also in this case, KcsA was detected solely as a monomer and SDS-PAGE analysis suggested that mixing reconstituted vesicles with TFE indeed results in destabilization of the tetrameric configuration. Interestingly, although protein-protein complexes were not observed, non-covalent complexes of KcsA and phospholipid molecules were detected. Most probably, these lipids are those that directly interact with the protein when incorporated in a lipid bilayer.

Measurements with KcsA reconstituted in vesicles of various composition revealed that the protein has a preference for association to certain classes of lipids. The order of preference of KcsA to associate with a phospholipid species was found to be PG ≈ PA > PE > PC. It was hypothesized that the preferential interaction of KcsA to the phospholipids PG, PA and, to a lesser extent, PE, reflects the order of affinity of KcsA to these lipids in the phospholipid bilayer. These preferences were assumed to be related to the specific physicochemical properties of these lipids. An obvious possible explanation for the preference of KcsA to anionic lipids is that they can interact with positively charged residues in the N-terminal α-helix or in the loop region. Possible explanations for the preferred interaction of KcsA to PE compared to PC may be the capacity of this phospholipid for hydrogen bonding to the protein, or the more favorable packing properties of this lipid at the protein/lipid interface due to its smaller headgroup.

The new aspect of the study presented in Chapter 5 is that the binding affinities of certain classes of membrane lipids to an integral membrane protein can be investigated by ESI-MS. The possibility to visualize such interactions opens perspectives for a better understanding of the association of proteins and surrounding lipids in biological membranes. A future challenge will be to improve experimental measurement conditions sufficiently to enable the detection of intact protein assemblies (e.g. the tetrameric form of KcsA) and complexes with phospholipids at physiological concentration levels. Also, peripherally bound membrane proteins and their interactions with the target membrane can in principle be studied in this way.

MS may also be useful in detailed studies on protein/lipid interaction in combination with proteolytic cleavage. For example, tryptic digestion experiments of bilayer incorporated KcsA showed that the proteolytic fragment corresponding to a part of the amphipathic N-terminal helix was associated with the membrane fraction after digestion and separation of membrane and supernatant fractions. This is in agreement with the membrane incorporation model of KcsA as proposed by Cortes *et al.* [41].

Covalent modification of KcsA

One aspect of this study that was not elaborated in Chapter 5, is the pursuit of the identification of an unknown compound in the KcsA sample. In the spectrum of KcsA in formic acid, besides

the full-length unmodified protein, an extra compound was observed with a mass of 19630 ± 1 Da, approximately 355 Da higher than that of KcsA (compound X). Variations in the cone voltage did not change the peak intensity proportions between compound X and KcsA peaks, suggesting that the unknown compound could be a non-covalent complex of KcsA with a 355 Da ligand. Both CID MS and in-source fragmentation MS experiments indicated that compound X represents a covalently modified KcsA species: fragmentation of the $[M + 11H]^{11+}$ ions of compound X and of KcsA revealed that the Y''_{54} to Y''_{87} fragment ions that were observed were identical, but that the B_n fragment ions of compound X all were 355 Da higher in mass. Since only fragment ions B_{49} to B_{57} were observed, it was concluded that the modification must be located somewhere in the N-terminal residues 1-48. In principle, it is even possible that compound X contains multiple modifications that result in a total mass difference of 355 Da.

Although the identity of compound X is not known, one could speculate about what it could be. KcsA has been described to contain two non-proteinaceous polymers, i.e. poly-(R)-3-hydroxybutyrate (PHB) and inorganic polyphosphate (polyP) [42]. PHB was detected in both tetramer and monomer species of KcsA and estimated as 28 monomer units of PHB that are covalently linked to KcsA. However, no information was obtained about the localization of these inorganic moieties. PolyP was detected in KcsA tetramers, but not in monomers. PolyP was estimated as 15 monomer units per tetramer and held together by ionic forces. It is possible that the modifications we have found are related to the above mentioned inorganic polymers, but there is no evidence for that yet.

Future perspectives

This section will describe in more detail potential applications of the proteoliposome ESI-MS approach.

Dependence of exchange kinetics in membrane-associated peptides on the lipid environment

In Chapters 2, 3 and 4, the interactions of various XALP peptides with lipid bilayers have been studied. However, in principle any transmembrane and/or membrane surface associated peptide can be investigated in much the same way, thereby gaining insight into factors like α-helix stability, localization in the interface, dynamics and conformational properties. This method also allows investigation of the dependence of these factors on environmental parameters, such as peptide concentration, or interactions with other components. Furthermore, although DMPC was mostly used as the lipid environment for investigation of the XALP peptides in these model studies, the unique possibilities of the described method in principle allow investigation of the influence of different lipid environments, such as length and degree of unsaturation of the acyl chains, various headgroups and packing properties, presence of cholesterol, etc. An interesting example in this respect would be the investigation of glycosphingolipid- and cholesterol-rich

lipid domains, called rafts or detergent-resistant membranes [43-45]. These rafts have been proposed to play a role in several biological processes in the eukaryotic cell membrane, such as signal transduction, viral budding and lipid sorting.

Alternatively, the direct environment of the peptide in a mixed lipid system could be probed by a cross-linking approach (see later in this section).

Integral membrane proteins studied by H/D exchange and MS

H/D exchange studies on integral membrane proteins can in principle be performed in order to find out which parts are membrane-embedded, but also to investigate structural properties. For instance, it would be very interesting to study the gating mechanism of a channel protein, by comparing H/D exchange between open and closed channel conformations. It was found that this can lead to major structural changes in KcsA [46]. In Chapter 5, we have shown that reconstituted KcsA can be analyzed directly using the proteoliposome ESI-MS approach. Subsequent pilot studies on H/D exchange properties in this channel protein, showed that the majority of the labile hydrogens in the protein exchanged after short incubation times. This is in agreement with H/D exchange studies on KcsA in lipid bilayers using FT-IR spectroscopy [47], which showed that almost 80% of KcsA amide hydrogens had exchanged within several hours of D_2O exposure. These results suggest that the channel is largely accessible to solvent exchange, and are consistent with the structure of KcsA [47]. Remarkably, these results are in contrast with similar FTIR studies [48], in which the protein was found to exhibit a low degree of H/D exchange and was suggested to be relatively rigid and inflexible.

Another strategy would be using simplified synthetic peptides with sequences corresponding to the putative transmembrane domains and/or the pore-lining regions that are deduced from the primary structures of ion channel proteins (other studies with such peptides have been reviewed in [49]). In addition to the ability to invoke ion channel activity, important issues are the secondary structures adopted and the mode of assembly of these short transmembrane peptides in reconstituted systems. H/D exchange in combination with ESI-MS may be a helpful tool in this respect.

Non-covalent interactions in a membrane environment

The idea that transient protein-protein interactions are crucial events in cell functioning [50], is nowadays a widely accepted concept in cell biology. At the biochemical level, proteins rarely act alone, instead they interact with other proteins to perform particular cellular tasks and form assemblies that represent more than the sum of their parts by having a new 'function' [51].

One way to study interactions between membrane-embedded segments of membrane proteins is by use of synthetic transmembrane peptides [52,53]. For instance, Engelman *et al.* have studied the leucine-zipper helix association phenomenon [53] by use of model peptides in a membrane environment. Furthermore, synthetic peptides corresponding to segments from the

hydrophobic core of the Shaker K$^+$ channel (S2, S3 and S4) have been used as a model system to study interactions between transmembrane segments [54,55]. These results have made clear that either specific or non-specific interactions exist between transmembrane segments of integral membrane proteins, and that these can contribute to their assembly and organization.

The great potential of ESI-MS in studying non-covalent biochemical interactions is now widely recognized and the field of applications is rapidly growing [56-58]. In principle, it should be possible to investigate non-covalent transmembrane helix-helix interactions in a lipid environment by ESI-MS on proteoliposomes. Even if it may be not clear yet whether MS is suitable for probing quantitative interaction energies between (bio)molecules, it should be possible to probe relative interaction energies between transmembrane-domains. In Chapter 5 of this thesis, we have tried to study non-covalent interactions between monomers of KcsA. Unfortunately, it was not possible to detect the KcsA tetrameric species in the mass spectrum. A possible reason may be the far from gentle experimental settings that were applied to obtain sufficient sensitivity. However, it may be possible to analyze non-covalently bound transmembrane α-helical peptides using improved sampling and instrumental conditions that allow non-covalent complexes to stay intact during the ESI process.

Another possibility to study non-covalent multi-protein complexes in membrane systems in a large-scale approach could be a tandem-affinity purification (TAP) based method [50]. Using this technology, membrane vesicular systems could be isolated and subsequently (directly) analyzed by mass spectrometric methods.

Finally, another different strategy to study protein-protein interactions in a membrane environment is the use of approaches based on cross-linking of the protein to other membrane proteins in their immediate surroundings (for a review on cross-linking see [59]). Cross-linked proteins can then be proteolytically digested and analyzed by mass spectrometry in order to determine the identity and location of the cross-linked product. Alternatively, the direct environment of the peptide or protein in a mixed lipid system could be probed by a cross-linking approach, whereby the cross-link probe could be attached either to the peptide or protein or to the specific lipid.

References

1. Mouritsen, O.G. and Bloom, M. (1984). Mattress model of lipid-protein interactions in membranes. *Biophys. J.* **46**, 141-53.
2. de Planque, M.R.R., Greathouse, D.V., Koeppe, R.E., II, Schafer, H., Marsh, D. and Killian, J.A. (1998). Influence of lipid/peptide hydrophobic mismatch on the thickness of diacylphosphatidylcholine bilayers. A 2H NMR and ESR study using designed transmembrane alpha-helical peptides and gramicidin A. *Biochemistry* **37**, 9333-45.
3. de Planque, M.R.R., Boots, J.W.P., Rijkers, D.T.S., Liskamp, R.M.J., Greathouse, D.V. and Killian, J.A. (2002). The Effects of Hydrophobic Mismatch between Phosphatidylcholine Bilayers and Transmembrane alpha-Helical Peptides Depend on the Nature of Interfacially Exposed Aromatic and Charged Residues. *Biochemistry* **41**, 8396-404.

4.   van der Wel, P.C.A., Strandberg, E., Killian, J.A. and Koeppe, I., R.E. (2002). Geometry and Intrinsic Tilt of a Tryptophan-Anchored Transmembrane alpha-Helix Determined by (2)H NMR. *Biophys. J.* **83**, 1479-88.

5.   de Planque, M.R.R., Kruijtzer, J.A.W., Liskamp, R.M.J., Marsh, D., Greathouse, D.V., Koeppe, R.E., II, de Kruijff, B. and Killian, J.A. (1999). Different membrane anchoring positions of tryptophan and lysine in synthetic transmembrane alpha-helical peptides. *J. Biol. Chem.* **274**, 20839-46.

6.   Kovacs, F., Quine, J. and Cross, T.A. (1999). Validation of the single-stranded channel conformation of gramicidin A by solid-state NMR. *Proc. Natl. Acad. Sci. U. S. A.* **96**, 7910-15.

7.   Iwata, S., Ostermeier, C., Ludwig, B. and Michel, H. (1995). Structure at 2.8 A resolution of cytochrome c oxidase from Paracoccus denitrificans. *Nature* **376**, 660-9.

8.   Landolt Marticorena, C., Williams, K.A., Deber, C.M. and Reithmeier, R.A. (1993). Non-random distribution of amino acids in the transmembrane segments of human type I single span membrane proteins. *J. Mol. Biol.* **229**, 602-8.

9.   Li, S.C. and Deber, C.M. (1992). Glycine and beta-branched residues support and modulate peptide helicity in membrane environments. *FEBS Lett.* **311**, 217-20.

10.   Javadpour, M.M., Eilers, M., Groesbeek, M. and Smith, S.O. (1999). Helix packing in polytopic membrane proteins: role of glycine in transmembrane helix association. *Biophys. J.* **77**, 1609-18.

11.   Seatter, M.J., Kane, S., Porter, L.M., Arbuckle, M.I., Melvin, D.R. and Gould, G.W. (1997). Structure-function studies of the brain-type glucose transporter, GLUT3: alanine-scanning mutagenesis of putative transmembrane helix VIII and an investigation of the role of proline residues in transport catalysis. *Biochemistry* **36**, 6401-7.

12.   Webb, D.C., Rosenberg, H. and Cox, G.B. (1992). Mutational analysis of the Escherichia coli phosphate-specific transport system, a member of the traffic ATPase (or ABC) family of membrane transporters. A role for proline residues in transmembrane helices. *J. Biol. Chem.* **267**, 24661-8.

13.   Wellner, M., Monden, I., Mueckler, M.M. and Keller, K. (1995). Functional consequences of proline mutations in the putative transmembrane segments 6 and 10 of the glucose transporter GLUT1. *Eur. J. Biochem.* **227**, 454-8.

14.   Sansom, M.S. and Weinstein, H. (2000). Hinges, swivels and switches: the role of prolines in signalling via transmembrane alpha-helices. *Trends Pharmacol. Sci.* **21**, 445-51.

15.   Wess, J., Nanavati, S., Vogel, Z. and Maggio, R. (1993). Functional role of proline and tryptophan residues highly conserved among G protein-coupled receptors studied by mutational analysis of the m3 muscarinic receptor. *EMBO J.* **12**, 331-8.

16.   Consler, T.G., Tsolas, O. and Kaback, H.R. (1991). Role of proline residues in the structure and function of a membrane transport protein. *Biochemistry* **30**, 1291-8.

17.   Deber, C.M., Glibowicka, M. and Woolley, G.A. (1990). Conformations of proline residues in membrane environments. *Biopolymers* **29**, 149-57.

18.   Brandl, C.J. and Deber, C.M. (1986). Hypothesis about the function of membrane-buried proline residues in transport proteins. *Proc. Natl. Acad. Sci. U. S. A.* **83**, 917-21.

19.   Deber, C.M., Sorrell, B.J. and Xu, G.Y. (1990). Conformation of proline residues in bacteriorhodopsin. *Biochem. Biophys. Res. Commun.* **172**, 862-9.

20.   Polinsky, A., Goodman, M., Williams, K.A. and Deber, C.M. (1992). Minimum energy conformations of proline-containing helices. *Biopolymers* **32**, 399-406.

21.   Papavoine, C.H., Christiaans, B.E., Folmer, R.H., Konings, R.N. and Hilbers, C.W. (1998). Solution structure of the M13 major coat protein in detergent micelles: a basis for a model of phage assembly involving specific residues. *J. Mol. Biol.* **282**, 401-19.

22.   Goormaghtigh, E., Raussens, V. and Ruysschaert, J.M. (1999). Attenuated total reflection infrared spectroscopy of proteins and lipids in biological membranes. *Biochim. Biophys. Acta* **1422**, 105-85.

23.   Sturgis, J., Robert, B. and Goormaghtigh, E. (1998). Transmembrane helix stability: the effect of helix-helix interactions studied by Fourier transform infrared spectroscopy. *Biophys. J.* **74**, 988-94.

24.   Zhang, Y.P., Lewis, R.N., Henry, G.D., Sykes, B.D., Hodges, R.S. and McElhaney, R.N. (1995). Peptide models of helical hydrophobic transmembrane segments of membrane proteins. 1. Studies of the

conformation, intrabilayer orientation, and amide hydrogen exchangeability of Ac-K2-(LA)12-K2-amide. *Biochemistry* **34**, 2348-61.

25. Henry, G.D., Weiner, J.H. and Sykes, B.D. (1987). Backbone dynamics of a model membrane protein: measurement of individual amide hydrogen-exchange rates in detergent-solubilized M13 coat protein using 13C NMR hydrogen/deuterium isotope shifts. *Biochemistry* **26**, 3626-34.

26. Chupin, V., Killian, J.A., Breg, J., de Jongh, H.H., Boelens, R., Kaptein, R. and de Kruijff, B. (1995). PhoE signal peptide inserts into micelles as a dynamic helix-break-helix structure, which is modulated by the environment. A two-dimensional 1H NMR study. *Biochemistry* **34**, 11617-24.

27. Pervushin, K.V., Orekhov, V., Popov, A.I., Musina, L. and Arseniev, A.S. (1994). Three-dimensional structure of (1-71)bacterioopsin solubilized in methanol/chloroform and SDS micelles determined by 15N-1H heteronuclear NMR spectroscopy. *Eur. J. Biochem.* **219**, 571-83.

28. Dempsey, C.E. and Butler, G.S. (1992). Helical structure and orientation of melittin in dispersed phospholipid membranes from amide exchange analysis in situ. *Biochemistry* **31**, 11973-7.

29. Matagne, A., Jamin, M., Chung, E.W., Robinson, C.V., Radford, S.E. and Dobson, C.M. (2000). Thermal unfolding of an intermediate is associated with non-Arrhenius kinetics in the folding of hen lysozyme. *J. Mol. Biol.* **297**, 193-210.

30. Akashi, S. and Takio, K. (2000). Characterization of the interface structure of enzyme-inhibitor complex by using hydrogen-deuterium exchange and electrospray ionization Fourier transform ion cyclotron resonance mass spectrometry. *Protein Sci.* **9**, 2497-505.

31. Deng, Y.Z., Pan, H. and Smith, D.L. (1999). Selective Isotope Labeling Demonstrates That Hydrogen Exchange at Individual Peptide Amide Linkages Can Be Determined by Collision Induced Dissociation Mass Spectrometry. *J. Am. Chem. Soc.* **121**, 1966-7.

32. Eyles, S.J., Speir, J.P., Kruppa, G.H., Gierasch, L.M. and Kaltashov, I.A. (2000). Protein conformational stability probed by Fourier transform ion cyclotron resonance mass spectrometry. *J. Am. Chem. Soc.* **122**, 495-500.

33. Akashi, S., Naito, Y. and Takio, K. (1999). Observation of hydrogen-deuterium exchange of ubiquitin by direct analysis of electrospray capillary-skimmer dissociation with courier transform ion cyclotron resonance mass spectrometry. *Anal. Chem.* **71**, 4974-80.

34. Anderegg, R.J., Wagner, D.S., Stevenson, C.L. and Borchardt, R.T. (1994). The Mass Spectrometry of Helical Unfolding in Peptides. *J. Am. Soc. Mass Spectrom.* **5**, 425-33.

35. Kim, M.Y., Maier, C.S., Reed, D.J. and Deinzer, M.L. (2001). Site-Specific Amide Hydrogen/Deuterium Exchange in E. coli Thioredoxins Measured by Electrospray Ionization Mass Spectrometry. *J. Am. Chem. Soc.* **123**, 9860-6.

36. Dongre, A.R., Jones, J.L., Somogyi, A. and Wysocki, V.H. (1996). Influence of peptide composition, gas-phase basicity, and chemical modification on fragmentation efficiency: Evidence for the mobile proton model. *J. Am. Chem. Soc.* **118**, 8365-74.

37. Wysocki, V.H., Tsaprailis, G., Smith, L.L. and Breci, L.A. (2000). Special feature: Commentary - Mobile and localized protons: a framework for understanding peptide dissociation. *J. Mass Spectrom.* **35**, 1399-1406.

38. Buijs, J., Hagman, C., Hakansson, K., Richter, J.H., Hakansson, P. and Oscarsson, S. (2001). Inter- and intra-molecular migration of peptide amide hydrogens during electrospray ionization. *J. Am. Soc. Mass Spectrom.* **12**, 410-9.

39. Wyttenbach, T., von Helden, G. and Bowers, M.T. (1996). Gas-phase conformation of biological molecules: Bradykinin. *J. Am. Chem. Soc.* **118**, 8355-64.

40. van Dalen, A., Hegger, S., Killian, J. and de Kruijff, B. (2002). Influence of lipids on membrane assembly and stability of the potassium channel KcsA. *FEBS Lett.* **525**, 33-8.

41. Cortes, D.M., Cuello, L.G. and Perozo, E. (2001). Molecular architecture of full-length KcsA: role of cytoplasmic domains in ion permeation and activation gating. *J. Gen. Physiol.* **117**, 165-80.

42. Reusch, R.N. (1999). Streptomyces lividans potassium channel contains poly-(R)-3-hydroxybutyrate and inorganic polyphosphate. *Biochemistry* **38**, 15666-72.

43. Jacobson, K. and Dietrich, C. (1999). Looking at lipid rafts? *Trends Cell Biol.* **9**, 87-91.

44.   Brown, D.A. and London, E. (1998). Functions of lipid rafts in biological membranes. *Annu. Rev. Cell Dev. Biol.* **14**, 111-36.

45.   Rietveld, A. and Simons, K. (1998). The differential miscibility of lipids as the basis for the formation of functional membrane rafts. *Biochim Biophys Acta* **1376**, 467-79.

46.   Jiang, Y., Lee, A., Chen, J., Cadene, M., Chait, B.T. and MacKinnon, R. (2002). The open pore conformation of potassium channels. *Nature* **417**, 523-6.

47.   Tatulian, S.A., Cortes, D.M. and Perozo, E. (1998). Structural dynamics of the *Streptomyces lividans* K+ channel (SKC1): secondary structure characterization from FTIR spectroscopy. *FEBS Lett.* **423**, 205-12.

48.   Le Coutre, J., Kaback, H.R., Patel, C.K.N., Heginbotham, L. and Miller, C. (1998). Fourier transform infrared spectroscopy reveals a rigid alpha- helical assembly for the tetrameric *Streptomyces lividans* K+ channel. *Proc. Natl. Acad. Sci. U. S. A.* **95**, 6114-7.

49.   Marsh, D. (1996). Peptide models for membrane channels. *Biochem. J.* **315**, 345-61.

50.   Gavin, A.C. et al. (2002). Functional organization of the yeast proteome by systematic analysis of protein complexes. *Nature* **415**, 141-7.

51.   Alberts, B. (1998). The cell as a collection of protein machines: preparing the next generation of molecular biologists. *Cell* **92**, 291-4.

52.   Gurezka, R., Laage, R., Brosig, B. and Langosch, D. (1999). A heptad motif of leucine residues found in membrane proteins can drive self-assembly of artificial transmembrane segments. *J. Biol. Chem.* **274**, 9265-70.

53.   Zhou, F.X., Cocco, M.J., Russ, W.P., Brunger, A.T. and Engelman, D.M. (2000). Interhelical hydrogen bonding drives strong interactions in membrane proteins. *Nat. Struct. Biol.* **7**, 154-60.

54.   Peled-Zehavi, H., Arkin, I.T., Engelman, D.M. and Shai, Y. (1996). Coassembly of synthetic segments of shaker K+ channel within phospholipid membranes. *Biochemistry* **35**, 6828-38.

55.   Papazian, D.M., Shao, X.M., Seoh, S.A., Mock, A.F., Huang, Y. and Wainstock, D.H. (1995). Electrostatic interactions of S4 voltage sensor in Shaker K+ channel. *Neuron* **14**, 1293-301.

56.   Loo, J.A. (2000). Electrospray ionization mass spectrometry: a technology for studying noncovalent macromolecular complexes. *Int. J. Mass Spectrom.* **200**, 175-86.

57.   van Berkel, W.J., van den Heuvel, R.H.H., Versluis, C. and Heck, A.J.R. (2000). Detection of intact megaDalton protein assemblies of vanillyl-alcohol oxidase by mass spectrometry. *Protein Sci.* **9**, 435-9.

58.   Robinson, C.V., Chung, E.W., Kragelund, B.B., Knudsen, J., Aplin, R.T., Poulsen, F.M. and Dobson, C.M. (1996). Probing the Nature of Noncovalent Interactions by Mass Spectrometry   A Study of Protein CoA Ligand Binding and Assembly. *J. Am. Chem. Soc.* **118**, 8646-53.

59.   Brunner, J. (1993). New photolabeling and crosslinking methods. *Annu. Rev. Biochem.* **62**, 483-514.

List of abbreviations

ac	acetyl
amu	atomic mass unit
ATR-FTIR	attenuated total reflection Fourier transform infrared
CD	circular dichroism
CHAPS	3-[(3-cholamidopropyl)-dimethylammonio]-1-propanesulfonate
CID	collision induced dissociation
DDM	n-dodecyl-β-D-maltoside
DEiPC	1,2-dieicosenoyl-sn-glycero-3-phosphocholine
DMPC	1,2-dimyristoyl-sn-glycero-3-phosphocholine
DOPA	1,2-dioleyl-sn-glycero-3-phosphate
DOPC	1,2-dioleyl-sn-glycero-3-phosphocholine
DOPE	1,2-dioleyl-sn-glycero-3-phosphoethanolamine
DOPG	1,2-dioleyl-sn-glycero-3-phosphoglycerol
DPoPC	1,2-dipalmitoleoyl-sn-glycero-3-phosphocholine
ESI-MS	electrospray ionization mass spectrometry
ESR	electron spin resonance
etn	ethanolamine
H/D	hydrogen/deuterium
K*	lysine residue with a di-methylated ε-amine nitrogen functionality
KcsA	potassium channel from *Streptomyces lividans*
LUVETs	large unilamellar vesicles prepared by extrusion
MALDI-MS	matrix-assisted laser desorption/ionization mass spectrometry
MLV	multilamellar vesicles
MS	mass spectrometry
MS/MS	tandem mass spectrometry
m/z	mass-to-charge ratio
nano-ESI-MS	nano-flow electrospray ionization mass spectrometry
NMR	nuclear magnetic resonance
PA	phosphatidic acid
PC	phosphatidylcholine
PE	phosphatidylethanolamine
PG	phosphatidylglycerol
PL	phospholipid
Q	quadrupole
RF	radio frequency
SDS	sodium dodecyl sulphate
TFE	2,2,2-trifluoroethanol

TM	transmembrane
ToF	time-of-flight
Tris	trishydroxymethylaminomethane
WALP16	ac-GWW(LA)$_5$WWA-etn
WALP16(+10)	ac-(GA)$_3$WW(LA)$_5$WW(AG)$_3$-etn
WALP19	ac-GWW(LA)$_6$LWWA-etn
XALP21	ac-GXX(LA)$_7$LXXA-am/etn sequence (X = F, W or Y)
XALP23	ac-GXX(LA)$_8$LXXA-am/etn sequence (X = H, K, K* or W)

Nederlandse samenvatting

In dit hoofdstuk zal ik voor niet-ingewijden uitleggen wat ik tijdens mijn promotie-onderzoek heb bestudeerd en wat de resultaten en perspectieven van het onderzoek zijn.

Elk levend organisme bestaat uit één (bijvoorbeeld een bacterie) of meerdere cellen (bijvoorbeeld de mens), die omgeven zijn door een beschermend omhulsel: de celmembraan. Membranen bestaan voornamelijk uit lipiden (vetten) en eiwitten en vormen een barrière voor wateroplosbare moleculen. Zo'n barrière is belangrijk om de gunstige omstandigheden voor biochemische reacties, die van levensbelang zijn voor de cel, te handhaven en de inhoud van de cel te beschermen tegen schadelijke externe invloeden. De lipiden in de membraan zijn moleculen die bestaan uit een hydrofiele (waterlievende) kopgroep en een hydrofobe (waterafstotende) staart en hebben daardoor speciale eigenschappen: in water zullen deze moleculen zich zo organiseren dat de hydrofiele kopgroep gepresenteerd wordt aan het water, terwijl de hydrofobe staarten vanwege hun onderlinge aantrekkingskracht bij elkaar zullen gaan zitten. Dit resulteert in de vorming van grote 'macromoleculaire' complexen van lipidemoleculen met een structuur die we 'bilaag' noemen: twee ('bi') lagen van lipidemoleculen in een plat vlak, waarbij de hydrofobe staarten elkaar raken en de hydrofiele kopgroepen grenzen aan de waterige oplossing die de membraan omringt (weergegeven in Figuur 1 op blz. 11). Dat water kan bijvoorbeeld het cytosol (celvloeistof) aan de ene kant zijn en het water van de buitenwereld aan de andere kant.

Hoewel de functie van de membraan als barrière dus belangrijk is moet de cel ook met de omgeving kunnen communiceren, voedingsstoffen kunnen opnemen en afvalstoffen kunnen uitscheiden. Zo 'voelt' een bacterie bijvoorbeeld dat de concentratie van essentiële voedingsstoffen in zijn omgeving afneemt en zal 'besluiten' zich te verplaatsen naar een omgeving met een hogere concentratie aan deze stoffen. Het 'voelen' geeft aan dat er signalen vanuit de omgeving moeten worden opgenomen en het opnemen van voedingsstoffen en het uitscheiden van afvalstoffen betekent dat er transport van deze stoffen door de membraan moet plaatsvinden. De moleculen die verantwoordelijk zijn voor al deze processen zijn eiwitten die in de membraan verankerd zitten. Deze membraaneiwitten vormen dus een heel belangrijke klasse van moleculen en het niet juist functioneren ervan kan fataal zijn voor de cel. Om vitale functies van cellen te verstoren of juist te stimuleren vormen membraaneiwitten zodoende een uiterst geschikte 'target'. Het is dan ook niet verwonderlijk dat veel geneesmiddelen die heden ten dage gebruikt worden, gericht zijn op membraaneiwitten.

Om de doelstellingen van mijn onderzoek duidelijk te maken is het noodzakelijk eerst iets uit te leggen over de opbouw van eiwitten. Eiwitten bestaan uit ketens van soms wel honderden aminozuren lang. Zoals woorden in onze taal worden opgebouwd uit 26 letters, zo worden eiwitten opgebouwd uit 20 verschillende aminozuren. Men kan zich voorstellen dat er dus een enorme variatie aan eiwitten mogelijk is. Dat is ook noodzakelijk, want elk eiwit moet een zeer specifieke functie uitoefenen. Zo ook de eiwitten die in de membraan verankerd zitten; veel van

deze eiwitten kun je beschouwen als minuscule machines. Sommige laten bijvoorbeeld specifiek natriumionen door, terwijl andere alleen kaliumionen doorlaten. Vergelijk het met een blokkendoos, waarbij een bal alleen via het ronde gat en een kubus alleen door het vierkante gat naar binnen kan. Op deze manier kan in de cel een delicaat evenwicht tussen deze ionen worden gehandhaafd. Dit evenwicht draagt er zorg voor dat de biochemische processen die plaatsvinden in de cel onder controle gehouden worden.

Hoewel elk eiwit dus verschilt van de ander en (daardoor) een specifieke functie heeft, blijken er ook enkele overeenkomsten te zijn tussen membraaneiwitten onderling. Zo weten we dat ze vrijwel allemaal ketens van hydrofobe aminozuren bezitten, die ervoor zorgen dat ze in de hydrofobe membraan verankerd zitten en dat de delen van het eiwit die uit de membraan in het omringende water uitsteken onveranderlijk georiënteerd blijven ten opzichte van het membraanoppervlak. Deze ketens noemen we de transmembraansegmenten of -domeinen van het eiwit. Gedetailleerde kennis over deze hydrofobe segmenten en over de manier waarop membraaneiwitten door middel van deze ketens in de membraan verankerd zitten ontbreekt echter. Zo is er veel variatie in lengte en in samenstelling van deze segmenten en de betekenis daarvan is tot nu toe onduidelijk. Toch zijn ze van cruciaal belang voor het eiwit, omdat zij de manier bepalen waarop het eiwit ten opzichte van de omringende lipiden in de membraan georiënteerd is. En dat is dan weer belangrijk voor het juist functioneren van het eiwit. Als men nu weet hoe die segmenten (en dus het eiwit) precies in de membraan verankerd zitten en weet welk deel van het eiwit uit de membraan steekt, is het bijvoorbeeld beter mogelijk geneesmiddelen te ontwerpen die erop gericht zijn specifiek aan het eiwit te binden en het zodoende te blokkeren.

Nu is het moeilijk om cellen en celmembranen gedetailleerd te bestuderen. Ten eerste zijn cellen zo klein dat je ze alleen met een sterke microscoop kunt bekijken. Om onderdelen van cellen - celmembranen bijvoorbeeld en, nog gedetailleerder, eiwitten in celmembranen - te bekijken zou je een nóg sterkere microscoop nodig moeten hebben en die bestaan niet. Er moeten dan dus andere methoden ontwikkeld worden om aan te kunnen tonen hoe een membraan en de eiwitten erin er precies uit zien. Hier kom ik zometeen op terug. Ten tweede bevatten celmembranen erg veel componenten en het is lastig om er één van gedetailleerd te onderzoeken. Het is handiger om er één component uit te lichten en de 'achtergrondruis' van componenten die op dat moment voor het onderzoek niet zo interessant zijn te verlagen. Een manier om de gewenste component kunstmatig te 'verrijken' is door modelsystemen te ontwerpen. Deze bestaan uit slechts enkele componenten en in hoeveelheden die men tot op zekere hoogte zelf kan bepalen, mits niet teveel van de biologische situatie wordt afgeweken.

Ik heb gebruik gemaakt van een modelsysteem om gedetailleerd te onderzoeken hoe eiwitten in membranen verankerd zitten. Omdat grote membraaneiwitten moeilijk uit organismen te isoleren en te zuiveren zijn en bovendien moeilijk te meten met de meeste biofysische technieken, hebben wij kleine eiwitjes (peptiden) ontworpen en gesynthetiseerd, die veel kenmerken van transmembraan segmenten bezitten en die we 'WALP' peptiden (een

acroniem) hebben gedoopt. We kunnen hele kleine variaties in deze peptiden aanbrengen (bijvoorbeeld het vervangen van slechts één aminozuur door een ander, of er een paar extra aminozuren aan plakken om zo het segment langer te maken), waarvan we dan het effect op de plaatsing in een membraan kunnen bestuderen. Als we die effecten systematisch bestuderen kunnen we deze ook uiteindelijk extrapoleren naar echte membraaneiwitten. Hiertoe maken we, naast modeleiwitjes, ook gebruik van modelmembranen die bestaan uit slechts één of twee soorten lipiden. Hier maken we dan hele kleine modelcelletjes van (minuscule vetbolletjes of 'vesicles') waar we het peptide dan in stoppen.

Membraaneiwitten kunnen vervolgens bestudeerd worden met behulp van verschillende biofysische technieken, die allemaal hun voor- en nadelen hebben. In het algemeen zijn hydrofobe moleculen erg moeilijk te bestuderen; vergelijk het met de moeite die het kost om een vetvlek met water uit kleding te verwijderen. Zoals zeep (detergens) in zo'n geval gebruikt kan worden om vet op te lossen, zo kunnen detergentia gebruikt worden voor het oplossen van membraaneiwitten. Hieraan kleven echter een paar ernstige nadelen en we wilden het gebruik hiervan dan ook voorkomen. Ik heb voor een tamelijk nieuwe techniek gekozen om eiwitten te bestuderen, namelijk electrospray massaspectrometrie. Hiermee kun je de moleculaire massa van peptiden en eiwitten heel nauwkeurig meten. Het belang van deze techniek voor het onderzoek in de biochemie werd vorige maand nog eens benadrukt met het uitreiken van de Nobelprijs voor scheikunde aan de uitvinder van de electrospray massaspectrometrie. Deze techniek wordt dan ook in heel veel laboratoria toegepast als algemene analytische techniek. Het meten aan membraaneiwitten met deze techniek is echter zeker nog geen standaardmethode die algemeen wordt gebruikt. Hoofdstuk 2 van dit proefschrift gaat dan ook over een nieuwe methode die we hebben opgezet en getest om deze moleculen beter te kunnen meten. Het nieuwe aspect van deze methode is dat we vesicles met de peptiden erin vanuit water direct kunnen meten met electrospray massaspectrometrie. Dit in tegenstelling tot verschillende andere biofysische technieken waarbij eerst het peptide uit de membraan moet worden gehaald en vervolgens moet worden opgelost in een organisch oplosmiddel of met behulp van detergentia, hetgeen minder goed overeenkomt met de biologische situatie. Op deze manier kunnen wij dus peptiden in hun natuurlijke omgeving, namelijk de membraan, wél bestuderen. Om de nieuwe methode te testen hebben we gebruik gemaakt van twee WALP peptiden: WALP16 en WALP16(+10). De eerste is 16 aminozuren lang en de tweede heeft behalve dezelfde 16 aminozuren ook nog eens 5 aminozuren die zich graag in water bevinden aan beide uiteinden. WALP16 is precies even lang als de membraan dik is (zie Figuur 1 op blz. 45). WALP16(+10) zit op dezelfde manier in de membraan, maar heeft staartjes waarvan we denken dat ze in het omringende water steken. We kunnen nu met waterstof/deuterium uitwisseling in combinatie met massaspectrometrie testen of dit werkelijk zo is. Sommige waterstofatomen in het peptide wisselen namelijk spontaan uit voor deuteriumatomen als vesicles in gedeutereerd water (D_2O of 'zwaar water') gebracht worden. De waterstofatomen die beter toegankelijk zijn voor D_2O zullen sneller uitwisselen dan de delen van het peptide die beschermd zijn in het hydrofobe gedeelte van de membraan waar

water moeilijk kan komen. Met de massaspectrometer kun je dan vervolgens bekijken hoeveel deuteriumatomen het peptide heeft opgenomen, omdat deuterium zwaarder is dan waterstof. Er vindt dus een verschuiving in massa plaats: hoe langer een peptide in aanraking is met D_2O, hoe meer deuteriumatomen het opneemt en hoe zwaarder het wordt. Zo kun je dus op een indirecte manier precies nagaan welk deel van het peptide in de membraan zit en welk stuk uitsteekt. Bovendien kun je met dissociatiemassaspectrometrie, waarbij het peptide in de massaspectrometer kapotgeschoten wordt, het deuteriumgehalte van de verschillende delen van het peptide bekijken. Zo weet je niet alleen *hoeveel* atomen uitgewisseld zijn, maar ook *welke*. We kunnen aan het eind van Hoofdstuk 2 concluderen dat het met deze methode inderdaad goed mogelijk is om te bekijken hoe deze modeleiwitjes in de membraan gepositioneerd zijn. Deze kennis kunnen we dan extrapoleren naar transmembraansegmenten van echte eiwitten.

In Hoofdstuk 3 hebben we vervolgens enkele eigenschappen van deze peptiden veranderd en het effect daarvan bekeken op de waterstof/deuterium uitwisseling en dus op de positionering van de peptiden in de membraan. Uitgaande van WALP16 zijn we begonnen met het verlengen van het peptide, terwijl we de dikte van de membraan constant hielden. Uit het effect op de uitwisseling konden we concluderen dat de membraan zich als het ware aanpast aan het langere transmembraansegment. Met andere woorden: om de interacties tussen het peptide en de membraan zo optimaal mogelijk te houden maakt het membraan zichzelf bij aanwezigheid van een langer peptide iets dikker. Dit effect was ook al eens gesignaleerd in een ander type experiment en hebben we nu beter kunnen kwantificeren. Verder hebben we gekeken naar het effect van een bepaald aminozuur (proline) dat vaak in bepaalde klassen van membraaneiwitten, bijvoorbeeld in 'transporter' of 'G-coupled receptor' eiwitten, wordt gevonden. De functie hiervan in die eiwitten is niet helemaal duidelijk, maar het vermoeden bestaat dat het aminozuur iets te maken heeft met het veranderen van de structuur van het eiwit op het moment dat er een signaal binnenkomt. Proline heeft namelijk een iets andere ruimtelijke structuur dan de andere aminozuren. Wij hebben met ons model aangetoond dat het aminozuur waarschijnlijk inderdaad een effect heeft op de structuur van het transmembraan segment. Een ander idee dat al wat langer bestaat is dat een ander aminozuur, tryptofaan, een speciale voorkeur heeft voor dat gedeelte van de membraan waarin zich de hydrofiele kopgroepen van de lipiden bevinden (de zogenaamde 'interface' regio). Wij hebben aangetoond dat het veranderen van de plaats van het aminozuur inderdaad een groot effect heeft op de positionering. Met andere woorden: tryptofaan zit graag op dezelfde plaats in interface, onafhankelijk van de positie in het peptide.

In Hoofdstuk 4 heb ik een meer fysisch-chemisch onderwerp aangesneden. Het bleek namelijk dat de resultaten van de dissociatiemassaspectrometrie experimenten wat verwarring opleverden toen we peptiden bestudeerden die in plaats van tryptofaan het aminozuur lysine bevatten. Het leek erop dat de deuteriumatomen in het peptide op plaatsen zaten waar we ze eigenlijk helemaal niet verwachtten. We kregen daardoor het vermoeden dat er in de massaspectrometer iets gebeurde waardoor de deuteriumatomen zich *random* verdelen in het peptide. Dit effect staat bekend onder de naam 'scrambling'. Scrambling is uiteraard een

ongewenst effect, omdat het lokaliseren van de deuteriumatomen extra informatie oplevert, terwijl die informatie in het geval van scrambling verloren gaat. In hoofdstuk 4 hebben we experimentele factoren bestudeerd die van invloed zijn op de hoeveelheid scrambling. Het blijkt dat bepaalde aminozuren het effect versterken en ook dat het effect kan worden tegengegaan door op het peptide een natriumion in plaats van een proton als lading aan te brengen. Behalve een waarschuwing voor onszelf zijn deze observaties ook een waarschuwing voor andere onderzoekers die dit soort experimenten doen: in bepaalde gevallen kan scrambling optreden en dit kan de interpretatie van de resultaten danig beïnvloeden.

In Hoofdstuk 5 heb ik een natuurlijk voorkomend membraaneiwit gebruikt om vergelijkbare experimenten mee uit te voeren als met de modeleiwitjes. Het eiwit, een kaliumkanaal, is afkomstig uit een bacterie en zorgt daar voor transport van kaliumionen over de membraan. Dit eiwit hebben we in membranen geplaatst om er vervolgens massaspectrometrie aan te doen. Het bleek echter moeilijker te zijn om een groot eiwit in vesicles te meten. Het was wel mogelijk, maar we konden er niet zo gedetailleerd naar kijken als in het geval van de modelpeptiden. Toch zagen we een verrassend verschijnsel: uit de resultaten van de metingen bleek dat aan het eiwit één of meerdere lipiden afkomstig uit de omringende membraan bleven hangen; dit is in het massaspectrum te zien aan de hogere massa voor het eiwit. Opvallend hierbij was dat het ene lipide beter op het eiwit bleef zitten dan het andere. Hieruit concludeerden we dat het eiwit een bepaalde voorkeur heeft in de keuze uit de lipiden waarmee het zich omringt. Met name negatief geladen lipiden hebben een grote voorkeur. Dit gegeven geeft nieuwe inzichten in het belang van de diversiteit van lipiden in membranen. Op grond van deze resultaten zou het goed kunnen dat de binding tussen de positieve ladingen op het eiwit en de negatieve ladingen op het lipide in de membraan een extra mogelijkheid voor het eiwit vormt, om zich stevig in de membraan te verankeren.

In het laatste hoofdstuk heb ik de in dit proefschrift verkregen resultaten en de betekenis ervan nog eens op een rijtje gezet. Het onderzoek heeft nieuwe inzichten opgeleverd in de interacties tussen eiwitten en membranen. Kennis over membraaneiwitten, d.w.z. hun structuur, functie, interacties met andere moleculen in de membraan en de onderlinge verbanden hiertussen, is belangrijk om het functioneren (of het *dis*functioneren) van celmembranen (en dus ook cellen) beter te kunnen doorgronden. Het is niet alleen fascinerend om te ontrafelen hoe celmembranen er precies uitzien en hoe ze functioneren, een beter begrip van membraaneiwitten stelt onderzoekers bovendien ook gemakkelijker in staat geneesmiddelen te ontwerpen die gericht zijn op deze eiwitten. Natuurlijk zijn de vragen die hier beantwoord zijn slechts enkele deelvragen in een veel groter geheel, maar het combineren van antwoorden op al die deelvragen uit kleine stukjes onderzoek en het puzzelen daarmee geeft uiteindelijk toch een aardig beeld over de werking van membranen en hun componenten. Uiteraard roept die verzameling antwoorden misschien zelfs wel meer nieuwe vragen op dan er ooit waren en die andere wetenschappers dan vervolgens proberen op te lossen. Wetenschap staat immers nooit stil.

Curriculum vitae

De schrijver van dit proefschrift werd geboren op 7 september 1975 te Bergen op Zoom. Na het behalen van het Voorbereidend Wetenschappelijk Onderwijs diploma aan de R.S.G. ' 't Rijks' in 1993 in diezelfde gemeente begon hij in oktober van dat jaar met de studie scheikunde aan de Universiteit Utrecht. Na het behalen van het propedeuse diploma (*cum laude*) werden vervolgens tijdens het doctoraal programma onderzoeksstages medische microbiologie bij het Eykman-Winkler Instituut van de Universiteit Utrecht (onder begeleiding van dr. J.A.G. van Strijp) en membraanbiochemie bij de sectie Biochemie van Membranen van de Universiteit Utrecht (onder begeleiding van prof. dr. Ben de Kruijff) gedaan, waarbij een deel van het onderzoek werd uitgevoerd bij de sectie Plantenfysiologie van de Landbouwuniversiteit Wageningen. In juni 1998 werd het doctoraalexamen behaald (*cum laude*). Een maand eerder was hij begonnen als onderzoeker in opleiding bij de secties Biochemie van Membranen en Biomolekulaire Massaspectrometrie van de Universiteit Utrecht op een door NWO gefinancierd project. In deze functie werd het in dit proefschrift beschreven onderzoek, dat onder leiding stond van prof. dr. J. Antoinette Killian, prof. dr. Albert J.R. Heck en prof. dr. Johan Haverkamp, verricht. Onderzoeksresultaten werden onder meer gepresenteerd tijdens lezingen op de jaarlijkse conferenties van de *American Society for Mass Spectrometry* in Chicago (2001) en Orlando (2002) en op verscheidene bijeenkomsten van NWO studiegroepen in Lunteren, alsmede door middel van posterpresentaties op conferenties in onder meer New Orleans en Barcelona. In mei 2002 werd hij uitgekozen om de '*best PhD publication*' lezing te mogen verzorgen tijdens het jaarlijkse Bijvoet Symposium in Utrecht.

List of publications

Van den Wijngaard, P.W.J., <u>Demmers, J.A.A.</u>, Thompson, S.J., Wienk, H.L.J., de Kruijff, B. and Vredenberg, W.J. (2000) Further analysis of the involvement of the envelope anion channel PIRAC in chloroplast protein import. *Eur. J. Biochem.* **267** (12), 3812-3817.

<u>Demmers, J.A.A.</u>, Haverkamp, J., Heck, A.J.R., Koeppe II, R.E. and Killian, J.A. (2000) Electrospray ionization mass spectrometry as a novel tool to analyze hydrogen/deuterium exchange kinetics of transmembrane peptides in lipid bilayers. *Proc. Natl. Acad. Sci. U.S.A.* **97** (7), 3189-3194.

<u>Demmers, J.A.A.</u>, van Duijn, E., Haverkamp, J., Greathouse, D.V., Koeppe II, R.E., Heck, A.J.R. & Killian, J.A. (2001) Interfacial positioning and stability of transmembrane protein segment models in lipid bilayers: a hydrogen/deuterium exchange and mass spectrometry study. *J. Biol. Chem.* **276** (37), 34501-34508.

<u>Demmers, J.A.A.</u>, Rijkers, D.T.S., Haverkamp, J., Killian, J.A. & Heck, A.J.R. (2002) Factors affecting gas-phase deuterium scrambling in peptide ions and their implications for protein structure determination. *J. Am. Chem. Soc.* **124** (37), 11191 –11198.

<u>Demmers, J.A.A.</u>, Van Dalen, A., De Kruijff, B., Heck, A.J.R. & Killian, J.A. (2002) Interactions of the potassium channel KcsA with phospholipid membranes studied by ESI mass spectrometry (*submitted*).

De Planque, M.R.R., Bonev, B.B., <u>Demmers, J.A.A.</u>, Van der Wel, P.C.A., Greathouse, D.V., Separovic, F., Watts, A., and Killian, J.A. (2002) Interfacial anchor properties of tryptophan residues modulate the membrane-associating properties of transmembrane peptides (*submitted*).

Adams, H., Teertstra, W., <u>Demmers, J.A.A.</u>, Boesten, R. & Tommassen, J. (2002) Interactions between Phage-shock proteins (Psp) in *Escherichia coli* (*submitted*).

<u>Demmers, J.A.A.</u>, *et al.* Properties of transmembrane peptides and integral membrane proteins studied by mass spectrometry. (Review*, in preparation*).

Dankwoord

"Well, well, so there *is* an audience…" – Aan het feit dat dit stukje van het proefschrift het meest gelezen wordt ben ik zelf mede schuldig…vandaar dat ik mijn best ga doen om er wat van te maken.

Wetenschap bedrijven is op een bepaalde manier wel te vergelijken met reizen naar onbekende landen: hoe meer je gezien hebt, hoe meer je wíl zien. Ik denk dat alleen daarom vier jaar lang werken aan een specifiek onderwerp mogelijk is. Wel met vallen en opstaan natuurlijk, en met de nodige frustraties af en toe. Maar met een mooi resultaat ben je meteen ook alle tegenslagen die daaraan vooraf gingen vergeten. Bovendien doe je het meeste werk ook niet alleen en daarom wil ik hier enkele mensen bedanken.

Allereerst mijn eerste twee promotoren Albert Heck en Antoinette Killian: jullie zijn het meest direct betrokken geweest bij het project en dankzij jullie specifieke vakkennis en enthousiasme was er al vrij snel sprake van een succesvolle synthese van 'water en vuur': hydrofobe membraanpeptiden en massaspectrometrie. Leuk dat ik voor jullie beiden de eerste 'echte' promovendus ben! Begeleiding wat meer vanachter de coulissen werd verzorgd door Ben de Kruijff en Johan Haverkamp. Ben, hoewel jij je bewust op de achtergrond hebt gehouden zijn jouw kennis van zaken, inzicht en kritisch oog met name bij het kaliumkanaal-werk zeer waardevol geweest. Johan bedank ik voor de vrijheid die je me hebt gegeven om dit onderzoek grotendeels op mijn eigen manier in te vullen.

Eén van de prettige kanten aan dit promotie-onderzoek was het feit dat ik mijn tijd kon doorbrengen in twee verschillende labs. Hoewel ik in het ene lab wat meer was dan in het andere, heb ik in beide met veel plezier gewerkt en 'gehobbied' en dat zeker dankzij iedereen die daar ook werkte. Een paar mensen wil ik in het bijzonder bedanken. 'WALP-goeroe' Maurits: bedankt dat je me wilde inwijden in de soms erg geheimzinnige wereld der hydrofobe peptiden. Verder waardeer ik je tips over postdocbeurzen, reizen, enzovoorts, altijd zeer. Succes in Oxford! Met Maurits, Matthijs en Hilde heb ik nog eens een avond op een terras op het Ledig Erf op een mooie zomeravond over alle aspecten van hydrofobe peptiden en hun interacties met lipide bilagen gediscussieerd. Ik geef toe: zelf zou ik als nietsvermoedende caféganger enigszins vreemd hebben opgekeken… Met mijn kamergenoot Edwin in het massa-lab heb ik veel lief, leed, frustratie (hoe vaak precies hebben we nu eigenlijk MassLynx geïnstalleerd?!), plezier, verbazing, bruingele rakkers en wat al niet meer gedeeld. Een terechte paranimf dus. Jouw zenuwen heb ik, zeker tijdens de eerste ASMS conferentie in Chicago, toen we elkaars slapie waren en allebei als ASMS-debutanten een lezing moesten geven (rollen toiletpapier op de 29^e verdieping van het Hyatt...), danig op de proef gesteld. Maar jij de mijne ook, dus ik denk dat we wat dat betreft wel quitte staan. De dagen na de tweede ASMS-conferentie (het *cruisen* door de straten van Clearwater en het luieren op Key Largo) zal ik niet snel vergeten. Ewald, we moeten ook allebei op zoek naar een nieuwe squash-partner de komende tijd. Kees: bedankt voor de nimmer

aflatende technische bijstand. Mocht de Q-Tof (die inmiddels toch al aardig op leeftijd is) ooit nog afgedankt worden, dan is Kees' bijkeuken volgens mij een uitstekende bestemming. I would also like to acknowledge prof. Roger Koeppe II and dr. Denise Greathouse for synthesizing some of the peptides that were used for the work described in this thesis. Het synthesewerk werd in Utrecht overgenomen door John Kruytzer en Dirk Rijkers: nooit geweten dat je peptiden zo snel en in zulke hoeveelheden kon maken! Annemieke: bedankt voor de discussies over het kaliumkanaalwerk en het beschikbaar stellen van je eiwitvoorraad – dat heeft me zeker een hoop werk gescheeld. Mijn studenten Esther, Hanneke, Nick en Mara wil ik bedanken voor al het verrichte werk. Vooralsnog is Esther de enige die het aangedurfd heeft om te gaan promoveren: succes! Verder de mensen van het Bijvoet AiO-platform, met wie ik heb geprobeerd om de AiO's van het Bijvoet Centrum wat meer het gevoel te geven dat we AiO's van het Bijvoet Centrum zijn: *keep up the good spirit*!

Natuurlijk lukt promoveren niet zonder de broodnodige ontspanning (wat wel eigenlijk?). Mijn andere paranimf, Remco (Cor voor intimi), is degene die je daarvoor bij uitstek moet hebben. Samen gestudeerd, samen op de Warande gewoond, samen afgestudeerd, (vrijwel) samen gepromoveerd en nu dan ook waarschijnlijk samen naar het Noord-Amerikaanse continent om te na-dokken (gaan we daar nu echt dichter bij elkaar wonen dan nu?!) Toch goed dat we die baan bij dat reisbureau in Havana niet aangenomen hebben…enne…zorg ervoor dat dit hier geen 'vies boekske' wordt! Hans, bedankt voor de weekendjes Londen, de bezoeken aan North Sea Jazz en andere concerten, de nieuwjaarsduiken en zo meer. En dan is er natuurlijk geen betere ontspanning dan muziek! Leden van Hortus, Zoroaster en de Utrechtse Muziekacademie: de komende tijd zullen jullie met een eerste viool minder verder moeten…Verder bedankt vrienden, familie en kennissen, die ik niet allemaal met name kan noemen, maar zonder wie het allemaal een stuk moeilijker zou zijn geweest: reizen, films, dineetjes, concerten, *cooking club* (ik hoop dat jullie destijds echt geen last meer hebben gehad van die - al zeg ik het zelf - overheerlijke Baskische rode-bonensoep met pepers en chorizo, hoewel jullie als een boer met kiespijn zeiden dat-ie 'best te doen' was...). Anneke en zwager Jeroen: ik zal er speciaal voor jullie in mei natuurlijk zijn! Uiteraard wil ik mijn ouders, die me altijd met raad en daad bijstaan, op deze plaats bedanken voor hun ondersteuning in alle mogelijke vormen: papa en mama, als jullie nu willen laten zien wat ik uitgespookt heb de afgelopen jaren kunnen jullie voortaan dit boekje laten zien in plaats van dat verfrommelde papiertje met de schets van een membraan en een massaspectrometer van ruim vier jaar oud!

En tenslotte, deze laatste zin van dit proefschrift is voor degene voor wie laatste zinnen van proefschriften altijd bedoeld zijn…

Vladimir: *That passed the time.*
Estragon: *It would have passed in any case.*
Vladimir: *Yes, but not so rapidly.*

From: *Waiting for Godot*, by Samuel Beckett (1955)